Structure of benthic microbial mat assemblages in Lake Fryxell, Antarctica

Colin Johnson Hillman

This thesis is presented and submitted in fulfilment of the requirements for the Master's Program in Antarctic Studies

Gateway Antarctica

College of Science

University of Canterbury

September, 2013

DECLARATION

I declare that, unless stated otherwise, all research presented in this thesis is my own work and has not previously been submitted for a degree at any tertiary education institution.

……

Colin Johnson Hillman

Acknowledgements

I would first like to express my warm gratitude to all of my supervisors. Professor Ian Hawes for constantly challenging me to perform to my best, combined with his never-ending supply of patience in even the most demanding work environments. Dr. David Collings for his invaluable assistance with the confocal microscopy. Dr. Paul Broady for his encyclopaedic knowledge in all matters cyanobacterial, along with his endless enthusiasm. Finally, thanks to Professor Bryan Storey for agreeing to take me on as a postgraduate student and ensuring that we met all our research deadlines.

I would also like to extend honourable mention and thanks to Graeme Bull, Manfred Ingerfeld, Alan Woods, Matthew Walters and Jackie Healy from the School of Biological Sciences for lending their experience, expertise and patience with the technical aspects of the sample analysis and data preparation. I am also extremely grateful for my colleagues at Gateway Antarctica for their friendship and help throughout the entirety of this project.

A special thank you as well to the vibrant and friendly staff at Scott Base for their help with the logistical, transport and training focussed aspects of our research expedition. I am also indebted to the Christchurch City Council for their generously provided CCC Scholarship, which helped to cover living expenses.

Finally, I wish to extend a sincere gratitude to my family for their constant love and support during this challenging research project.

And to all those concerned, there are no polar bears in the Antarctic.

Abstract

Microbial mats are important components of perennially ice-covered Antarctic lakes in the McMurdo Dry Valleys, where they often comprise the dominant biomass in this cold, shaded environment. These lakes represent some of the most extreme lacustrine environments on Earth, including a persistent ice-cover, stable, stratified water columns, with strong salinity related density gradients. In these low-disturbance environments, the microbial consortia develop macroscopic emergent structures such as pinnacles and ridges. Such structures are speculated to confer advantageous survival traits and have also been found in the Precambrian fossil record as "conophyton" stromatolites – arguably some of the earliest evidence of life – and it has been suggested that a better understanding of the growth dynamics of modern "conophyton" will inform our understanding of what was required for these early fossils to be produced.

Despite decades of research, there are few studies of the structural basis of conophyton producing microbial mats in Antarctic lakes. To help address this gap, complex microbial mats along a transect established in Lake Fryxell, one of the McMurdo Dry Valley lakes, were examined; with the aim of documenting the distribution of different types of photosynthetic organisms and mat morphologies along environmental gradients such as light, conductivity, oxygen concentration and depth. Microbial mat samples were taken along the transect and analysed in New Zealand using confocal laser scanning microscopy, along with conventional pigment extraction techniques.

Correlations between mat morphology, pigment content and lake properties were found. The appearance of bacteriochlorophylls, characteristic of green sulfur bacteria within and below the oxycline confirm a shift from aerobic to anaerobic metabolism that was consistent with mats taking on a prostrate appearance. The cyanobacterial pigment phycoerythrin was only found in the hyperoxic, relatively well lit region of the transect, and was associated with the mats forming a distinctive macroscale morphology with dense fields of cm-scale cuspate pinnacles. Between these, a hypoxic region was characterised by a relatively flat mat within which were many cm-scale pits. Structural investigations were focussed on two distinct morphologies, pinnacle and honeycomb mat. Nearly all photosynthetic organisms were located in the upper 2 mm of both pinnacle and

honeycomb mats, mainly comprising diatoms and cyanobacteria. Pinnacle mats were dominated by a narrow cyanobacterium, probably a species of *Leptolyngbya*, which were mostly oriented vertically, which placed trichomes parallel to the direction of pinnacle extension. The honeycomb mat contained fewer narrow trichomes, rather the bulk of photosynthetic organisms were diatoms from the genera *Muellaria*, *Navicula* and *Diadesmis,* together with broad-trichome cyanobacteria that formed a thin skin on the surface of the mat, though absent from the pits. The type of emergent structure that is formed appears to be related to species composition, and this in turn appears to be related to the growth conditions. A model was developed to explain how species-specific growth mechanisms are involved in emergent structure formation for honeycomb and pinnacle mats.

Abbreviations

CLSM Confocal laser scanning microscopy

DBL Diffusive boundary layer

EPS Extracellular polysaccharides

MDV McMurdo Dry Valleys

NA Numerical aperture

OD Optical density

PAR Photosynthetically available/active radiation

SRB Sulfate-reducing bacteria

Table of Contents

List of Figures

List of Tables

Glossary

Euphotic zone: The zone of water in which there is sufficient sunlight for photosynthesis to occur.

Lambda mode: In confocal microscopy, lambda scanning is the recording of a series of individual images within a user defined wavelength range, and the quantification of these to provide the emission spectrum of fluorescent molecules at specific locations within the image.

Lamination: A layered accretion of organic and/or inorganic material formed by the trapping and binding of sedimentary detritus with microbial life-forms, such as cyanobacteria. Laminations can also be preserved in the fossil record.

Meromictic: A lake characterised by a lack of mixing between the water layers.

Numerical aperture: A description of how much light a microscope lens permits to enter. A higher aperture means that the angle of light coming through the sample is higher.

Oxycline: A sharp gradient in oxygen concentration.

Tile scan mode: A confocal microscopy program that permits the user to automatically assemble an image from a series of smaller images by digitally merging the smaller images. A tile scan area is defined by selecting two opposite positions within a sample, which define the outer positions of where the scan will be undertaken.

Trichome: An entire chain of cyanobacterial cells. A filament is a trichome, plus the enclosing sheath.

Z-stack: In confocal microscopy, the collection of a series of images at different depths within a sample at the same location. Z-stacks can be used in conjunction with Tile Scans and Lambda scans.

1. Introduction

1.1 Microbial mats

Microbial mats are stratified, heterogeneous consortia of microorganisms that can be up to several centimetres thick, and which can be found in a wide range of environments (Sharma *et al.,* 2003; Franks and Stolz, 2009; Gerdes, 2010). They are often regarded as 1-dimensional systems, since they contain strong vertical stratification of organisms and physical processes in conjunction with steep resource gradients. The stratification within microbial mats is primarily determined by gradients in the concentration of oxygen and other gases (such as methane and hydrogen sulfide), irradiance and nutrient supply (Figure 1).

Cyanobacteria frequently dominate microbial mats and their photosynthesis provides the main oxygen source (Hawes *et al.,* 1992). The cyanobacteria and other oxygen phototrophs are however, limited to the upper layers of the mats due to the decreasing light penetration with depth. Beneath the cyanobacteria, a reddish-pink stratum of purple sulfur bacteria, and a deeper layer of green sulfur bacteria, are often present (Fenchel, 1998; Dupraz *et al.,* 2009). While capable of photosynthesis, these sulfur bacteria use hydrogen sulfide (H_2S) and not water as an electron donor, and generate sulfate (SO_4) rather than oxygen as a by-product. These sulfur bacteria are typically located at the bottom of the oxygenic zone with sulfate reducers, which produce H_2S from the sulfate. Anoxia at these depths is caused by anaerobic decomposition of the organic material, which is buried by new growth and sediment deposition from above (Paerl and Pinckney, 1996). The deepest layers of microbial mats are dominated by anaerobic organisms such as nitrate (NO_3) reducing bacteria, methanogens and fermenters. This layer is predominately black, with occasional grey bands due to the presence of iron sulfide (Barghoorn and Nichols, 1961; Karr *et al.,* 2005).

During the daytime, the oxygenic photosynthesis from the cyanobacteria and diatoms releases dissolved organic compounds - such as glucose, along with oxygen, which are then utilised by heterotrophic bacteria, generating carbon dioxide and water. These by-products are then recycled for use in photosynthetic

reactions. This situation is reversed during night-time. Sulfate-reduction is also reduced during day-time, but increases during night-time. The sulfate reducing bacteria (such as *Desulfovibrio*) reduce sulfate to hydrogen sulfide using electron donors such as H_2, sterols and alcohols. While sulfate can be reduced to sulfide at an intracellular level, under oxygenic external conditions, large-scale biogeochemical reduction of sulfate to sulfide must occur in anoxic environments. The sulfide diffuses to the site of daytime anoxygenic photosynthesis - an example of efficient metabolic coupling within the microbial mat. In addition to close coupling of the S-cycle (Figure 1), another example of microbial mat efficiency is found in N-cycling. Aerobic respiration consumes oxygen, which is a potent inhibitor of the nitrogen-fixing enzyme *nitrogenase*, creating anoxic zones where denitrification can occur (Barghoorn and Nichols, 1961; Jorgensen and Des Marais, 1986; Paerl and Pinckney, 1996).

The organisational and metabolic networking of microbial mats can be attributed to complementary functions existing in close proximity at micrometre scales over which diffusion is an effective process (Decho, 1990). Efficient coupling over short distances allows for mats to accrue and recycle nutrients and allows them to be relatively independent of the water column. Mats interact with the water column via the diffuse boundary layer (DBL), the thin layer of water that covers all submerged microbial mat surfaces (Lorenzen *et al.,* 1995).

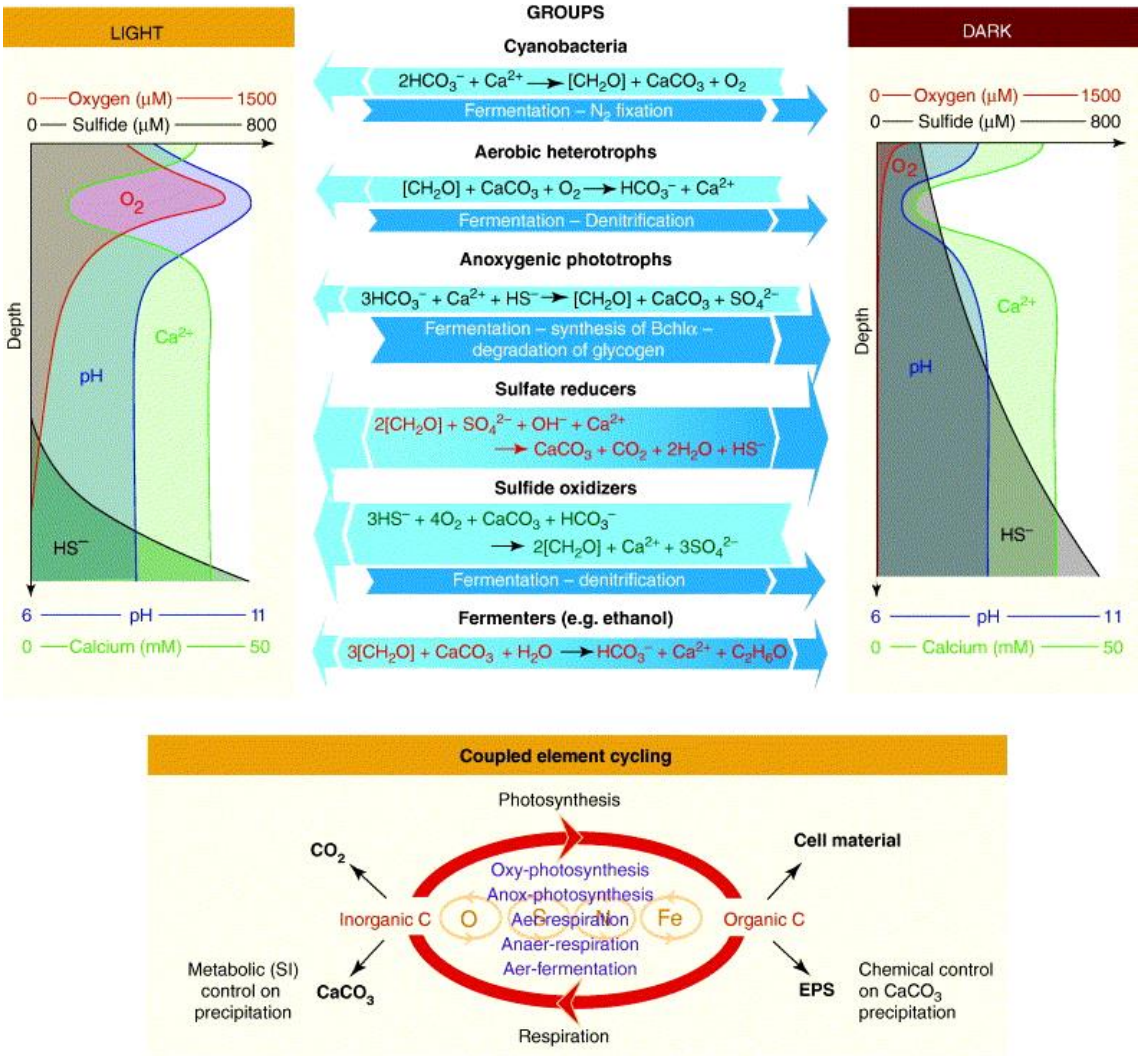

Figure 1. Diagram of an archetypal microbial mat (modified from Dupraz and Visscher, 2005).

1.2 Modern emergent structures

While microbial mat communities are often seen as 1-dimensional, in the absence of significant physical and biological disturbances, they can develop 3-dimensional macroscopic frameworks such as ridges and peaks. These are referred to as *emergent structures*, as they emerge as from the main body of the microbial mat as extensions of it. Emergent structures are comprised of microbial cells that grow in a mix of extracellular polymeric material (polysaccharides, lipids and proteins), detritus and calcium carbonate. All these components mechanically bind together and rise above the main body of the microbial mat (Burne and Moore, 1987; Decho, 1990; Klock *et al.,* 2007). Gross mat morphology and emergent structure formation are affected by a number of variables, including species composition, environmental factors (irradiance, salinity, nutrient loads and water depth) and the type of sediment on which the microbial mat is located (Castenholz, 1968; de los Rios *et al.,* 2004; Gerdes, 2010). For example, the peaks and ridges formed in microbial mats are dominated by filamentous cyanobacteria (trichomes) and filament motility seems to be required for emergent structure formation (Flannery and Walter, 2012).

Since the pinnacles and ridges are rising out of and extending away from the mat, this indicates that they are also growing at a more rapid rate than the rest of the mat. One explanation for this is that it is due to a positive phototaxis from the resident cyanobacteria, which would account for greater biomass of these photoautotrophs in the peaks and ridges themselves. (Bauld, 1981; Gerdes, 2010; Shephard and Sumner, 2010) The positive phototaxis/photokinesis hypothesis has been suggested by Dillon *et al.* (2009) and is supported with evidence from Kilian *et al.* (2007). Other possible mechanisms include unoriented, gliding motility (Shepard and Sumner 2010), movement along nutrient gradients to minimise resource competition (Petroff *et al.,* 2010) or a combination of these factors that may be further complicated by species specific behaviours, such as competition (Andersen *et al.,* 2011). These contemporary cyanobacteria-dominated microbial communities frequently exhibit emergent structure features, such as cuspate pinnacles, that are strikingly similar to those found in preserved Precambrian "conophyton" material (Hofmann, 1969; Jorgensen *et al.,* 1983).

1.3 Precambrian stromatolites

1.3.1 General overview

Stromatolites (Kalkowsky, 1908) are accretionary, organosedimentary deposits which form a dominant component of the early Earth's fossil record. All accrete upwards by the addition of laminae and can be divided into 4 main morphological classes: coniform, branched, flat and domical. They are distinguished from other sedimentary deposits by their laminated structure, as opposed to thrombolites (clotted morphology) or dendrolites (dendritic morphology). While stromatolites are usually made up of calcium carbonate ($CaCO_3$), other documented types include siliceous, evaporite and carbonate-siliciclastic forms (Riding, 2000; Allwood *et al.,* 2009). These structures are shaped by complex physical and chemical interactions and can range in size from thin millimetre-scale sheets to formations extending for hundreds of metres vertically and hundreds of kilometres laterally (Grotzinger and Knoll, 1999). Stromatolites were dominant during the Archean and Proterozoic Eons in the Precambrian, between 3100-510 million years ago (Walter *et al.,* 1976; Parker *et al.,* 1981; Batchelor *et al.,* 2003; Allwood *et al.,* 2009;).

As presumed indicators of physical and chemical dynamics in the water and sediment from the Precambrian, stromatolites remain one of most studied and debated topics in geobiology (Allwood *et al.,* 2009; Bosak *et al.,* 2013). Structural similarities between contemporary benthic microbial communities and fossilised Precambrian specimens may imply formation under similar conditions. Modern microbial mats are frequently used as model systems to infer and study the hypothesised functions of the world's earliest microbial communities. In particular, pinnacle morphology terminates to form a 'cuspate' apex which appears only to be found in Precambrian specimens of a disputed biogenic origin. Hofmann (1969) classified these stromatolite morphology traits into several main categories, based on the types of documented surfaces, peaks and apices (Figure 2).

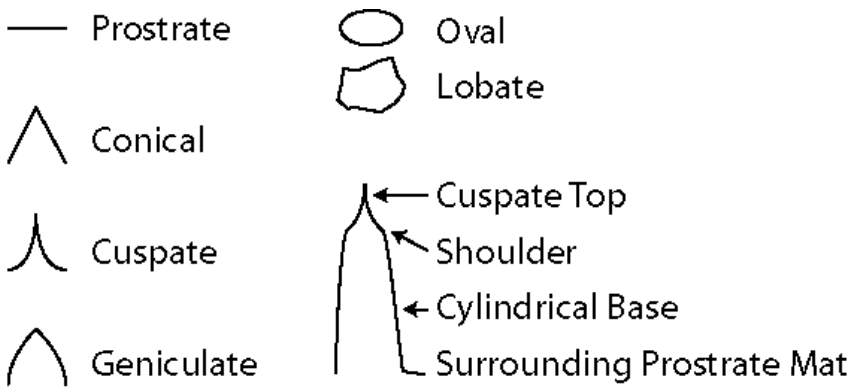

Figure 2. Terms used in describing stromatolite morphology. Note that the oval and lobate definitions refer to transverse sections (modified from Hofmann, 1969).

1.3.2 Physical and biological models for stromatolite formation

Kalkowsky (1908), one of the pioneers in the systematic study of stromatolites, was convinced that stromatolites were biotic in origin, even though he was not able to prove it. The lithification process removes traces of extracellular polymeric material and metabolites and identifying structures that are definitively associated with a biotic origin is problematic at best (Allwood *et al.,* 2009; Petroff *et al.,* 2010; Tice *et al.,* 2011). As a result, morphology is often the only indicator to gauge the presence of possible past life and the associated environmental conditions (Bosak and Newman, 2005; Stevens *et al.,* 2011).

While stromatolites have been interpreted as the first fossilised organisms, a universal biological origin is still fiercely challenged and two paradigms exist for stromatolite formation; primarily abiotic and primarily biotic. Grotzinger and Rothman (1996) and Grotzinger and Knoll (1999) proposed that stromatolites are formed through abiotic mechanisms. They postulate that the preserved Precambrian material is indicative of physical and chemical processes alone such as mineral re-crystallisation and carbonate deposition. They further argued that the emphasis on modern 'analogues' for stromatolite formation, discussed below, is overplayed and may have limited relevance to interpretation of Precambrian structures due to differing compositions of seawater and atmosphere then and now (Bosak *et al.,* 2013). Thus, Grotzinger and Rothman (1996) proposed the following in their abiotic model of stromatolite formation:

(1) Fallout of suspended sediment,

(2) Diffusive smoothing of settled sediment

(3) Surface-normal precipitation of carbonates, and,
(4) Uncorrelated 'random noise' of micro-scale environmental fluctuations.

They caution that microbial activity in stromatolite growth cannot be exclusively ruled out, simply that their exact potential role in stromatolite formation is unclear due to a lack of fossil evidence.

Recently Flannery and Walter (2012), supported by evidence from Shepard and Sumner (2010) have challenged the paradigm of abiotic formation and provided more evidence in support of the biotic model of stromatolite formation. They argue that some of the structures are undoubtedly biological in origin due to the presence of tufted and pustular morphologies that are inconsistent with a sedimentary origin. Tufted mats in particular are complex and possess a variety of recurring structures (tufts) which arise from otherwise flat surfaces. Flannery and Walter (2012) further note that the structures include centimetre-scale tufts, pinnacles and ridges arranged into radial, parallel and reticulate patterns that have been observed in a wide array of modern global environments – such as Yellowstone National Park, Wyoming, USA, Lake Vanda in Antarctica and Shark Bay in Western Australia (Walter *et al.,* 1976).

At present, it seems necessary to acknowledge that some stromatolites may have been formed entirely through abiotic mechanisms while others had a biotic origin. Even so, it will be easier to infer the biological and physical processes of fossil assemblages if the development of emergent structures in modern 'stromatolites' can be more closely analysed, which continues to be problematic due to the sheer complexities involved in stromatolite morphogenesis. To better understand how these formations develop, it is important to analyse the modern analogues, which are found in several global locations - such as the McMurdo Dry Valleys (MDV) in Antarctica. Several perennial ice-covered lakes in the MDV – Lakes Bonney, Chad, Vanda, Hoare and Fryxell possess benthic microbial communities that are striking analogues of Precambrian stromatolites. MDV microbial mats provide researchers with unique opportunities, due to a number of key factors:

1) Studied Antarctic lakes (such as Lakes Vanda and Fryxell) have been well documented since the 1960s.

2) The benthic mats are internally laminated, with evidence indicating that these laminae record previous annual growth (Hawes *et al.,* 2001).
3) Perennial ice-covered lakes are amongst the components of the Antarctic ecosystem most sensitive to ecological changes over time.
4) Some of the best developed modern stromatolites/benthic mats are located in these lakes (Andersen *et al.*, 2011).
5) The water levels in several ice-covered lakes in the MDVs are rising due to increased glacial inflow in response to an increase in solar radiation and a gradual summer warming trend. As lake levels rise, growth conditions can change. For example, irradiance at specific locations on the lake floor decline as water depth above them increases. This can render it impossible for photosynthetic microbial communities and their emergent structures to persist, and in at least one lake, Lake Joyce, microbial formations only persist as "legacy" structures – communities that grew only when environmental conditions were more favourable and are now deceased (Bomblies *et al.,* 2001; Hawes *et al.,* 2011).

1.4: Microbial mats in the lakes of the McMurdo Dry Valleys

The McMurdo Dry Valleys (MDVs) are located to the west of McMurdo Sound (Figure 3). This region is characterised by low humidity, a mean annual temperature of -20°C, a lack of ice cover and less than 50 mm precipitation each year (Fountain *et al.,* 2009). The MDVs remain ice-free due to the katabatic winds which sweep down from the Polar Plateau and because the outflow of glaciers from the East Antarctic ice sheet have been blocked by the uplift of the Transantarctic Mountains (Gleadow *et al.,* 1984; Craig *et al.,* 1992).

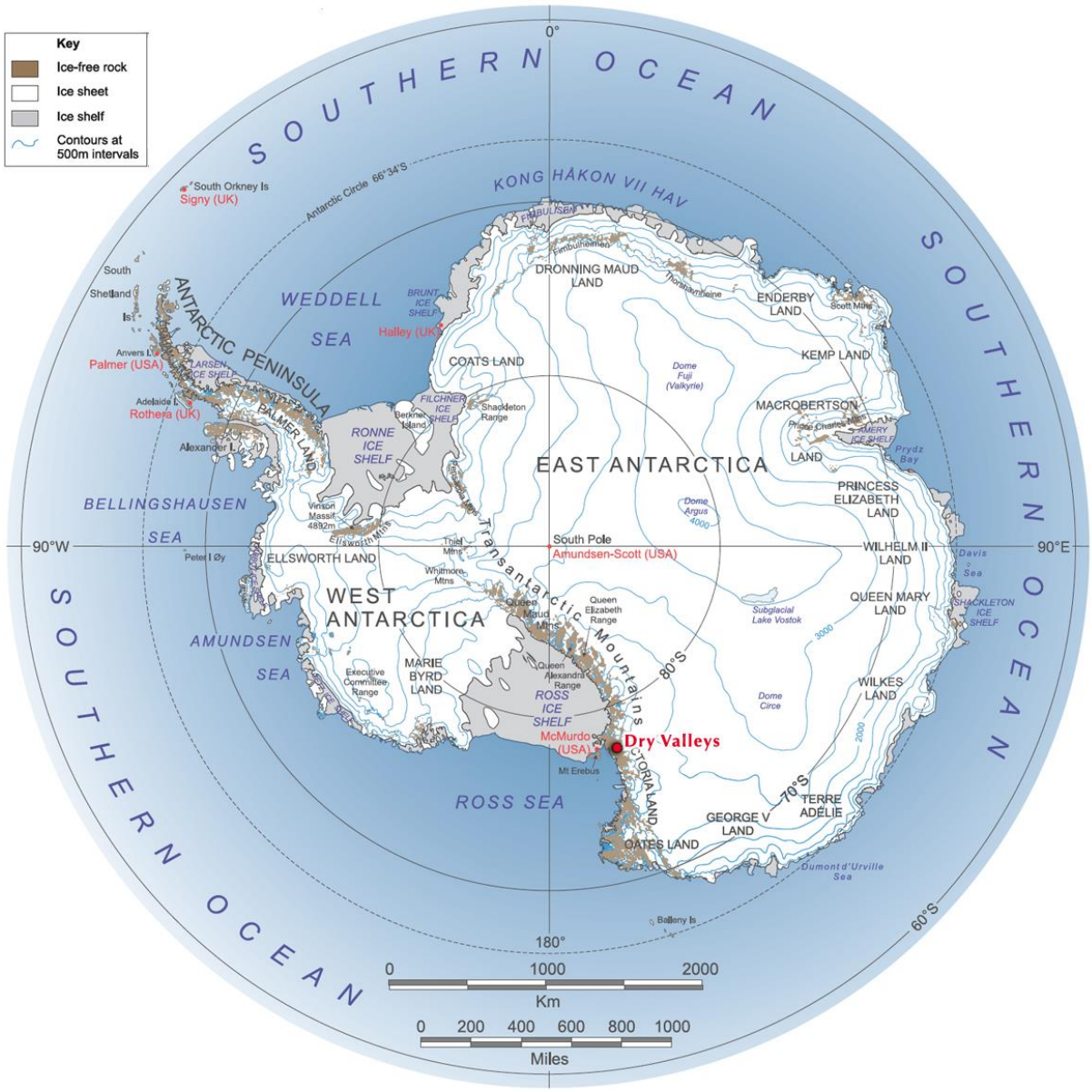

Figure 3. The location of the McMurdo Dry Valleys in Antarctica (modified from Kowalewski, 2009).

Perennially ice-covered lakes are a prominent feature of the MDVs and occupy the lowest parts of closed drainage basins (Canfield and Green, 1985). The thick ice cover insulates the water from the extremely low atmospheric temperatures, and the heat balance is re-established in summer by solar heating and inflowing water. The latent heat released as ice thickens in winter also prevents complete freezing of the lakes (Wilson, 1967; Vincent, 2000). The ice cover has profound effects on the lakes as it reduces light penetration, and restricts gas-exchange between the atmosphere and the water column. It also prevents wind-induced mixing of the lake. As a result of this, the upper part of the lakes are supersaturated with oxygen (over 14.6 mg/L at O°C in freshwater), while at depth the lakes are anoxic (Wharton *et al.,* 1982; Wharton *et al.,* 1983 Lampert and Sommer, 1997; Vopel and Hawes, 2006). Dissolved gases derive from several sources. They are supplied by inflowing summer glacial melt-water and, in the case of oxygen, by photosynthesis occurring below the ice, although low light conditions especially during winter frequently limit photosynthetic activity (Craig *et al.,* 1992; Moorhead *et al.,* 1997; Hawes and Schwarz, 2001). The lakes lack outflow streams, but receive limited inflow from the glacial melt-water, which provides sediment, nutrients and salts (Wilson, 1967; Parker *et al.,* 1981; Canfield and Green, 1985).

MDV benthic microbial mats frequently dominate the total biomass (carbon), despite the considerable environmental stresses (Parker *et al.,* 1981; de los Rios *et al.,* 2004; Quesada *et al.,* 2008). These benthic communities are well-adapted to anaerobic conditions, oxygen super-saturation, pH extremes, oligotrophic nutrient levels (especially nitrate and phosphate), cold temperatures, saline water and freshwater (Parker *et al.,* 1981; Dore and Priscu, 2001; Hawes *et al.,* 2001). Furthermore, the absence of vascular plants, vertebrate animals, insects and crustaceans mean that grazing/predation and competition for resources are almost entirely absent (Hawes and Howard-Williams, 1998; Moorhead *et al.,* 2005). While the composition and abundances of the resident mat species varies between locations, the benthic microbial mats are predominantly composed of cyanobacteria (primarily *Phormidium*, *Oscillatoria* and *Lyngbya*), along with several pennate diatoms and heterotrophic bacterial species (Wharton *et al.,* 1983; Vincent, 1988). A unique feature of many of the benthic mats is their

development into modern cold freshwater stromatolites, which are unknown elsewhere on Earth. These formations have been undisturbed for centuries (Wharton *et al.,* 1983; Vincent, 1988; Andersen *et al.,* 2011; Hawes *et al.,* 2011). Lake Fryxell, in the Taylor Valley is one such lake.

1.4.1 Lake Fryxell

Lake Fryxell (77° 36´S, 162° 6´ E) (Figure 4) is a strongly stratified, meromictic lake located near the eastern end of Taylor Valley. The lake is 5 by 1.5 kilometres in extent and permanently covered by 4.5 metres of ice. Less than 1% of surface irradiance penetrates the ice cover (Hoare *et al.,* 1965; Vincent and Vincent, 1982; Dore and Priscu, 2001; Karr *et al.,* 2006; Whittaker *et al.,* 2008) The maximum depth of the lake is 20 metres (including the ice cover), with an oxycline depth at approximately 11 metres (Taton *et al.,* 2003). The oxycline is a sharp gradient change in oxygen concentration. Frxyell has an irregular topography (Figure 5). The submerged architecture of the lake seems to have been partially buried by a sediment fan deposited by water that flowed into the eastern end of the basin. Lake sediment cores contain 5 recognised units, with 3 being calcareous (Lawrence and Hendy, 1985). Six zones were defined using diatom assemblage changes based on Konfirst *et al.* (2011).

While Lake Fryxell remains ice-covered throughout the year, a marginal melt-water moat does form around the edges of the lake during summer when a network of 13 streams discharge fresh glacial melt-water into the lake (Figure 5) from the Canada and Commonwealth glaciers (Aiken *et al.,* 1996; Konfirst *et al.,* 2011). The lake is fresh-water near the top and reaches a salinity of 1% NaCl near the bottom. The principal minerals are sodium chloride and sodium bicarbonate (Angino *et al.,* 1962: Lawrence and Hendy, 1985).

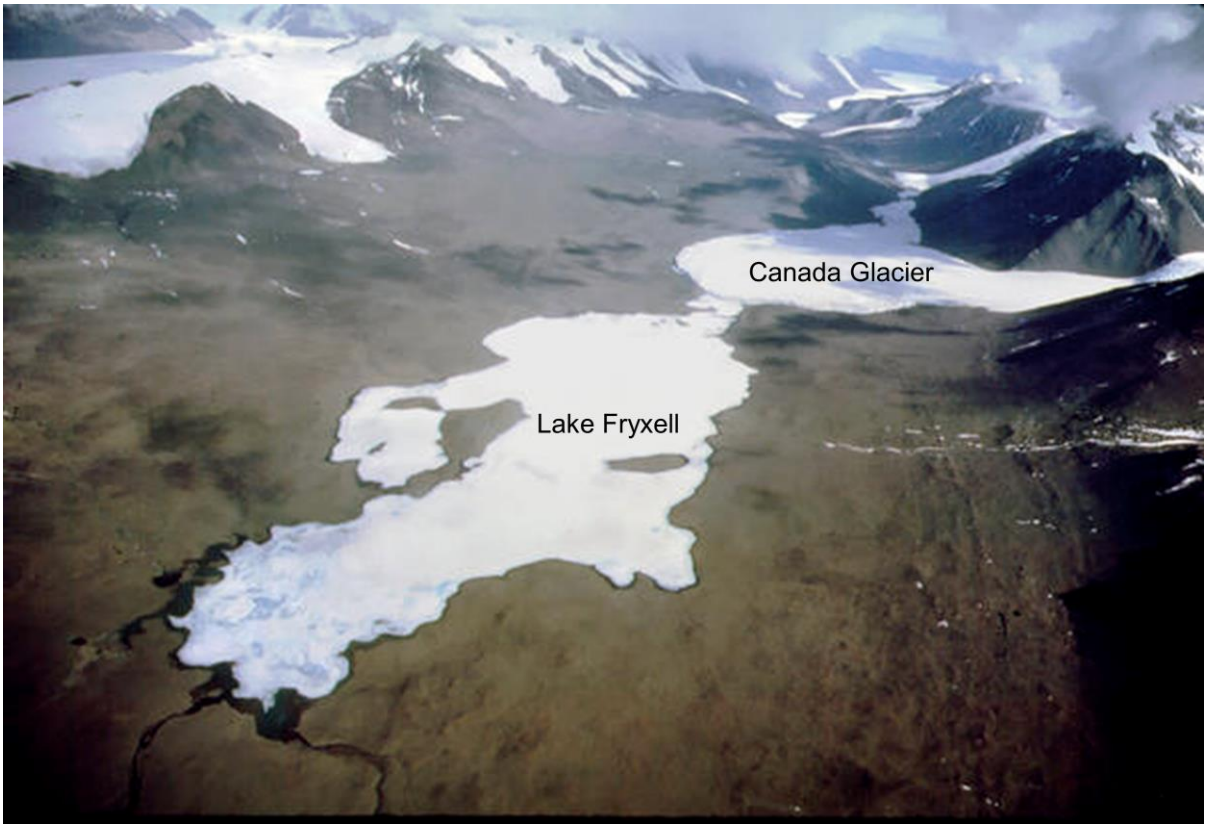

Figure 4. Annotated aerial photograph of Lake Fryxell and the Canada Glacier, looking westwards up the Taylor Valley.

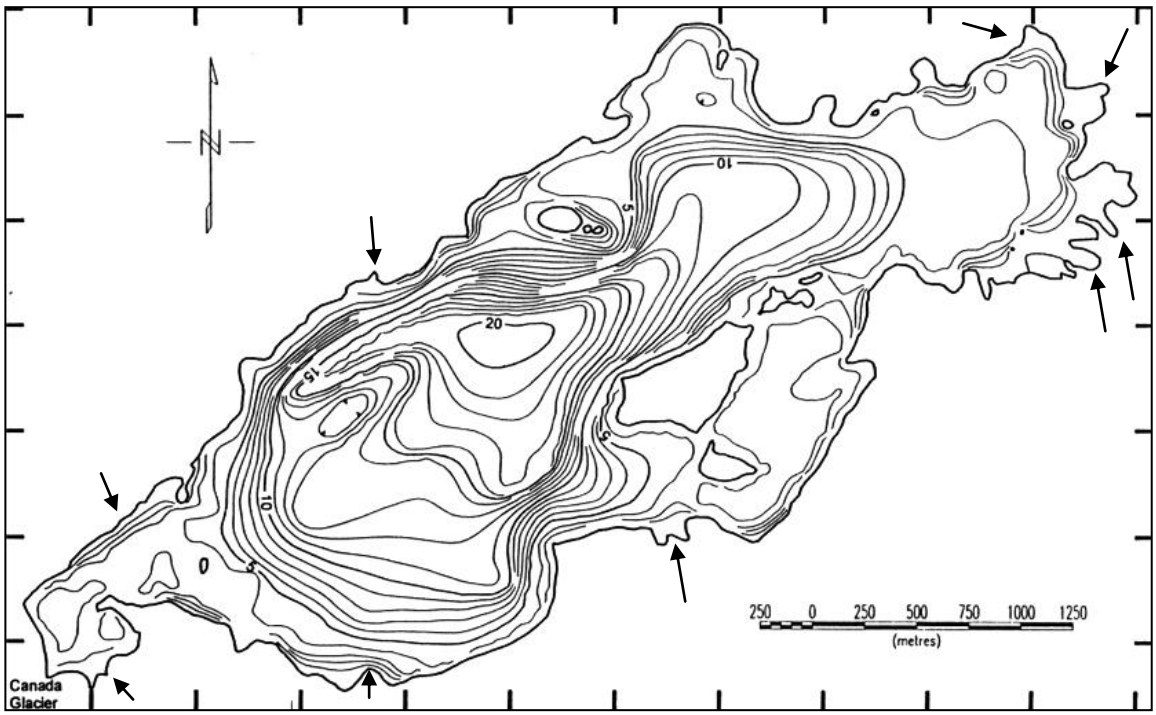

Figure 5. Bathymetric map of Lake Fryxell, with arrows highlighting the entry points of the main glacial stream inflows (modified from Kepner *et al*., 2000).

While organic carbon input (dissolved organic carbon) is minimal, Lake Fryxell supports significant sulfur and methane cycles (Karr *et al.,* 2005; Karr *et al.,* 2006; Sattley and Madigan, 2010). Methane is produced in the sediments and consumed in the anoxic water column where sulfate reduction also occurs (Smith *et al.,* 1993). The water column possesses a strong sulfide concentration that exceeds 1 mM immediately above the sediment at the deepest point in the lake, decreasing above the oxycline as the sulfide diffuses upwards. Conversely, sulfate concentration decreases with depth (Figure 6) (Howes and Smith, 1990; Karr *et al.,* 2005; Karr *et al.,* 2006; Sattley and Madigan, 2010).

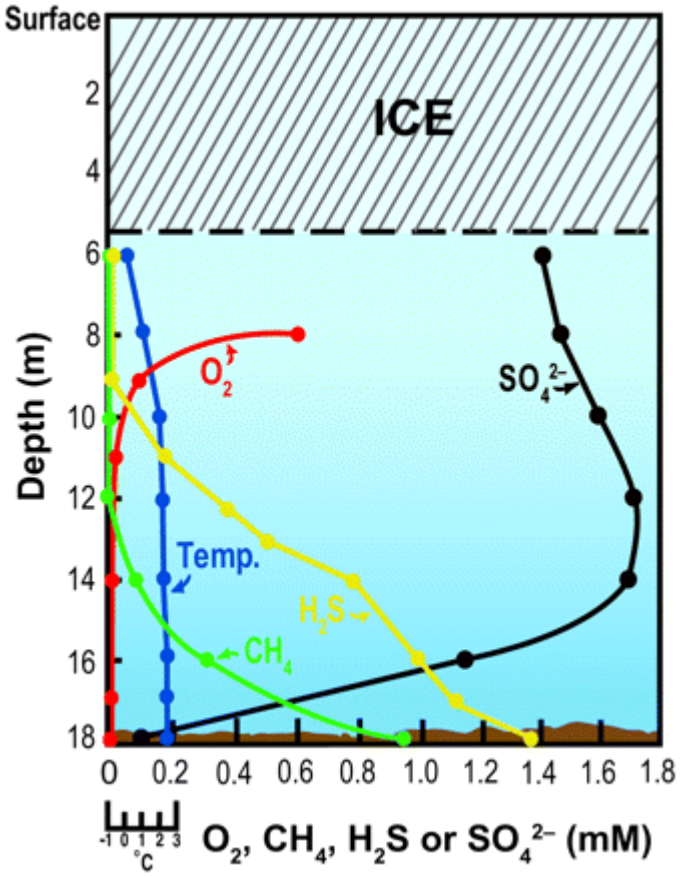

Figure 6. Geochemistry profile summary of Lake Fryxell (Karr *et al*., 2006).

1.4.2 Lake Fryxell microbial communities

While there have been extensive studies on Lake Fryxell's geochemistry, only few studies have reported on the microbial communities present within the lake (Karr *et al.,* 2003). Phytoplankton diversity is low (56 algal taxa collected), and consist primarily of cryptophyte and chlorophyte flagellates, and filamentous cyanobacteria (Spaulding *et al.,* 1994). In contrast, benthic microbial communities are abundant in Lake Fryxell, primarily in the more shallow parts of the lake (Wharton *et al.,* 1983). As described by Wharton *et al.* (1982), these communities have a top layer that was 2 to 10 mm thick that consists mainly of the cyanobacterium *Phormidium frigidum,* pennate diatoms and heterotrophic bacteria. The mat communities are also characterised by pinnacles within the top layer, which are found mainly in the euphotic zone (sufficient sunlight for photosynthesis) and are also internally laminated. Underneath this top layer, layers of sediment and organic material continue to a depth of 50 cm. These have an average organic matter content of 8.7%. Embedded in those sediment layers are laminated and unbranched calcite structures which have either developed a horizontal or vertical orientation. The vertical structures (1-5 cm diameter and 1-10 cm long) are frequently hollow, terete (cylindrical and tapering to an apex) and covered by a 0.2 to 1 cm thick algal mat (Parker and Simmons, 1978; Wharton *et al.,* 1982). They were described as *modern Antarctic stromatolites* by Parker *et al.* (1981).

While several molecular, ecological and descriptive studies have documented the diversity of benthic microbial communities in Lake Fryxell, - such as identifying 11 cyanobacteria taxa (Brambilla *et al.,* 2001; Taton *et al.,* 2003), few studies have investigated the functional or structural significance of the emergent structures or the exact spatial arrangements within the resident benthic mats. Similarly, few studies have investigated biogeochemical cycling in benthic mats, as the majority of research has focussed on nutrient cycling in the water column. It is also important to note that molecular diversity samples were only obtained from the shallow summer moat by Taton *et al.* (2003). Therefore, it is not likely that the studies are representative of the entire species diversity at Lake Fryxell.

1.5 Research Aims

The primary goals of this study were to help facilitate improved understanding of 1) benthic mat organisation, 2) the growth and development of macroscopic emergent structures and to assist in 3) the interpretation of ancient stromatolite communities. Specifically, it was necessary to ascertain how different photosynthetic organisms were distributed in benthic mats from Lake Fryxell, Antarctica. This was accomplished by:

- Developing techniques that exploit the different fluorescent properties of dissimilar groups of organisms in order to map their distribution in microbial mats using confocal laser scanning microscopy (CLSM).

- Trialling new preservative techniques to maintain microbial mat structure and photosynthetic pigment brightness for later analyses.

- Developing fluorescence "fingerprinting" to characterise different groups of photosynthetic organisms.

- Producing 3-D maps of photosynthetic organism distribution within microbial mats based on the previous objectives.

2. Materials and Methods

2.1 Field sampling

2.1.1 Transect and sampling stations

Sampling at Lake Fryxell was undertaken in November and December 2012 by the K081 Field Team, NZ Antarctic Program. A dark-tent laboratory was established on the lake ice (77° 36.404´S, 163° 9.071´E) and a dive hole was melted through the ice using a Hotsy ethylene glycol circulating heater. A 60 m long transect was then established by a SCUBA diver from just below the dive hole towards the centre of the lake and marked with a fixed rope. Nine stations were established along the transect at depths of 9.1, 9.4, 9.7, 9.9, 10.3, 10.4, 10.8, 11.2 and 11.5 m (values include the approximate 4.5 m depth of the ice layer). The stations were designated D1 through to D9.

2.1.2 In situ *measurements*

PAR (photosynthetically available radiation) was measured using a LiCor 192 sensor connected to a LiCor 1400 meter. The latter was in a waterproof housing, which permitted operation by a diver. The first series of PAR measurements were conducted by a diver swimming in radial patterns immediately under the ice. Measurements were made at 2-3 m intervals, while holding the Li192 sensor against the underside of the ice. A LiCor 190 terrestrial quantum sensor was used to obtain simultaneous measurements of incident irradiance above the ice to allow the underwater readings to be recalculated as percentage transmission of surface irradiance. Light measurements were then taken with the underwater sensor at each sample station along the transect, again in conjunction with the surface measurements, to determine the percentage of light transmission at each station.

Water samples were then collected into two, acid-washed 60 ml syringes from immediately above the mat surface at each station, and were taken into the dark-tent laboratory next to the ice-hole. The tip of one of the syringes was

capped and the plunger withdrawn to allow water temperature and conductivity to be measured with a Hach portable CTD meter. The conductivity-temperature probe was then swapped for a freshly-calibrated pH probe and pH recorded. Dissolved oxygen was measured in the second syringe using a Pre-sense needle optode that could be inserted through the syringe tip to minimise gas exchange with the atmosphere.

2.1.3 Microbial mat sampling

2.1.3.1 Quantitative sampling

Mat samples for quantitative analysis were collected from all nine sampling stations (D1-D9) using a 38 mm diameter coring device. Four replicates were taken per station and transferred to 50 ml Falcon tubes (while still underwater). On return to the surface, water was drained and the samples were frozen for return to New Zealand. At D4, the mat samples were strongly stratified by marked colour changes (Figure 7). For this reason, all samples from D4 were divided into 3 layers; A – the brownish-purple top layer, 2 mm thick, B - the green, middle layer, approximately 10 mm thick and C - a cream under-layer, approximately 10 mm thick.

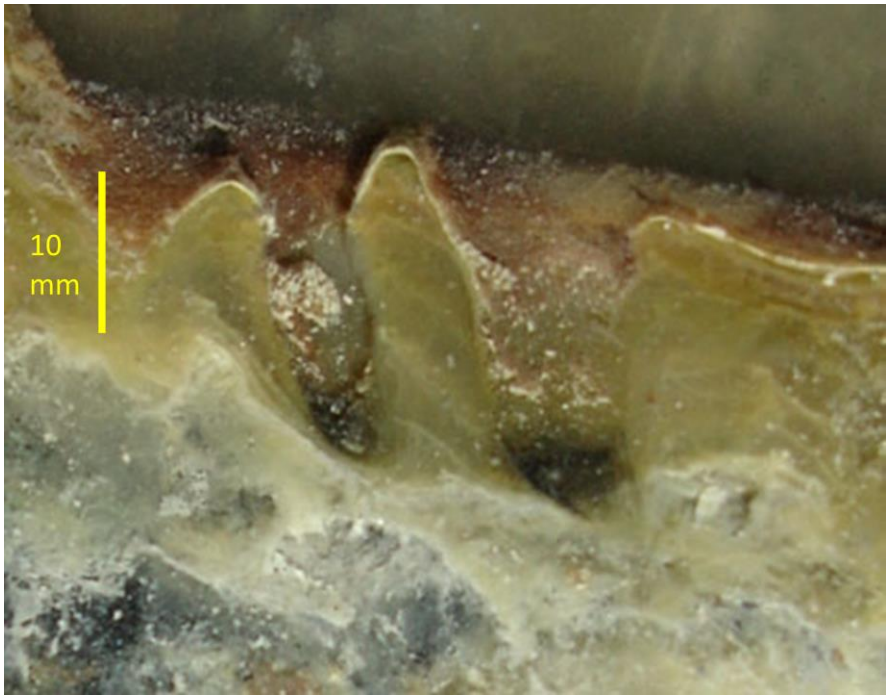

Figure 7. Vertical section of a honeycomb mat from the D4 sample station at Lake Fryxell showing strong colour stratification. Photo is courtesy of Ian Hawes.

2.1.3.2 Qualitative sampling

Mat samples for qualitative studies were retrieved by SCUBA diver from the "active layer" of the microbial mats at water depths 8.9, 9.4, 9.5 and 10.9 m, along the same transect used for quantitative sampling (and, as far as possible, at similar depths). Mat active layers are characterised by high densities of photosynthetic pigments, mat cohesiveness and ease of separation from the underlying layers of un-pigmented organic material (Hawes and Schwarz, 1999). These samples were carefully removed from the underlying materials and transferred into opaque polyethylene boxes with water-tight lids (while still underwater). To ensure that the acquired specimens were representatives of the sampling depths, replicates were obtained for each depth (Table 1). A total of 46 samples were obtained and were immediately photographed and analysed by bright-field microscopy at the lakeside laboratory.

Table 1. Acquired benthic microbial mat samples for specimen preservation

Depth (m)	Sample type (structure)	Quantity	Acquisition date
8.9	Pitted pinnacles	2 frozen (small) 4 embedded (small) 4 embedded (large)	22/11/2012
9.4	Pitted pinnacles	4 fixed (large) 7 frozen (small) 3 frozen (large)	27/11/2012
9.5	Honeycomb pinnacles	8 frozen 8 fixed 4 embedded	26/11/2012
10.9	Prostrate	2 frozen	28/11/2012

2.1.3.3 Preservation

Three different preservation methods were used to stabilise the mat structures so that they could be taken back to New Zealand for observation, comparison and analysis. A series of vertical cuts were made in the mat samples to allow cross sections of mat to be studied. The first set of samples were fixed in 4% (v/v) formaldehyde in phosphate buffered saline (PBS, 131 mM NaCl, 5.1 mM Na_2HPO_4, 1.56 mM KH_2PO_4, pH 7.2; Table A1.1 in Appendix 1) in 50 ml pottles which were sealed with parafilm. Secondly, an acrylamide embedding technique was employed as it was suspected that the mat integrity could be lost during transport of samples that were simply fixed. Samples were first fixed in 4% (v/v) formaldehyde (Table A1.2 in Appendix 1) for minimum of 24 h before being rinsed 3 times in filtered lake water. Each rinse was for a period of no less than 1 h. The samples were then infiltrated with 16% (w/v) acrylamide in PBS (Table A1.3 in Appendix 1) for a minimum of 24 h. Acrylamide polymerization was initiated with the addition of tetramethylethylenediamine and ammonium persulfate. Finally, a third set of samples were frozen in lake-water in plastic containers.

2.1.3.4 Photography and field microscopy

Field photography was conducted at Lake Fryxell, both within the lake and at the lakeside laboratory. Visible/optical microscopy of freshly collected material was carried out at Lake Fryxell with a Nikon binocular microscope and a Leica compound microscope.

2.2 Analysis in New Zealand

2.2.1 Pigment extraction and analysis

Samples were freeze dried and then ground to a fine powder and weighed aliquots were taken for various analyses. Chlorophylls and carotenoids were extracted from the weighed aliquots in 5 ml of 95% (v/v) acetone at 4°C for 24 h. Samples were then centrifuged at 3000 RPM for 15 min. Subsamples of the extract were then pipetted into a quartz cuvette and placed into an acetone-blanked Jasco scanning spectrophotometer. Absorbance spectra were then measured between 350 and 900 nm. A second series of extract subsamples were then prepared for fluorescence studies. An Agilent Technologies Cary Eclipse Fluorescence Spectrophotometer was used at excitation wavelengths of 405, 488, 561 and 633 nm to measure emission spectra beginning at 425, 508, 581 and 653 nm and running through to 900 nm. These excitation wavelengths were selected on the basis of known absorption peaks of photosynthetic pigments, and were matched to the available excitation wavelengths on the confocal microscope. Absorbance and fluorescence intensity were normalised on the basis of mat freeze-dried weight and after any required dilution factors, necessary where undiluted absorbance readings exceeded an optical density (OD) of 1.

Phycobilins were extracted from a second series of weighed aliquots using 5 ml 0.1 M tris(hydroxymethyl)aminomethane (Tris) buffer at pH 7.6. Extraction was aided by sonication for 25 seconds using a Misonix XL-2000 (15 watts output power) and extracts were then refrigerated at 4°C overnight. Samples were then also centrifuged at 3000 RPM for 15 min. Absorption of aqueous extracts was again scanned from 350 to 900 nm, though using a Cary 100 Bio UV-Vis Scanning spectrophotometer. Fluorescence emission of aqueous extracts was measured using excitation wavelengths 405, 488 and 550 nm. Again, these excitation wavelengths were selected on the basis of known absorption peaks of photosynthetic pigments, and were matched to the available excitation wavelengths of the confocal, or (in the case of 550 nm excitation) were sufficiently close to the necessary excitation laser. Absorbance and fluorescence intensity were again normalised to sample weight after corrections for dilution factors.

2.2.2 Confocal microscopy

Techniques were developed that used the differing fluorescence properties of different microorganisms to map their distribution using confocal laser scanning microscopy (CLSM). CLSM is an advanced form of epifluorescence microscopy that uses a laser beam to illuminate a specimen via the objective lens of the microscope. The objective lens collects fluorescence which is passed through a pinhole to eliminate out-of-focus light. Selection of specific excitation laser wavelengths permits the user to excite different types of substances, such as photosynthetic pigments for visualisation. It is also possible to use z-stacking: by accurately moving the microscope stage in the z-direction (depth). Z-stacking allows closely spaced optical sections to be collected through an object which can then be converted into a 3-dimensional model. The strategy employed approached the analysis through a series of systematic objectives:

i) Evaluation of the efficacy of the 3 preservation methods (fixed, embedded and frozen) in maintaining structure preservation and photosynthetic pigment brightness.
ii) Evaluation of the fluorescence properties of the different groups of constituent organisms in the microbial mat samples.
iii) Development of a robust analytical protocol using CLSM.
iv) Production of 3-D maps of photosynthetic organism distribution on the basis of fluorescent characteristics and visual identification

This process was supplemented as necessary using traditional bright-field and epifluorescence microscopy.

2.2.3 Fluorescence microscopy and photography

As limited facilities were available at the Lake Fryxell field site, most of the photography and microscopy was conducted back in New Zealand at the University of Canterbury. Frozen samples were analysed with a Leica epifluorescent microscope using a 63x NA 1.3 glycerol-immersion objective lens under blue (long pass), green and transmitted light emission filters. Photography was undertaken using a Leica DFC310 FX digital colour camera.

2.2.3.1 Sample preparation

Samples were imaged on the confocal microscope in 25 mm diameter Petri dishes whose base was a circular glass cover-slip. For frozen and fixed samples, this required preparation of a flat surface. Flat surfaces were produced from the polymerised acrylamide blocks using a razorblade, by hand. Flat surfaces for the frozen sections were prepared using a combination of hacksaw and razorblade. Fixed and embedded specimens were kept at 4°C when not in use. All frozen samples were maintained at -20°C when not in use.

2.2.3.2 Sample observations

Samples were examined with a Leica SP5 Confocal microscope using 10x NA 0.1 dry objective and a 20x NA 0.3 glycerol-immersion objective. Laser excitation wavelengths of 405, 488, 561 and 633 nm were used to excite the phycobiliproteins and chlorophylls with these corresponding to violet, blue, green and red light. Emission wavelengths, which can be set independently on the Leica SP5 confocal system, were varied from experiment to experiment as required. Concurrent transmitted light images were also recorded.

2.2.3.3 Spectral analyses and relative wavelength intensity

To characterise the organisms, the CLSM was initially used in wavelength scanning mode, known as λ (lambda) scanning mode. Lambda scanning allows the spectrum of fluorescent light emanating from the analysed specimen to be recorded. This requires a region of interest (ROI) in the image to be defined (manually, by the user) and this emission spectra is then automatically

calculated by the Leica software program. Six ROIs for each type of organism seen were collected, and then averaged for each treatment (frozen, fixed, fixed and embedded), were viewed in vertical-section and illuminated using 405, 488, 561 and 633 nm laser excitation. All samples were viewed under a x 20 NA 0.3 glycerol-immersion objective. Spectral image acquisition involved setting up a scan ranging from a wavelength 10 nm longer than the excitation laser, and finishing at 800 nm. The scan increment interval was set at 4 nm, and the detector integrated a band of 10 nm width. Each ROI was then scanned 3 times and an average recorded. As the purpose of the first experiment was to document the spectral "fingerprint" of each species group, all collected data was normalised to 100%. The relative wavelength intensity experiments involved comparing emission intensity between preservative treatments. All image acquisition settings on the confocal microscope were kept identical and the data was not normalised.

2.2.3.4 Investigations of the structural organization of the mats

To map the distribution of cyanobacteria and diatoms within the embedded samples, three replicates, both of honeycomb and pinnacle were viewed in vertical section using 633 nm laser excitation. All samples were viewed under a 10x NA 0.1 dry objective lens. Image acquisition also involved setting up three fluorescence detection windows (photon multiplier tubes) to differentiate between diatoms and cyanobacteria. Based on developmental experiments, the fluorescent waveband widths were set at 633 nm (to collect reflections), and between approximately 650 – 679 nm (for cyanobacteria) and 680 - 700 nm (for diatoms). A fourth window was used to collect transmitted light. For each defined field, a z-stack of optical sections, each 10 µm thick was recorded. Depths from which fluorescence was collected varied on the basis sample size. All individual images were then digitally assembled by the Leica software into a summa projection known as a tile scan. Tilescanning permits the user to automatically assemble an image from a series of smaller images by digitally combining them. A scan area is defined by selecting two opposite positions within a sample, which define the perimeter of where the scan will be undertaken.

3. Results

3.1 Physical properties of Lake Fryxell

Both pH and temperature varied little between stations (pH 7.4 to 7.6 and 2.6 to 2.8 °C respectively). In contrast, conductivity increased steadily with depth, from 5.24 mS/cm at D1 to 8.18 mS/cm at D9, confirming that the stations lay in the salinity-stabilised part of the water column. Within this density gradient, dissolved oxygen and irradiance both decreased with depth. Water overlying D1 and D2 had oxygen concentrations of >18 mg/L, (which is above oxygen saturation in freshwater at 0°C; 14.6 mg/L), falling below saturation at D3 and then falling steadily to reach anoxia between D6 and D7, at approximately 10.5 metres. Based on oxygen concentration, the transect could be divided into 3 zones, the hyperoxic zone (stations D1-D3); the hypoxic zone (stations D4 to D6) and the anoxic zone (stations D7-D9). Divers also reported sulfide becoming detectable by smell through the rubber of the dive masks from D7 onwards. Irradiance had declined to 0.8% of surface-incident value by D1 and D2, diminishing continually with increasing depth to 0.04% at D9 (Figure 8).

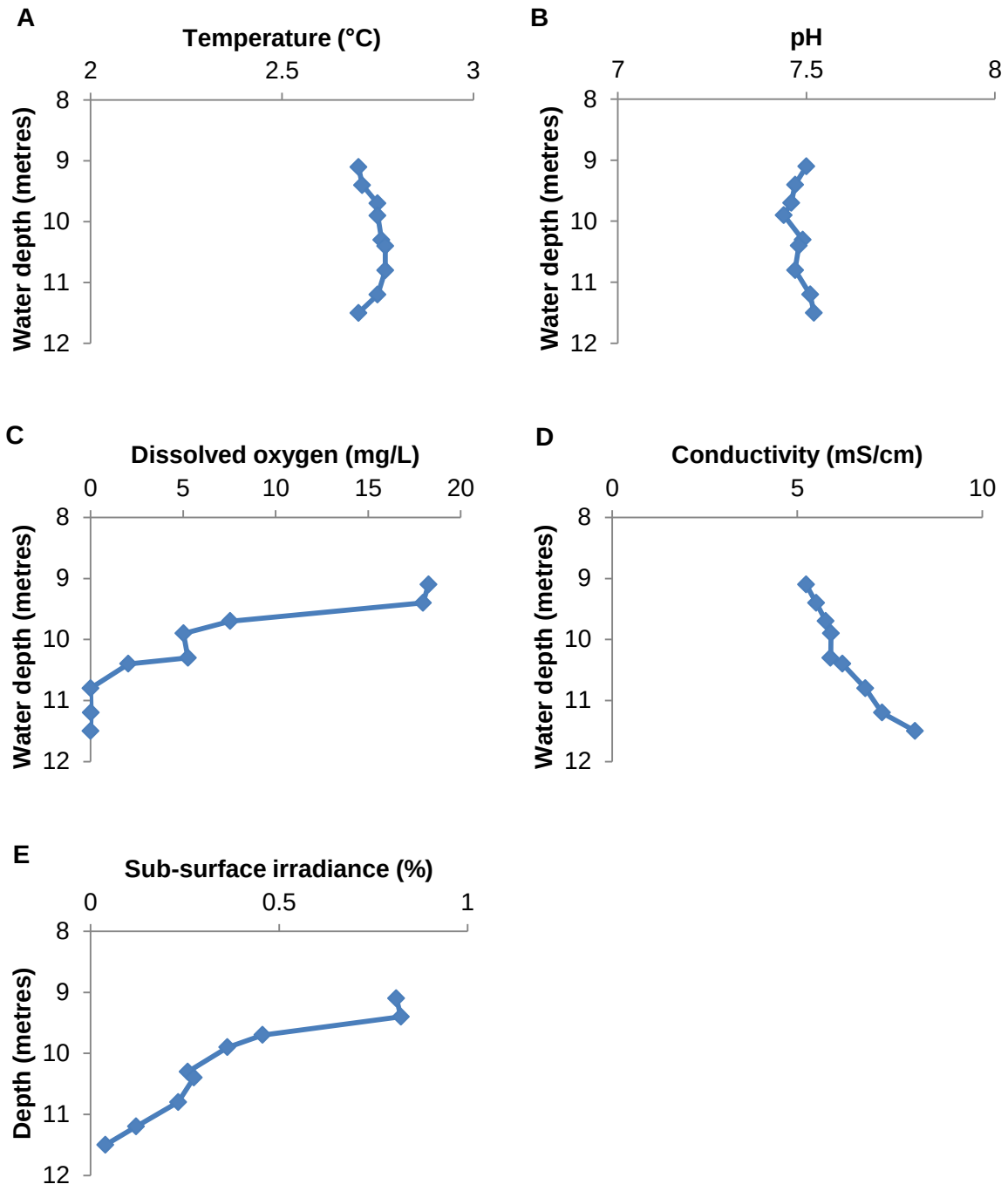

Figure 8. Physical properties of the sampling stations at different depths in Lake Fryxell. Each point on the graphs represents 1 of the 9 sampling stations.

- **A:** Temperature
- **B:** pH
- **C:** Dissolved oxygen
- **D:** Conductivity
- **E:** Sub-surface irradiance

3.2 Mat morphologies

Microbial mat communities were present along the entire transect, and displayed changes in colour and morphology with depth. Three main types of mat could be recognised; pinnacle, honeycomb and prostrate (Figure 9). The distribution of mat morphologies appeared to correlate with water column properties; pinnacle mats were only found in the hyperoxic zone (D1-D3), honeycomb mats predominated in the hypoxic zone (D4-D6), while prostrate mats were mainly located in the anoxic zone (D7-D9).

Pinnacles: Hyperoxic mats were characterised by numerous pinnacles up to 5 cm tall that tapered to a delicate apex (Figure 9A). The pinnacles were pink and cuspate often having pits between the apices, which could be linked by narrow ridges in vertical cross section.

Honeycomb: Hypoxic mats possessed an overall orange-brown colouration interspersed with occasional cream-coloured patches. The honeycomb mats had few, if any pinnacles. Instead, the mat had a rather flat surface, but also had regular pits of 10 to 20 mm depth (Figure 9B; Figure 10). The pits could be separated by flat mat, or could be sufficiently close to give a ridged, honeycomb appearance, for which the mat was named. Pits were often characterised by black staining at their bottoms. The honeycomb structures did not fit the Hofmann style classification in vertical section.

Prostrate: In the anoxic zone were prostrate mats, which were predominantly dark brown or green in colour, and lacked either pinnacles or pits in vertical section (Figure 9C). The prostrate morphology has also been described by Hofmann (1969) for Precambrian stromatolites.

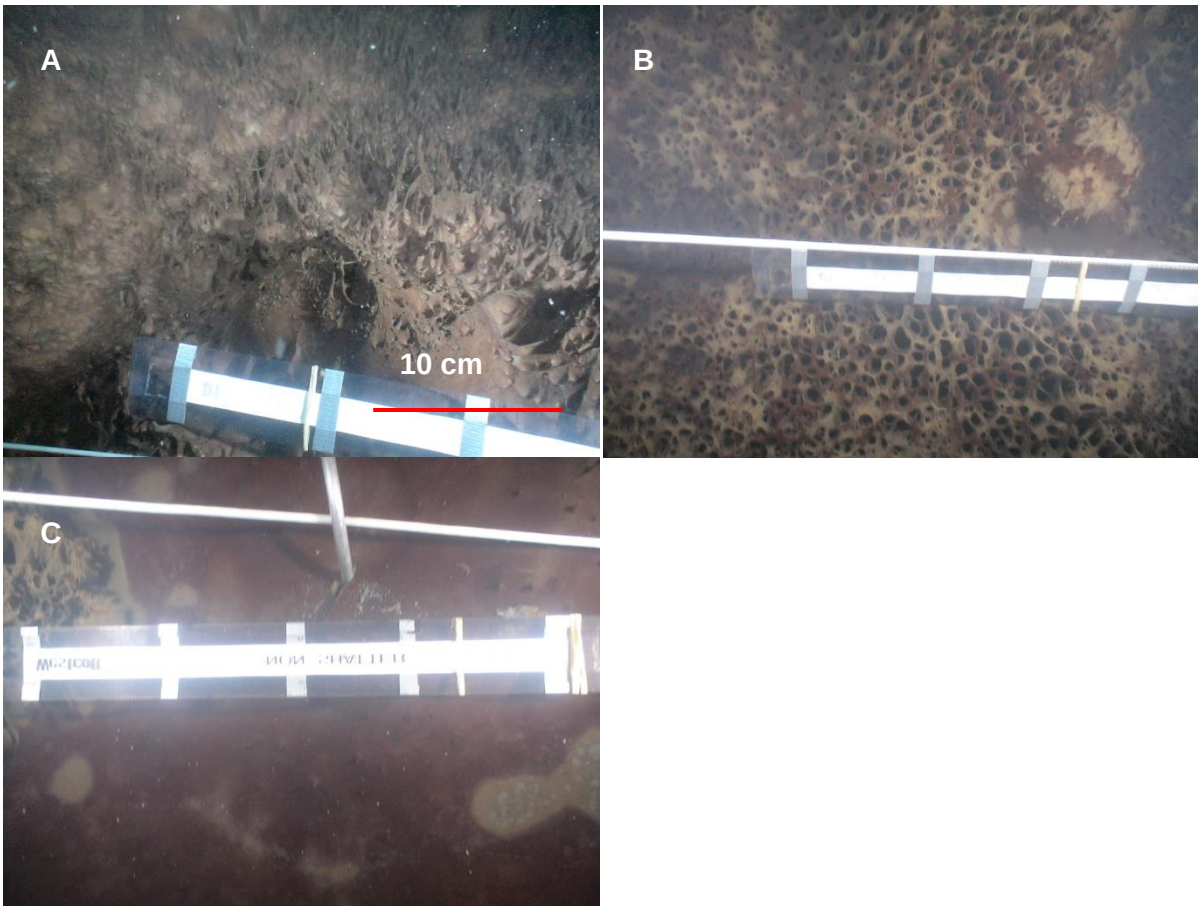

Figure 9. The 3 main microbial mat morphologies/types taken at Lake Fryxell. Photographs are courtesy of Ian Hawes. Scale bar in A = 10 cm for each image.

- **A** Pinnacle mats.
- **B** Honeycomb mats.
- **C** Prostrate mats.

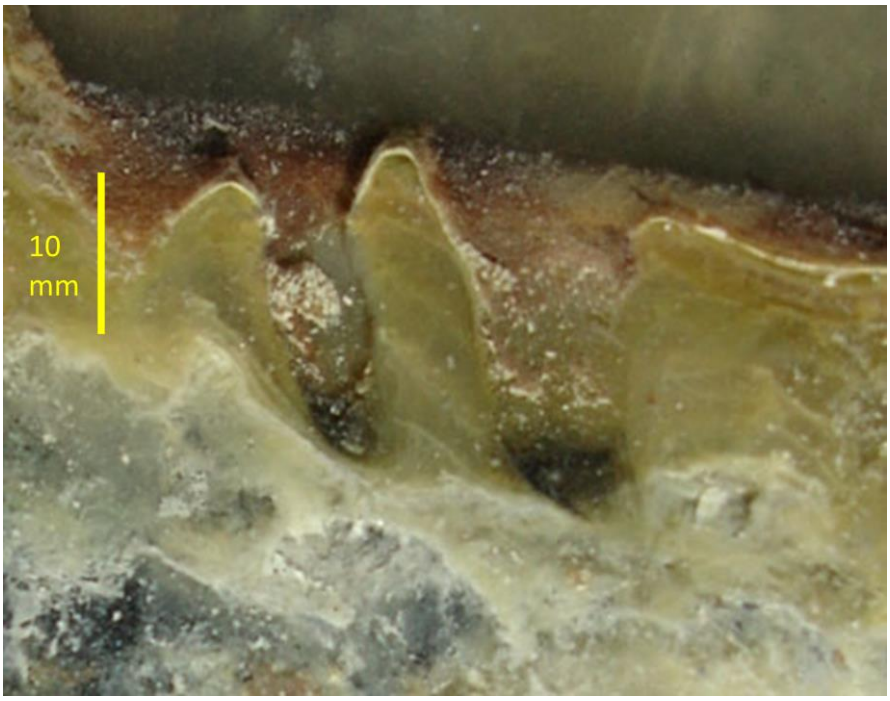

Figure 10. Vertical section of honeycomb microbial mat from D4 station at Lake Fryxell. Photo is courtesy of Ian Hawes.

3.3 Pigment analysis

As a first approach to characterising the mat samples from all transect stations, the absorption spectra were measured for acetone and aqueous extracts of hydrophobic and hydrophilic pigments respectively. The goal was to determine if pigment complements varied with transect site and mat morphology. In both acetone and aqueous pigment extractions, quantitative and qualitative differences between sample spectra were evident. Scanning spectrofluorometry was used to further examine shifts in pigment content with depth in the lake and provided similar data interpretations to the absorbance peaks.

3.3.1 Acetone extracts

3.3.1.1 Scanning spectrophotometry

Acetone extracts of hydrophobic pigments from all stations possessed a distinctive absorbance peak between 660 and 670 nm and a second, broader absorption peak from 350 nm to approximately 500 nm. Beginning at D5, a third distinct absorbance peak was detected at approximately 750 nm (Figure 11). These absorbance peaks corresponded to the changes in the oxygen regime, so all stations were divided into 3 main zones – A (hyperoxic, D1-D3), B (D5-D6, hypoxic) and C (D7-D9, anoxic). D4 was also located in the hypoxic zone, but the colour stratification (Figure 10) warranted it being classified separately (Figure 11D).

Based on published pigment absorption spectra (Frigaard *et al.,* 1996), the 660-670 nm peak region was likely due to one of several chlorophylls or bacteriochlorophylls. Traditionally absorption of acetone extracts at 670 nm is taken as a proxy for chlorophyll-a content. However, the only pigment likely to be contributing to the 750 nm peak is bacteriochlorophyll-a. This pigment is typically found in green sulfur bacteria, a group that also contains bacteriochlorophyll-c, which has an absorption maximum at 670 nm (Gerola and Olson, 1986; Frigaard *et al.,* 1997). Thus the size of the 670 nm absorption peak (Figure 12) could not be specifically related to any one pigment, and from D5 downwards is likely to include substantial contributions from bacteriochlorophyll-a.

The broad absorbance peak in the 400-500 nm band region may include contributions from carotenoids and chlorophylls (Vermaas, 1998). While the obvious change in the spectral shape through the transect sites indicates a shift in pigment composition and concentration along the transect, as with the 667 nm peak, it is not possible to ascribe this to specific pigment changes. The broad absorbance band between 400 and 500 nm generally increased in height with depth, from approximately 44 g^{-1} to a maximum absorbance of 160 g^{-1} by D7 before decreasing abruptly to approximately 30 g^{-1} by stations D8 and D9. The 750 nm peak was not present from D1 to D4, but was detected at D5 and increased to its highest absorption at D7. The 660-670 nm absorbance band peaked at 44 g^{-1} in the hyperoxic zone (D1-D3), increasing to 50 g-1 by D4, then decreased to approximately 20 g^{-1} before suddenly increasing again to a maximum of 55 g^{-1} in the anoxic zone. The differing ratios of 660:480 and 660:750 indicated increasing changes in carotenoid composition, combined with declining biomass of chlorophyll-a with depth, and a deep maximum of bacteriochlorophyll-a at D7 (Figures 11 and 12).

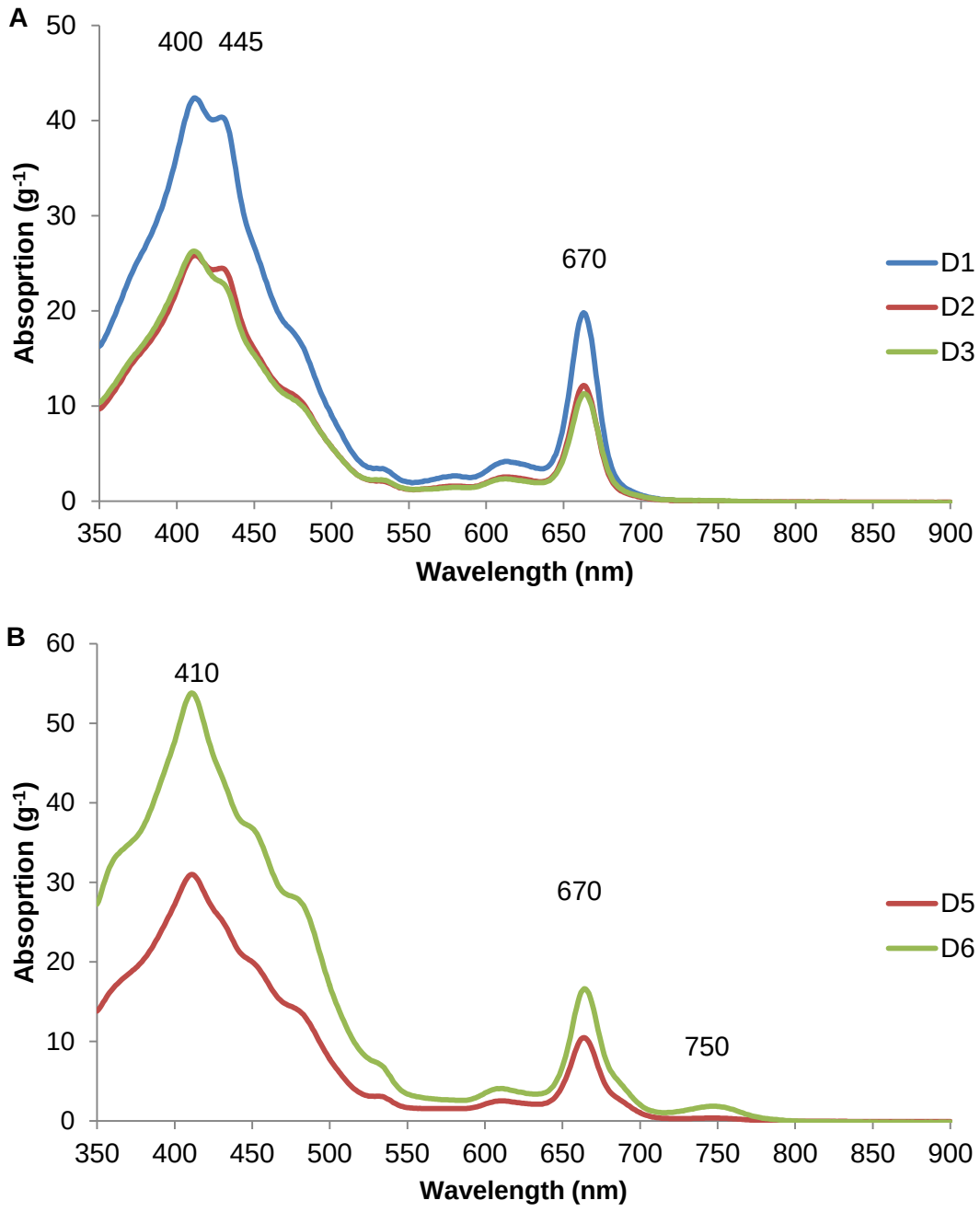

(Figure 11 continued over page)

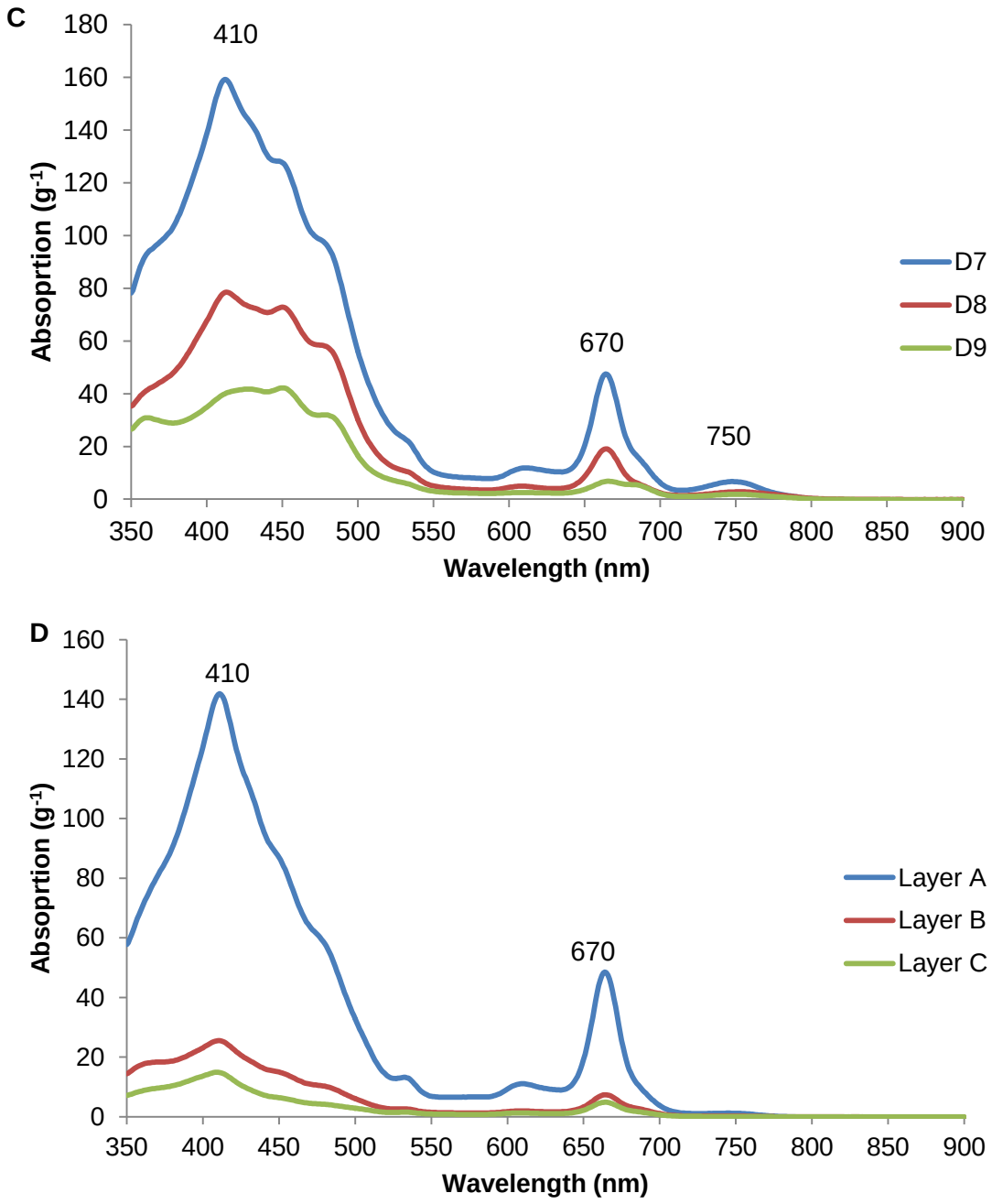

Figure 11. Mean absorption spectra (per gram) for acetone extracts of microbial mats from Lake Fryxell. Numbers above peaks indicate the wavelength of the absorption peak.

- **A** Samples from the hyperoxic zone (stations D1 to D3).
- **B** Hypoxic zone samples (stations D5 andD6).
- **C** Anoxic zone samples (stations D7-D9).
- **D** The 3 layers from D4 samples at the top of the hypoxic zone (A to C).
- All stations are a mean of 3-4 replicates.

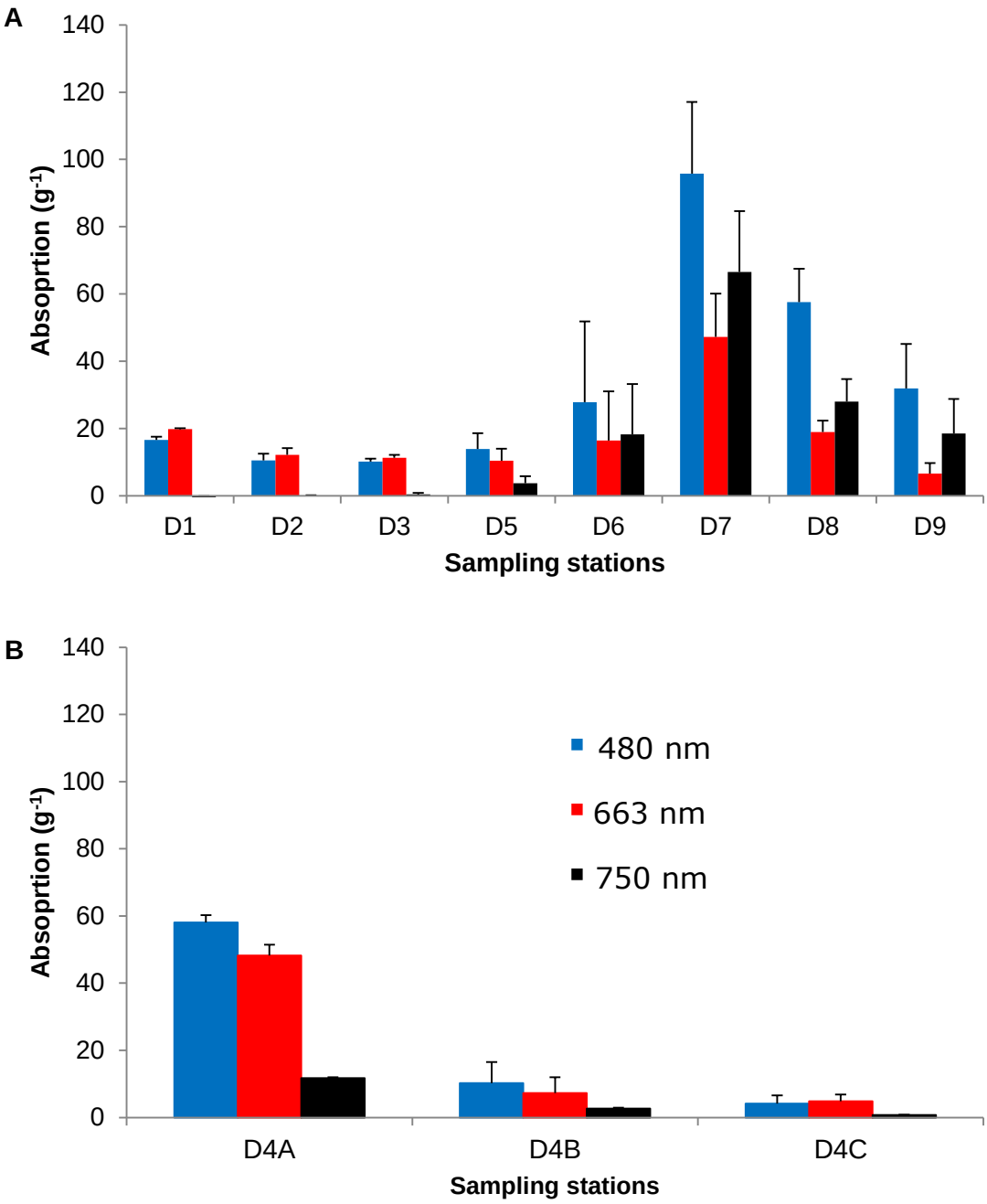

Figure 12. Mean absorption (per gram) for acetone extracts of microbial mats from Lake Fryxell, measured at key wavelengths (480, 663 and 750 nm). Values shown as mean ± S.E. (n= 4).

- **A** Stations D1 to D3, and D4 to D9.
- **B** The three different components of the D4 station (D4A, D4B and D4C).

3.3.1.2 Scanning spectrofluorometry

The fluorescence emission spectra for the acetone extracts were measured using multiple excitation wavelengths. A single fluorescence peak was evident at 670 nm, with a distinct shoulder at 720 nm, for all excitation wavelengths. Figure 13 shows example spectra from each of the defined oxygen zones. The ratio of 670:720 nm emissions in the acetone extracts did not change with sample origin and indicated either that only one pigment was likely present, or that a single pigment dominated the sample. All stations displayed this peak, which gradually decreased with depth, with the exception of D7 which displayed the highest peak intensity of all the stations, as with absorbance at 633 nm excitation (Figure 14). The emission spectra of chlorophyll-a and bacteriochlorophyll-c are similar (Frigaard *et al.,* 1996), and the bimodal appearance of Figure 12 is again consistent with a declining biomass of chlorophyll-a with depth, and a deep maximum of bacteriochlorophyll-c centred on D7. No bacteriochlorophyll-a peak was detected, probably because the excitation wavelengths were poorly absorbed by this pigment or it was only present in trace amounts. It would have been expected beyond 750 nm.

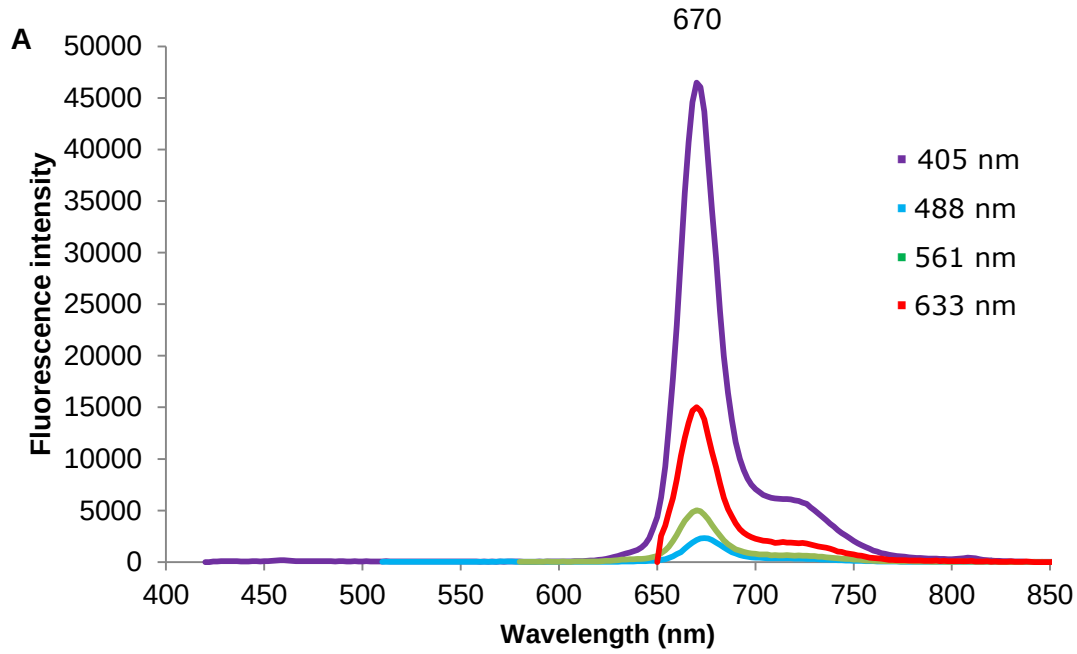

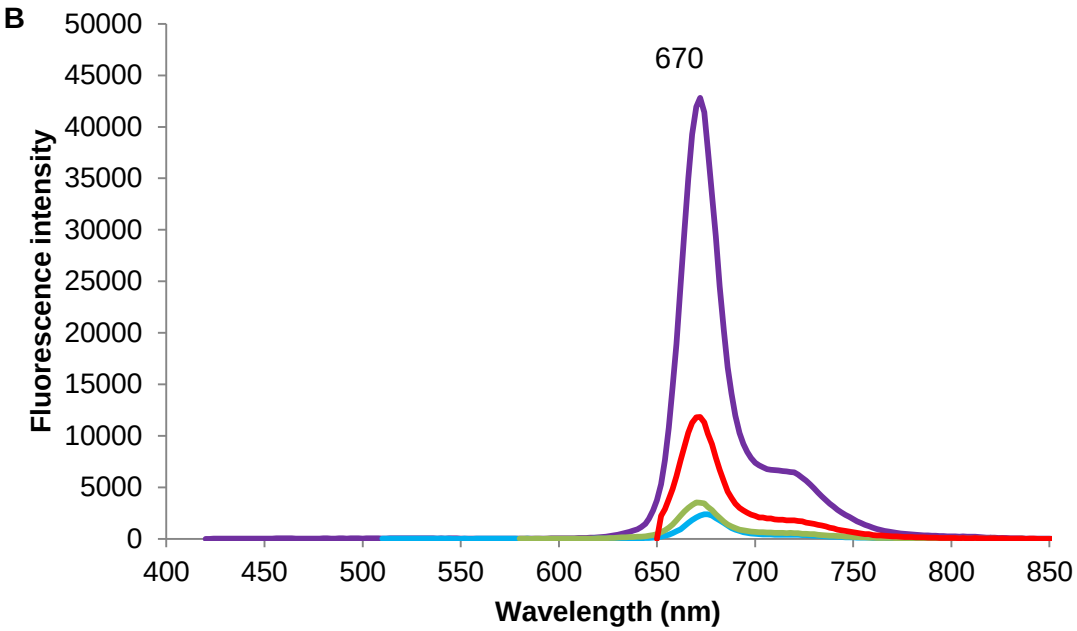

(Figure 13 continued over page)

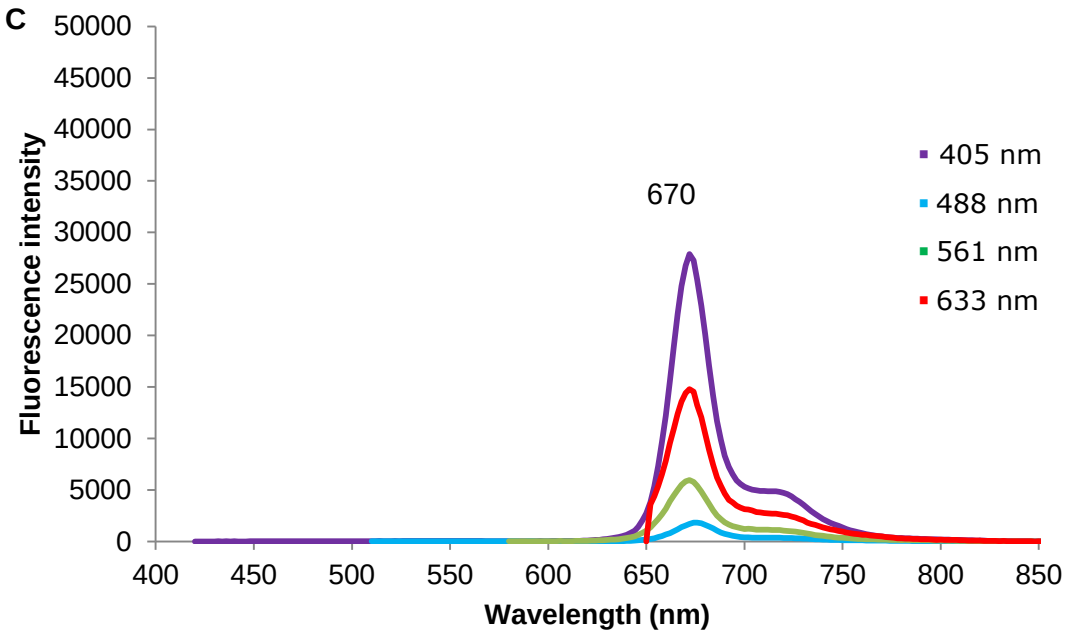

Figure 13. Emission spectra of microbial mat samples from Lake Fryxell, measured at 4 different excitation wavelengths (405, 488, 561 and 633 nm). Spectra are averages of 3-4 replicate runs. Numbers above peaks indicate the wavelength of the emission peak.

- **A** Station D2 (hyperoxic).
- **B** Station D5 (hypoxic).
- **C** Station D8 (anoxic).

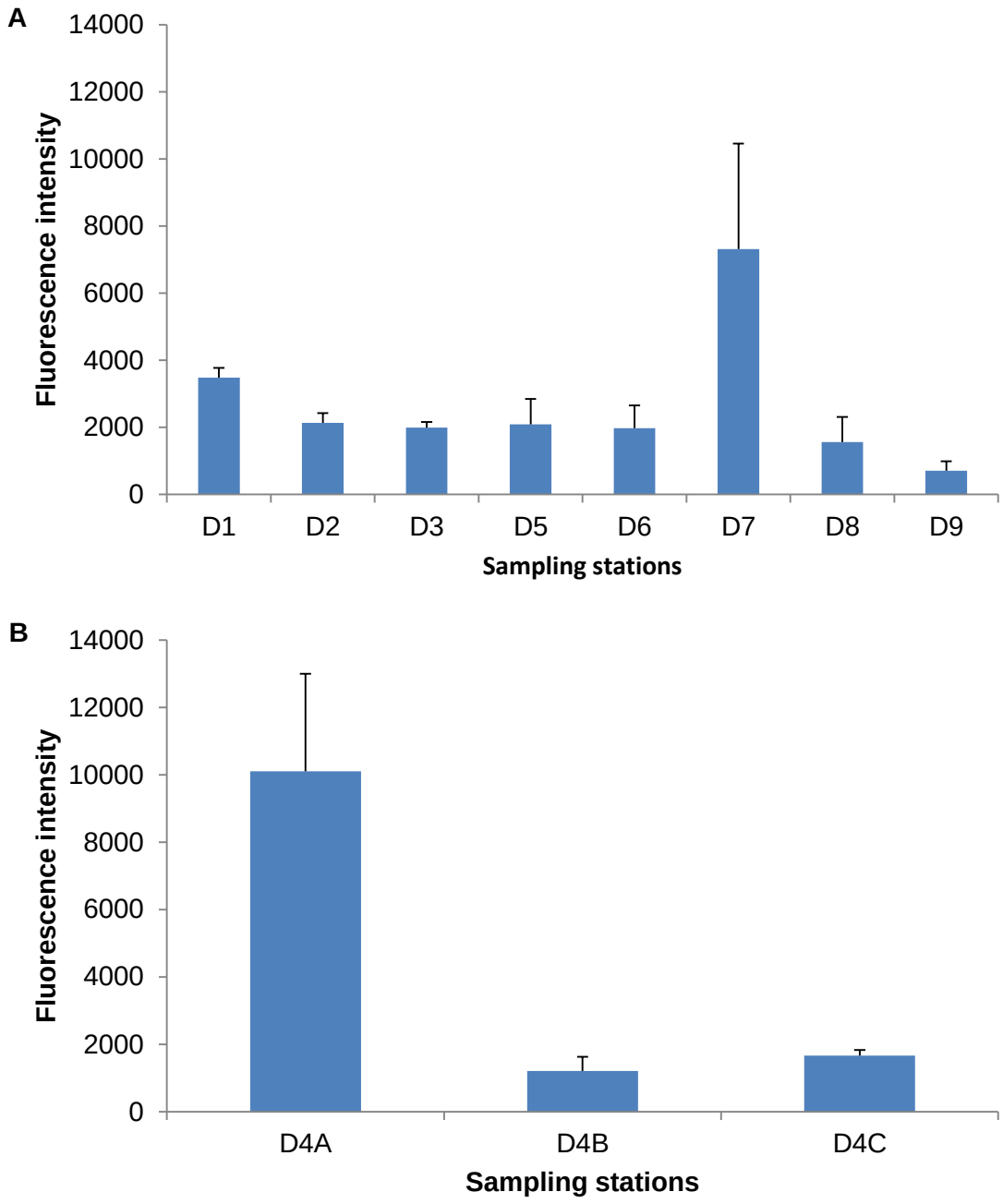

Figure 14. Mean fluorescence intensity at the 670 nm peak using 488 nm excitation for acetone extracts of microbial mats from all 9 sampling stations. Values shown as mean ± S.E. (n= 4).

- **A** Stations D1 - D3 and D5 - D9 from the transect.
- **B** The three different extracts from the D4 station.

3.3.2 Aqueous extracts

3.3.2.1 Scanning spectrophotometry

Absorbance spectra of aqueous extracts from the hyperoxic zone showed a rising trend with decreasing wavelengths, overlain on which were at least two distinct peaks at 550 nm and 660 nm (Figure 15A). This rising trend was seen in all samples and was interpreted as a result of a rising baseline due to the absorption properties of the wide range of organic materials extracted with the aqueous medium.

The absorbance peak at 550 nm is consistent with the absorbance region for phycoerythrin, a red pigment that is part of the light harvesting apparatus of many cyanobacteria (Rowan, 1989). Phycoerythrin was present at stations D1 to D3, decreasing in relative absorption from 1.21 g^{-1} to 0.59 g^{-1}, but was virtually absent from all deeper stations (Figures 15 and 16). A trace of phycoerythrin was detected in the sample from D4, but only in the layer A (Figure 15). This was consistent with the pink colouration of the mats at sites D1 to D3, and the gradual shift to a green or brown colour at greater depth. To estimate the size of the phycoerythrin peak, a method had to be developed to remove the rising baseline. This was accomplished by designating a start and end for the phycoerythrin peak region as 480 and 600 nm, and calculating a "baseline" over that waveband as a straight line between absorption at these two wavelengths. Calculating the height of the 550 nm absorption peak above this line allowed the relative size of the phycoerythrin peak to be estimated (Figure 16). The calculation returned slight negative values from station D5 and beyond, suggesting that the method was not perfect, but the most significant finding was the effective disappearance of phycoerythrin from stations deeper than D4 (i.e. > 9.9 m).

The second absorbance peak was detected at approximately 660 nm in samples from D1 through D7, and this is consistent with allophycocyanin, a blue-green light harvesting pigment also found in cyanobacteria (Barber *et al.*, 2003) (Figure 15). However, this pigment was only found in trace amounts. As the allophycocyanin peak was less distinct than phycoerythrin, its actual absorbance could not be reliably calculated. A third absorbance peak at 840 nm was also detected, but only in the D7 sample.

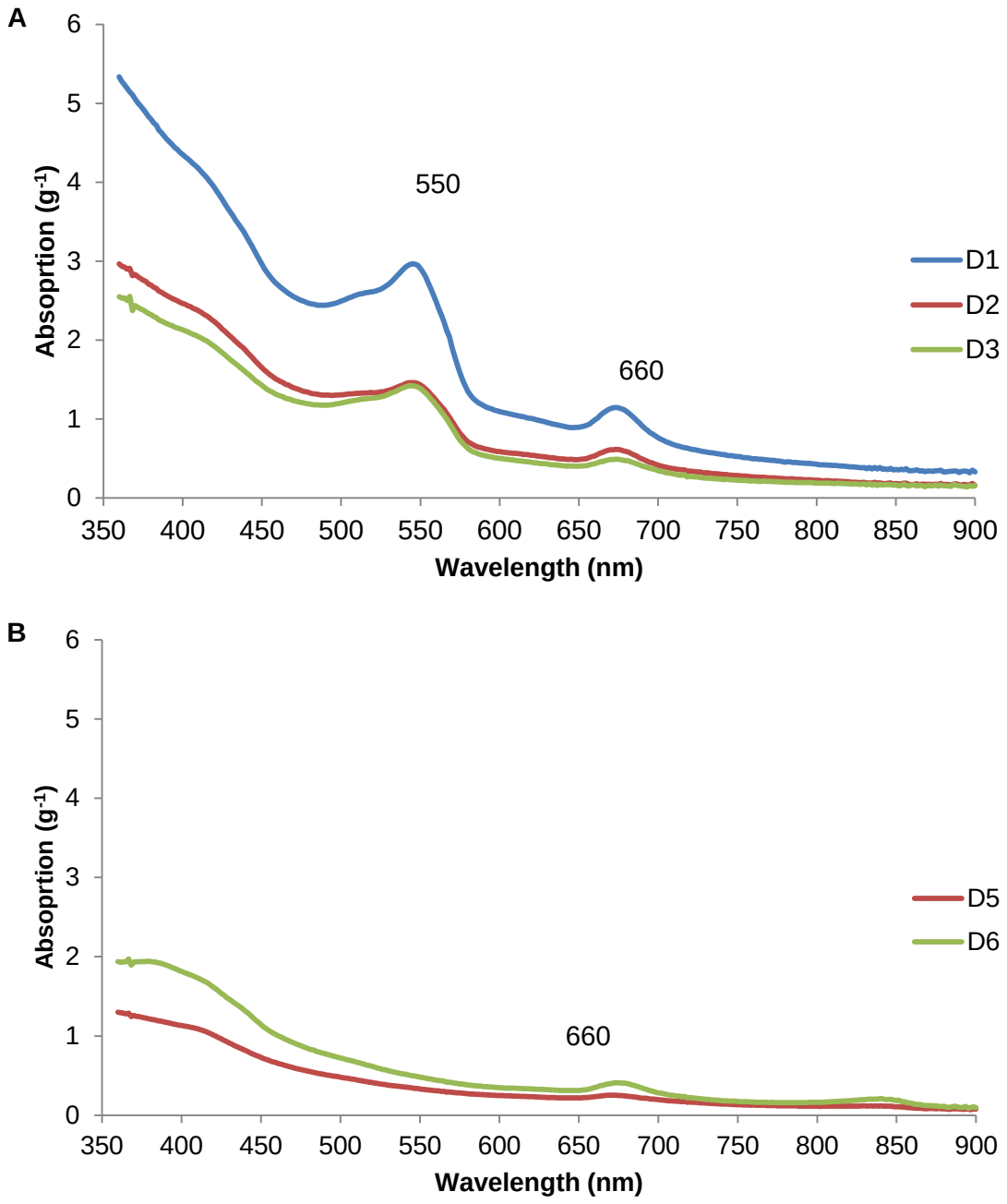

(Figure 15 continued over page)

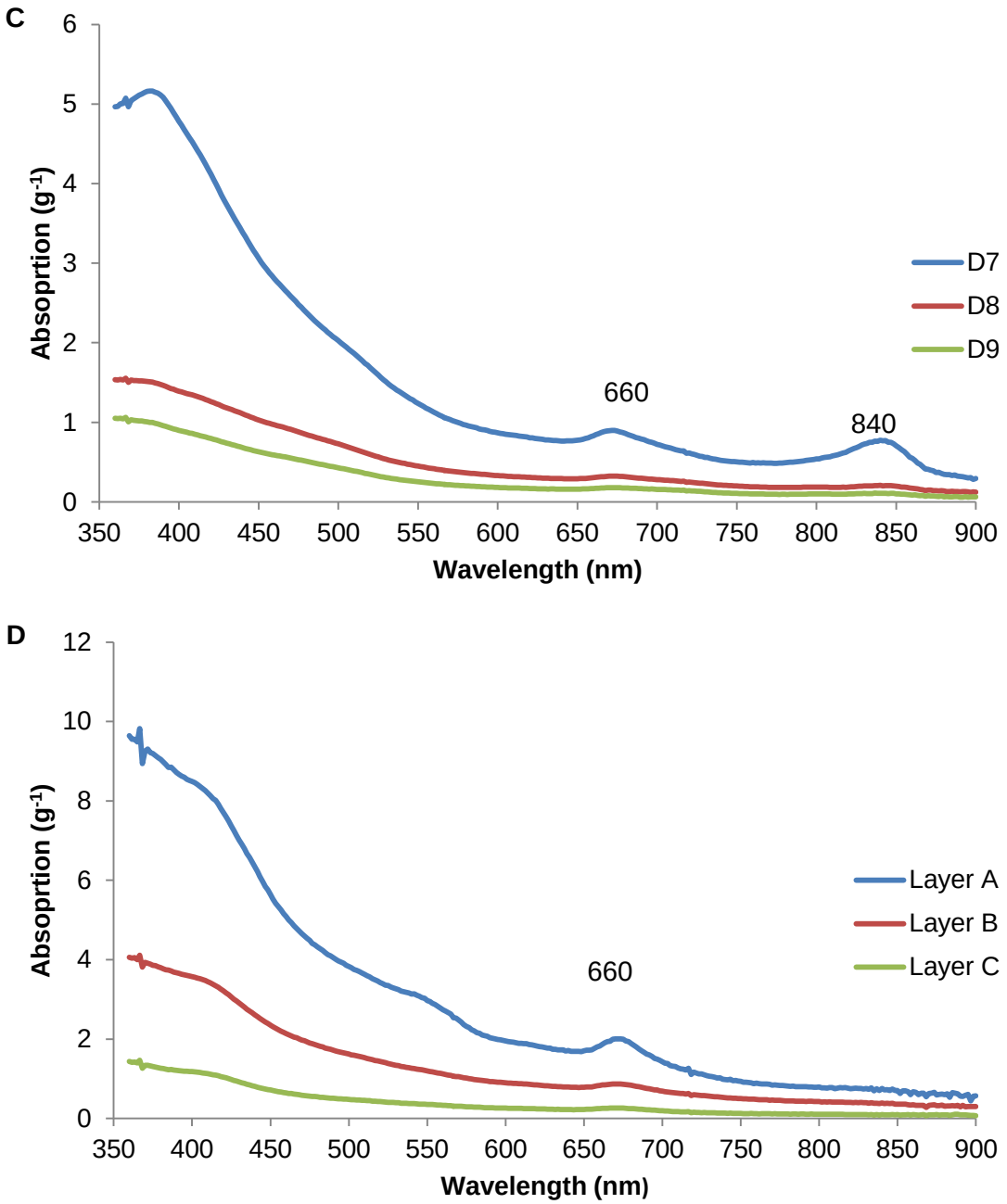

Figure 15. Mean absorption spectra (per gram) for aqueous extracts of microbial mat samples from Lake Fryxell. All stations are a mean of 3-4 replicates. Numbers above peaks indicate the wavelength of the absorption peak.

- **A** Samples from the hyperoxic zone (D1 to D3).
- **B** Hypoxic zone samples (D5 to D6).
- **C** Anoxic zone samples (D7 to D9).
- **D** The 3 layers from D4 samples (A to C).

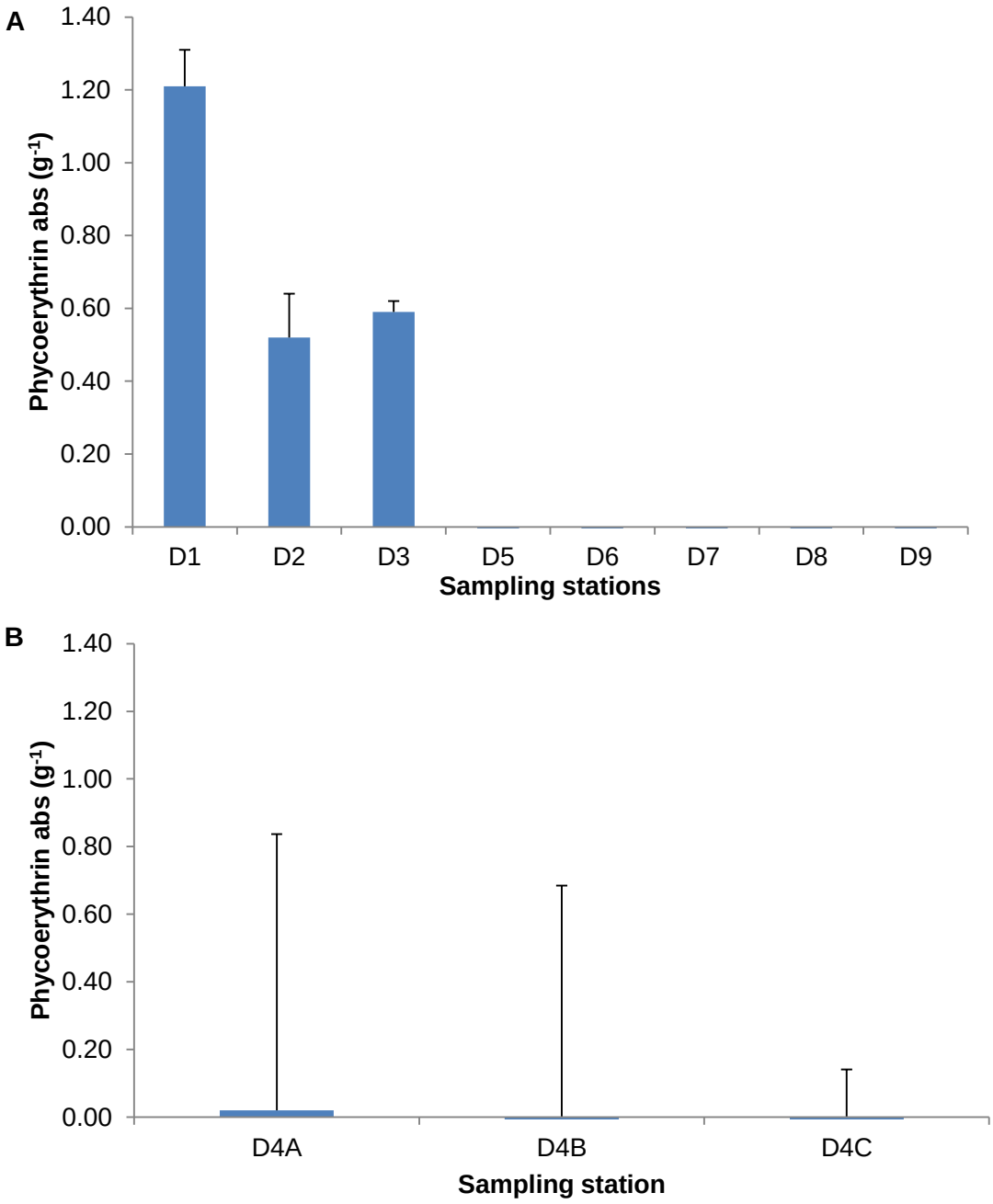

Figure 16. Mean absorption (per gram) for extracted phycoerythrin from microbial mat samples from Lake Fryxell, with shown values as mean ± S.E. (n= 4).

- **A** Stations D1 - D3 and D5 - D9 from the transect.
- **B** The three different extracts from the D4 station.

3.2.2.2 Scanning spectrofluorometry

Spectrofluorometry of aqueous extracts showed a distinct emission peak at approximately 580 nm, consistent for phycoerythrin. As with spectrophotometric detection, the pigment was present in stations D1 to D3 and the surface layer of D4 before disappearing beyond station D4 (Figures 17 and 18). An intense peak at 805 nm, generated by 405 nm excitation was not identified and was not seen at either 488 nm or 550 nm excitation (Figure 17). In the upper layer of D4, phycoerythrin was present (accounting for the red hue). Layers B and C were characterised by pale green and black-grey colouration, indicating a paucity of pigments. The emission peak at 670 nm was relatively consistent for allophycocyanin, which was only detected in trace amounts. However, the pigment persisted to greater depths than phycoerythrin – notably at D7 (Figure 18), and possibly at D8 (Figure 17) and was more evident in samples from D4A.

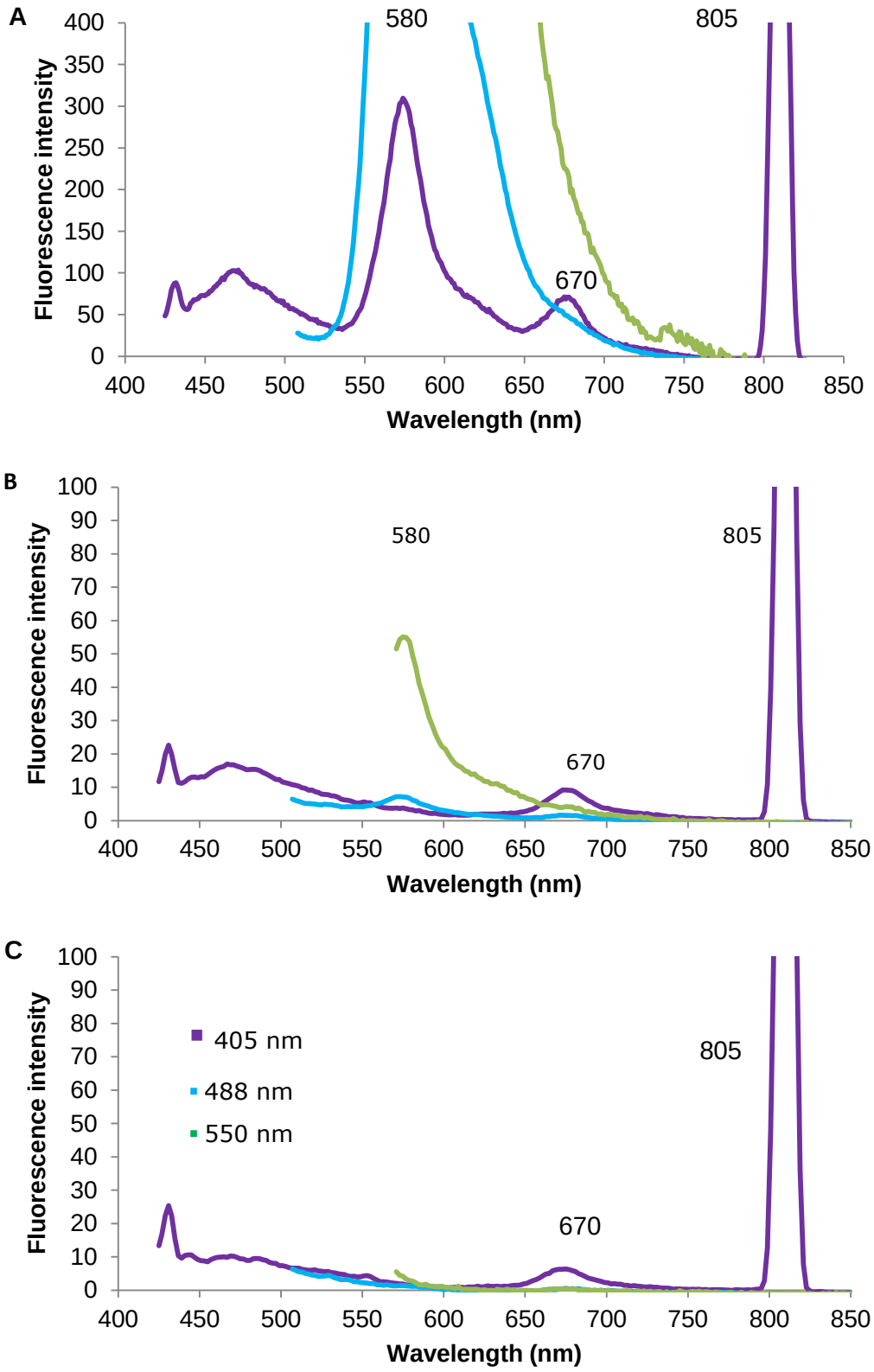

Figure 17. Emission spectra for aqueous extracts of microbial mat samples from different depths in Lake Fryxell, for 3 different excitation wavelengths. Spectra are averages of 3-4 replicates. Numbers above peaks indicate the wavelength of the emission peak. Spectra at A went off the scale due to high emission intensity.

- **A** Station D2 (hyperoxic).
- **B** Station D5 (hypoxic).
- **C** Station D8 (anoxic).

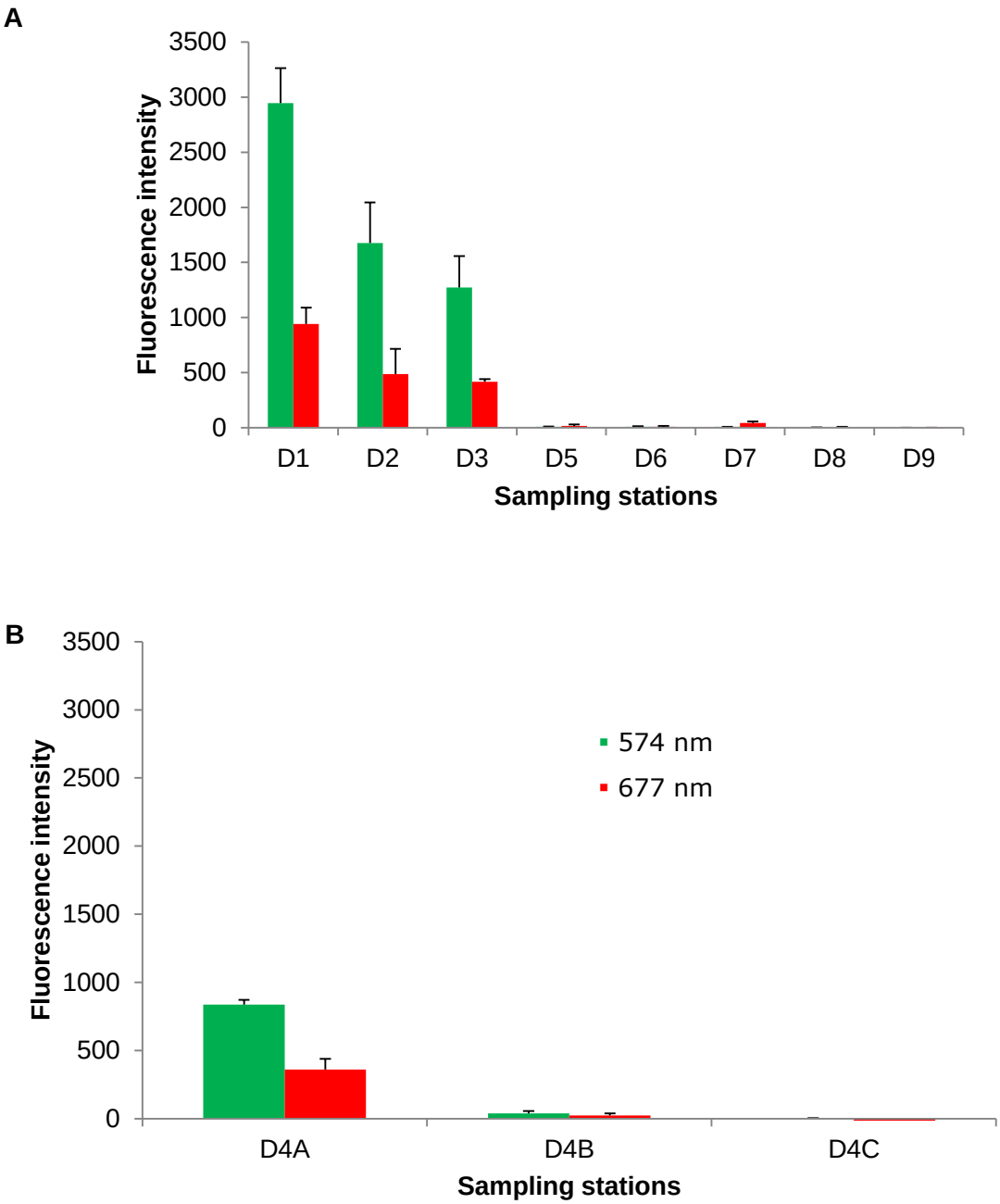

Figure 18. Mean fluorescence intensity for aqueous extracts of microbial mat samples from all 9 sampling stations at Lake Fryxell, using 488 nm excitation. Emission at 574 nm and 677 nm (multiplied by a factor of 10) are shown. Values are means ± S.E. (n= 4).

- **A** Stations D1 - D3 and D5 - D9 from the transect.
- **B** The three different extracts from the D4 station.

3.4 Summary of transect data

All collated data demonstrated that there was a strong, positive correspondence between mat morphology, pigment content and physical lake properties. Phycoerythrin was present in the pinnacle mats and in high oxygen environments, yet was either only present in trace amounts or was entirely absent in both the honeycomb and prostrate samples. Allophycocyanin was only detectable in smaller quantities than phycoerythrin, yet persisted at greater depths than the latter pigment. This coincided with an increase in bacteriochlorophyll-a, which begins in the honeycomb samples and positively correlates with decreased irradiance and oxygen concentration. Based on these findings, the Lake Fryxell transect could be broadly divided into 3 zones based on oxygen concentration, mat morphology and the presence of key pigments (Table 2).

Table 2. Summary of the distribution of mat morphologies, notable pigment transitions and oxygen zones at all nine sampling along the transect at Lake Fryxell.

	Sampling station								
	D1*	D2	D3*	D4*	D5	D6	D7*	D8	D9
Oxygenation	Hyperoxic			Hypoxic			Anoxic		
Mat morphology	Pinnacle			Honeycomb			Prostrate		
Phyocerythrin	Present			Absent					
Bacteriochlorophyll -a	Absent			Trace			Present		
Allophycocyanin	Present			Trace			Absent		

* Locations from which preserved samples were collected.

3.5 Confocal microscopy

3.5.1 Constituent mat components

Four key mat constituents were identified on the basis of fluorescent microscopy and lambda scanning; diatoms, at least 2 different types of cyanobacteria (possessing thick and thin trichomes respectively) and chlorophytes. Diatoms and thin trichome cyanobacteria were the two most frequently documented components of all observed mat samples. The chlorophytes and thick trichomes were far less numerous and only encountered occasionally. All samples analysed here had been preserved by freezing.

3.5.1.1 Diatoms

Figure 19 shows two example sets of images taken under bright field (Figures 19 A, B), and with green (Figures 19 C, D) and blue (Figures 19 E, F) excitation. The diatoms are visible under bright field, and were characterised by bright orange-red fluorescence under both blue and green excitation. While visible under green excitation, they were more easily discernable under blue excitation owing to the increased colour contrast with the other organisms which were mainly cyanobacteria. At least 3 different morphotypes were recognised which could be tentatively identified as *Muelleria peraustralis*, *Navicula gregaria* and *Diadesmis contenta*, based on Spaulding *et al.* (1997). Spectral imaging (Figure 19G) demonstrated that the diatoms emitted strongly at approximately 680 nm when stimulated with all the different excitation lasers, indicating the presence of a chlorophyll. This is likely to be chlorphyll-c. At 561 nm excitation, the absolute signal was very low compared to the other excitation wavelengths. Thus, the signal to noise ratio was lower and the background appeared to be relatively higher

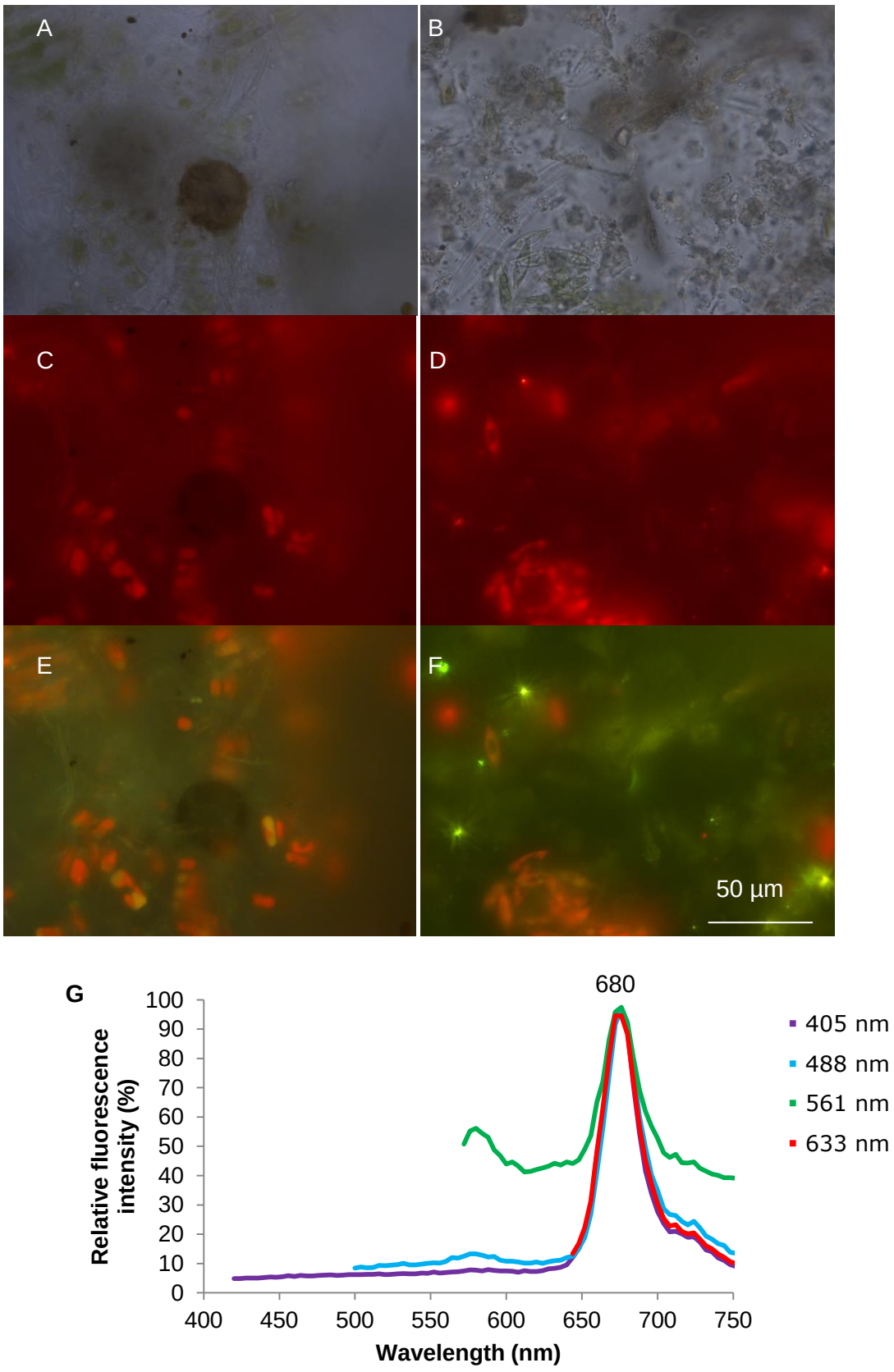

Figure 19. Diatoms in a frozen pinnacle mat sample viewed under bright field (A, B) and fluorescence microscopy, using green (C, D) and blue (E, F) excitation with suitable long-pass filters. Scale bar in F = 50 µm for all images. (G) - Normalised fluorescence emission spectra for diatoms obtained by confocal microscopy in λ mode, obtained using 4 different excitation lasers.

3.5.1.2 Cyanobacteria

a) Thin trichomes

The thin trichomes (< 10 µm thick) fluoresced strongly under both blue and green excitation, appearing bright yellow under blue excitation and red under green excitation (Figure 20 A-C). Two excitation peaks were documented during Lambda scanning, one at approximately 580 nm (yellow) and the other at 660 nm (red). The 580 nm peak confirmed the presence of phycoerythrin, while the 660 nm peak represents either an allophycocyanin or a chlorophyll pigment, or a combination of the two (Figure 20D). The 660 nm peak was clearly seen under 633 nm excitation due to a higher signal to noise ratio.

b) Thick trichomes

The thick trichomes (>10 µm thick) displayed similar fluorescent and spectral characteristics to their thinner counterparts (Figure 21A-C), although the peak at approximately 660 nm was more noticeable than in the thin trichomes (Figure 21D), possibly indicating a higher concentration of the allophycocyanin pigment in the observed samples.

3.5.1.3 Green algae (Chlorophytes)

All observed green algae displayed similar fluorescent properties to the diatoms – namely a strong emission peak at approximately 680 nm (Figure 22D), though green algae were not visible under green excitation. Under transmitted light, the green algae were visible as 5-lobed green circles encapsulated within an outer membrane (Figure 22A-C). At least two of these circles did not fluoresce under blue excitation, suggesting that both were moribund.

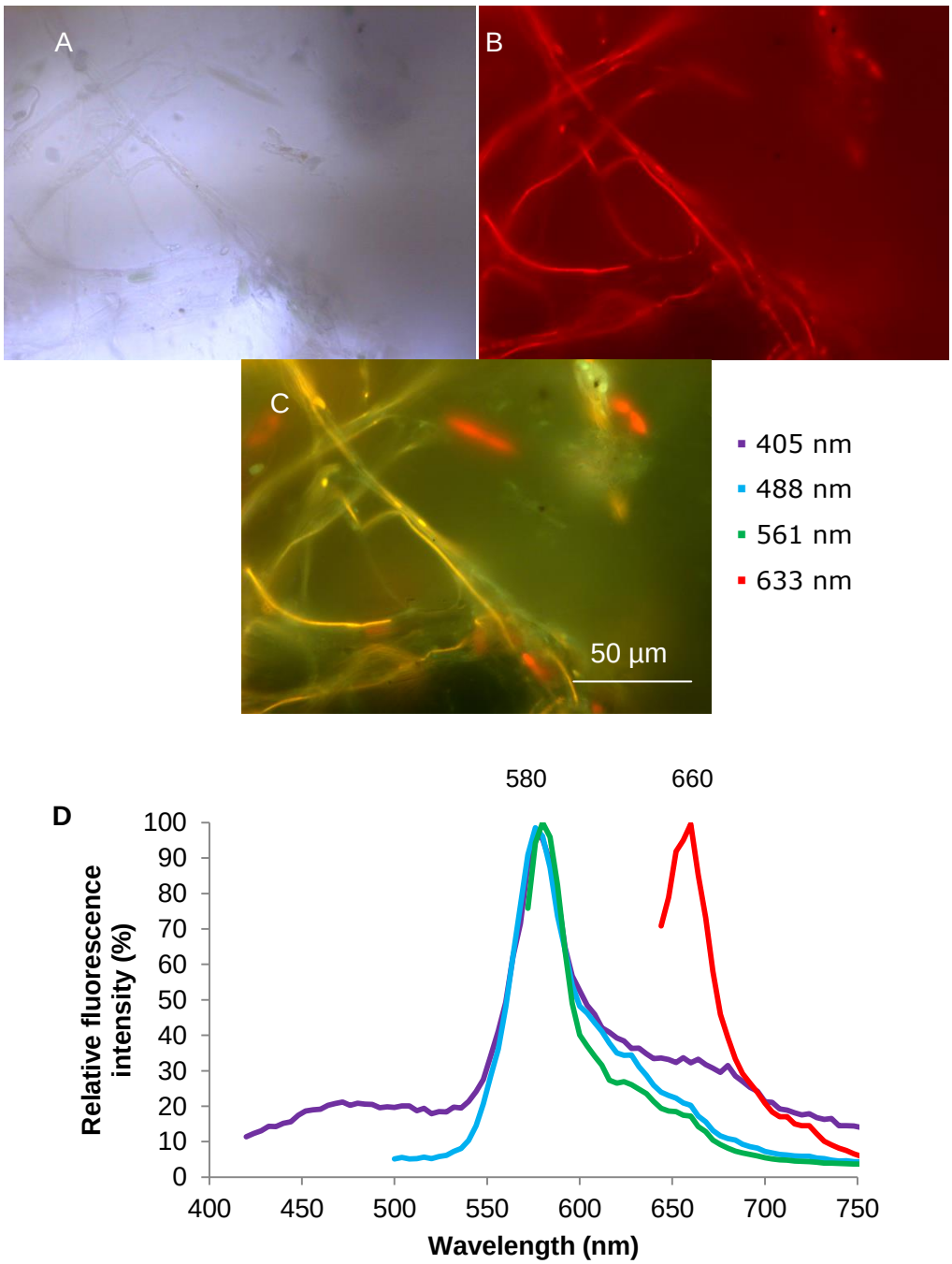

Figure 20. Thin trichomes in a frozen pinnacle mat sample viewed under bright field (A) and fluorescence microscopy, using green (B) and blue (C) excitation with suitable long-pass filters. Scale bar in F = 50 µm for all images. (D) - Normalised fluorescence emission spectra for thin trichomes obtained by confocal microscopy in λ mode, obtained using 4 different excitation lasers.

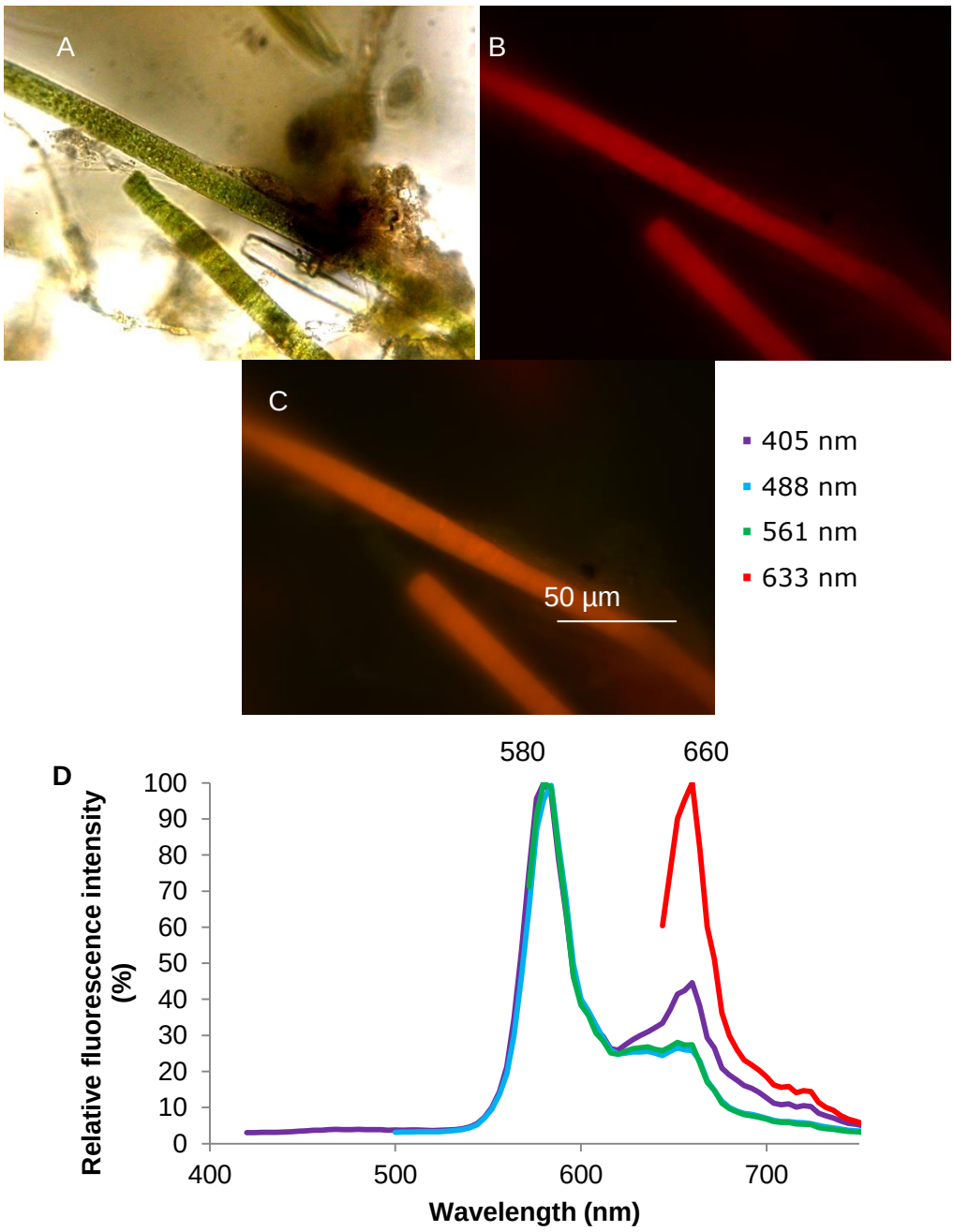

Figure 21. Thick trichomes in a frozen pinnacle mat sample viewed under bright field (A) and fluorescence microscopy, using green (B) and blue (C) excitation with suitable long-pass filters. Scale bar in F = 50 µm for all images. (D) - Normalised fluorescence emission spectra for thick trichomes obtained by confocal microscopy in λ mode, obtained using 4 different excitation lasers.

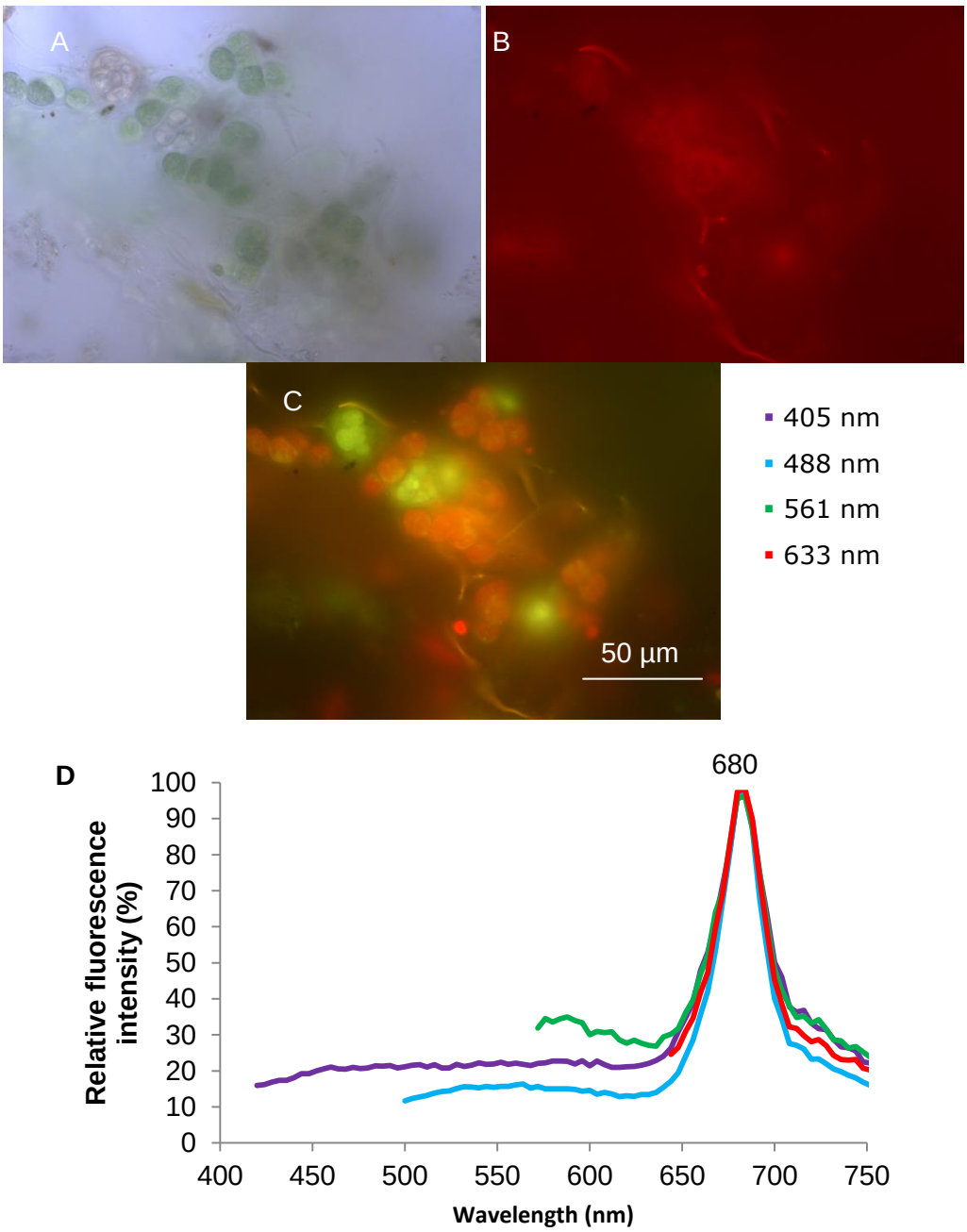

Figure 22. Green algae in a frozen pinnacle mat sample viewed under bright field (A) and fluorescence microscopy, using green (B) and blue (C) excitation with suitable long-pass filters. Scale bar in F = 50 µm for all images. (D) - Normalised fluorescence emission spectra for green algae obtained by confocal microscopy in λ mode, obtained using 4 different excitation lasers.

3.6 Effect of preservation treatments on structural integrity and fluorescence properties

3.6.1 Structural integrity

Of the 3 preservation techniques that were employed, the fixed samples suffered severe disruption during transport, such that structural integrity was lost (Figure 23A). However, individual components were well preserved and were still useful for some purposes, such as spectral emission studies. Only the frozen (Figure 23B) and embedded specimens (Figure 23C) were useful for structural studies. While frozen samples were well preserved, out-gassing was observed as bubbles within the matrix, causing potential changes to structural integrity. Acrylamide treatments were generally successful in retaining structure, though the cuspate peaks in the pinnacle mats suffered collapse due to acrylamide contraction during transport while wrapped in aluminium foil. Honeycomb mat specimens, which were transported in sealed plastic containers, were better preserved than the pinnacle mats in the acrylamide treatment.

3.6.2 Emission intensity

Documenting changes in emission intensity in confocal microscopy images of specimens preserved by the three different methods was a key component in assessing how the photosynthetic pigments were affected by the fixative and embedding process, and thus in determining how reliably different pigments and organisms could be detected during later analyses. Only the most numerically abundant fluorescing organisms - diatoms and thin cyanobacteria - were assessed.

Samples were scanned with the four different excitation lasers using a fixed set of imaging conditions for each laser so that direct comparisons might be map between the samples (Figure 24). Frozen samples consistently displayed the greatest emission intensity across all 4 laser excitations. They were at least 50% brighter on average than either fixed or embedded trichomes. The fixed samples and embedded samples were characterised by markedly lower emission intensities, indicating that both preservative techniques eliminated large

quantities of pigments from the samples. Phycobilins (phycoerythrin and possibly allophycocyanin) were particularly depleted, as indicated by the much higher 580 nm emission peak of frozen trichomes than that of preserved or embedded trichomes. In contrast, the chlorophyll containing cells (the diatoms) were relatively well preserved in all treatments. Individual emission peak shifts in the 670-680 nm band between 633 nm (Figure 24D) excitation and 405 nm (Figure 24A) laser excitations suggested that the fixative and embedding treatments may have altered the emissive properties of the photosynthetic pigments found in the fixed and embedded samples (Figure 24).

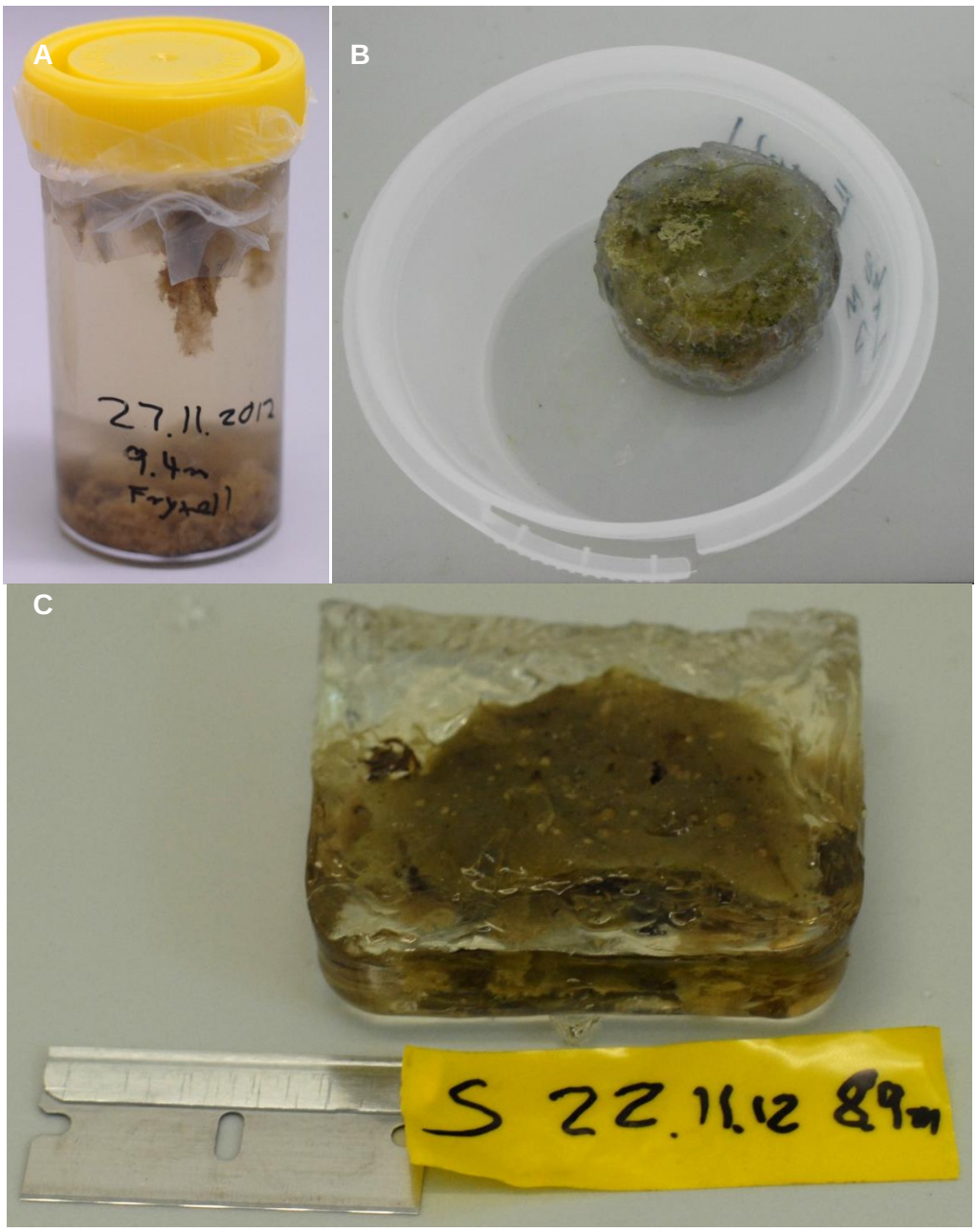

Figure 23. Preserved samples of microbial mats from Lake Fryxell after their return to New Zealand.

- **A** Fixed tissue
- **B** Frozen tissue.
- **C** Acrylamide embedded tissue.

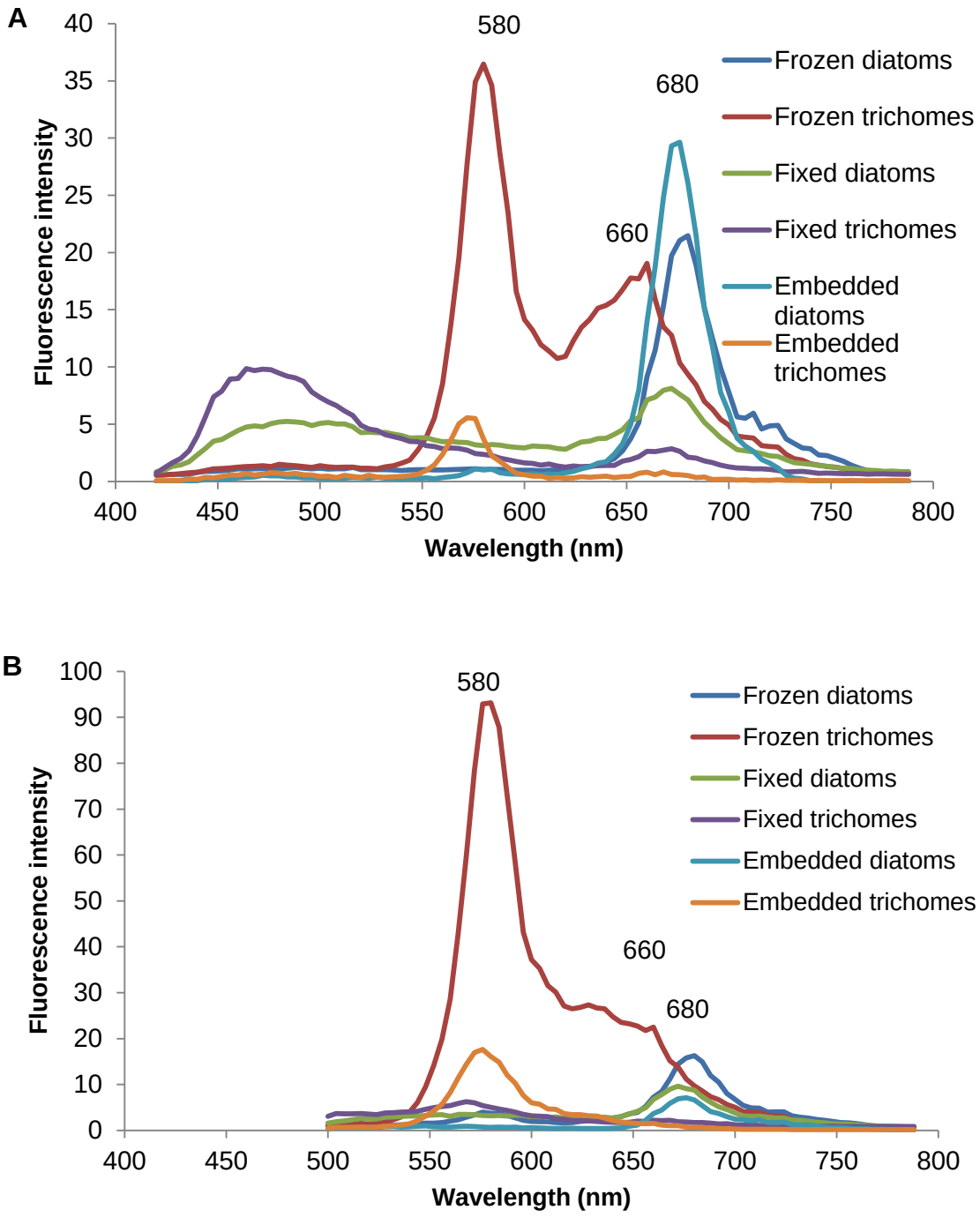

(Figure 24 continued over page)

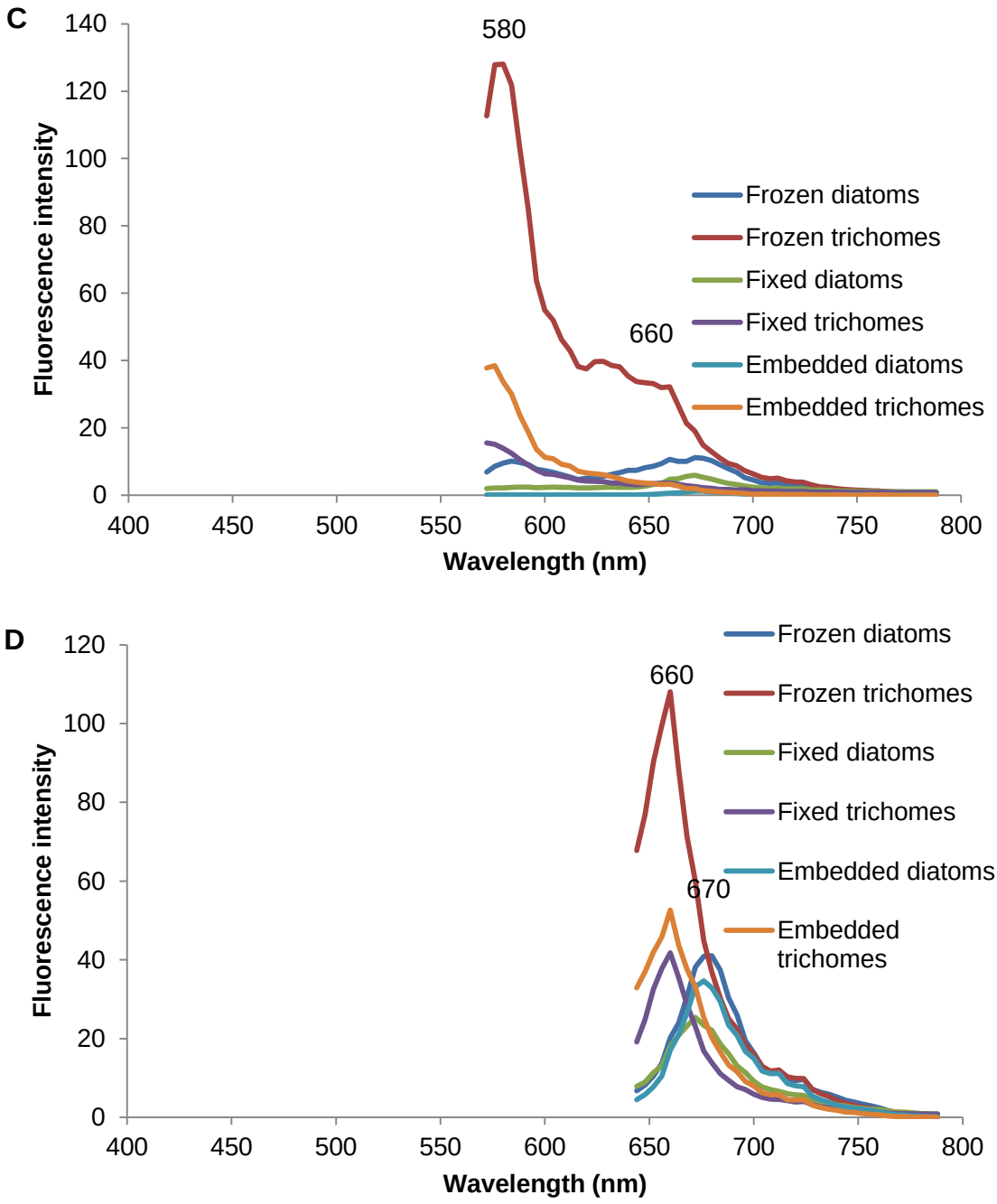

Figure 24. Fluorescent emission spectra of cyanobacterial trichomes and diatoms from microbial mat samples from Lake Fryxell, preserved in different ways (frozen, fixed and embedded). Samples are averages of 3 or 4 replicate runs for each treatment and sample. Numbers above peaks indicate the wavelength of the emission peak.

- **A** 405 nm excitation.
- **B** 488 nm excitation.
- **C** 561 nm excitation.
- **D** 633 nm excitation.

3.7 Structural organization within the mats

The final objective in characterising the mat samples from the transect was to map the distribution of the resident organisms using their ascertained fluorescent properties from the previous experiments. The specific goal was to determine if species composition, orientation and distribution varied with mat morphology. Although fixation and embedding had extracted much of the phycobiliproteins (see section 3.6), enough chlorophyll remained present for the samples to fluoresce strongly when excited at 633 nm. More importantly, the differences in fluorescence between diatoms and cyanobacteria - excitation maxima were 680 and 660 nm respectively - meant that the confocal microscope could be adjusted to provide species information. Confocal detection windows were set to 650-679 nm and 680-700 nm.

In both the honeycomb (Figures 25 and 27) and pinnacle mats (Figure 30), notable differences in species composition were evident, although poor packing of the pinnacle samples rendered it difficult to draw definitive conclusions. No prostrate samples were examined. The embedded samples were used in this analysis. These were the best structurally preserved of all samples recovered from Lake Fryxell, were readily sectioned, unlike the frozen samples were not affected by thawing during the long-exposure on the microscope. They also retained sufficient pigments to allow some resolution of the diatom and cyanobacterial components using the 633 laser on power settings that caused minimal fading of pigment brightness.

3.7.1 Honeycomb mats

Due to more adequate packaging prior to transport, the embedded honeycomb mats were better preserved than the pinnacle mats. Under the confocal microscope, it was evident that nearly all fluorescent cells were concentrated in the upper mat layers (Figure 26), pit sides and small peaks (Figure 28). The sides of the pits and the tops of the inter-pit spacers were characterised by the most intense fluorescent emission, and these also showed the thickest growth layers – approximately 1 to 2 mm thick. The thickness of the growth laminae diminished as the pits deepened, before tapering away to less than 0.5 mm at approximately 10 mm in depth, by when little or no fluorescence was seen. This

thick growth at the tops of the inter-pit walls also seemed to reinforce the pits themselves by promoting relative wall growth away from the pit base. Black precipitate/stains were found in the bottoms of pits, and here almost no fluorescing organisms were detected deeper than 10 mm (Figure 29). The majority of the resident cells were thick-trichome cyanobacteria and diatoms that interspersed amongst each other. These organisms were typically oriented parallel to the mat surfaces. This arrangement was similar to a mosaic and was constant in this taxa composition across the pit slopes, and upper layers (Figure 26). Immediately below the diatom-thick trichome mosaic were thin trichomes arranged vertically and about 3 mm thick. These organisms were far less numerous than either the thicker trichomes or the diatoms, and did not penetrate deeper than 1-2 laminae.

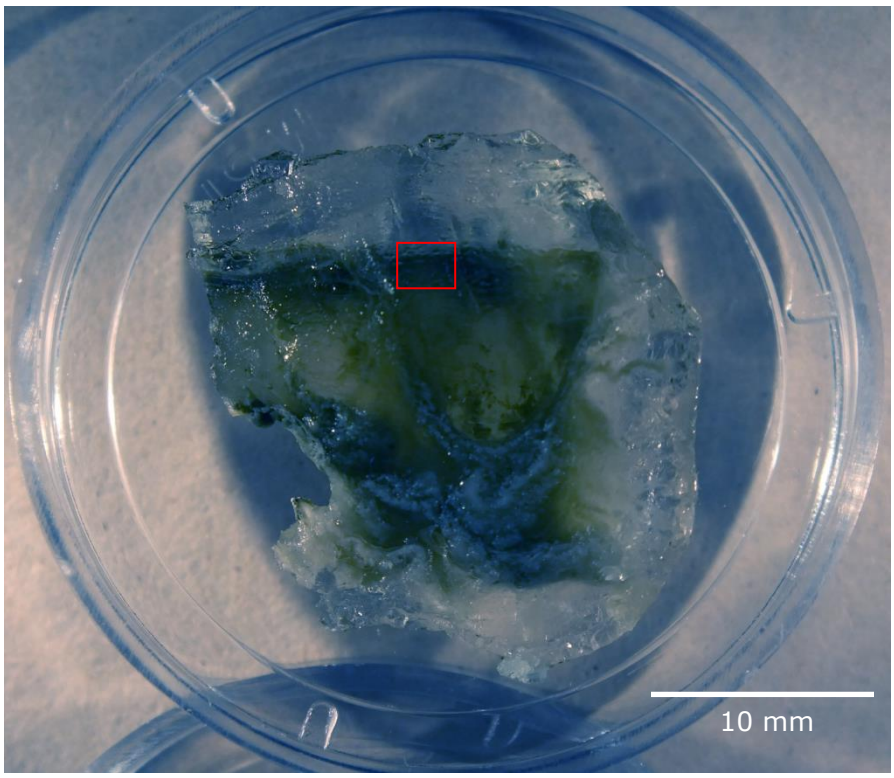

Figure 25. Vertical section of an acrylamide-embedded honeycomb mat collected from Lake Fryxell. The top of the microbial mat is oriented towards the top of the image. The red rectangle represents the location imaged by confocal microscopy and shown in Figure 26.

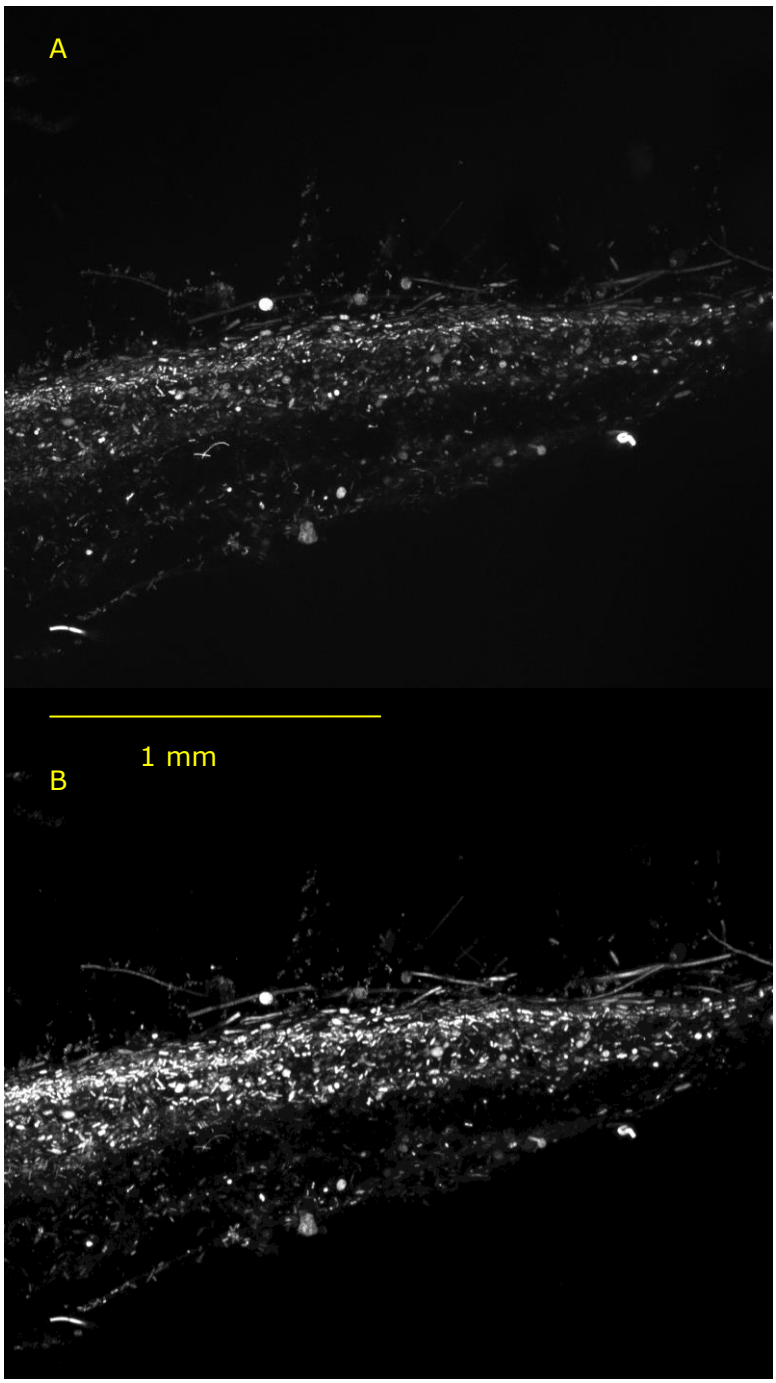

Figure 26. CLSM single image at 10 x magnification detailing the surface of a honeycomb mat collected from Lake Fryxell. The scale bar in B represents 1 mm for all images.

- **A** Fluorescence between 650 and 679 nm.
- **B** Fluorescence between 680 and 700 nm.

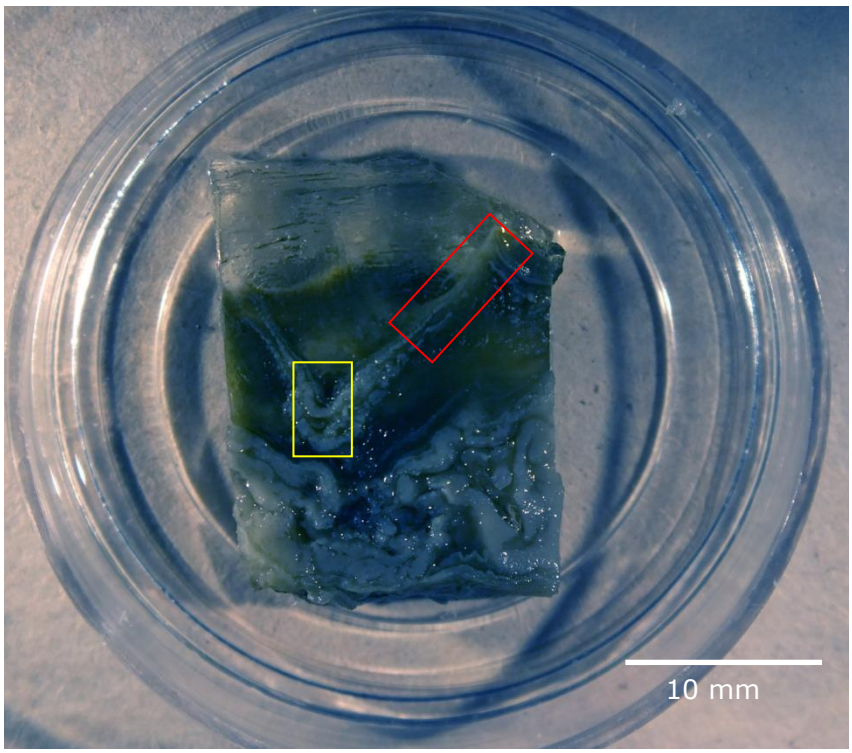

Figure 27. Vertical section of an acrylamide-embedded honeycomb mat collected from Lake Fryxell. The top of the microbial mat is oriented towards the top of the image. The red square represents the location scanned in Figure 28 while the yellow square represents the area scanned in Figure 29.

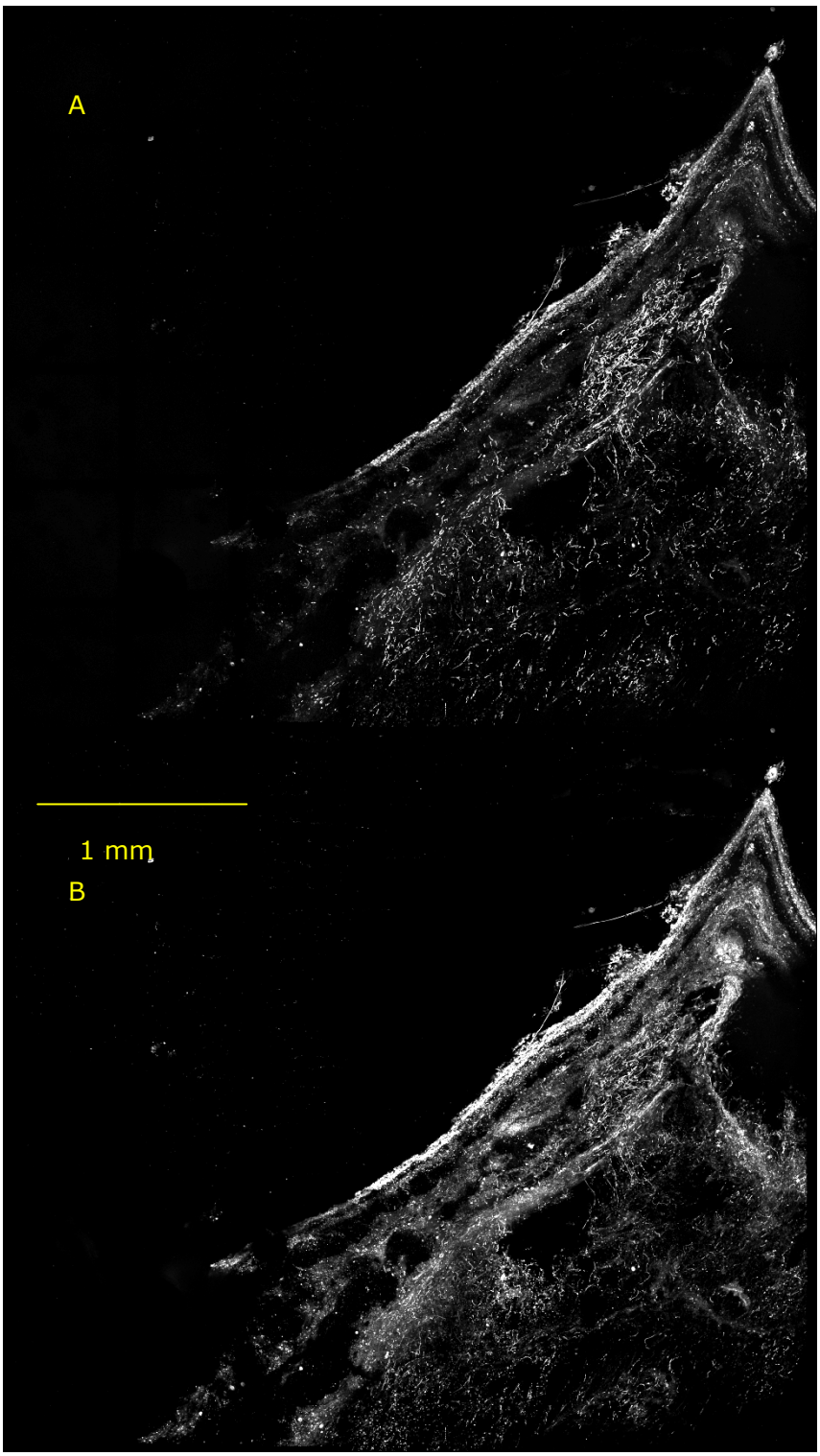

Figure 28. CLSM tilescan at 10 x magnification detailing a honeycomb mat from Lake Fryxell, with a pit slope and small peak. The scale bar in B represents 1 mm for all images.

- **A** Fluorescence between 650 and 679 nm.
- **B** Fluorescence between 680 and 700 nm.

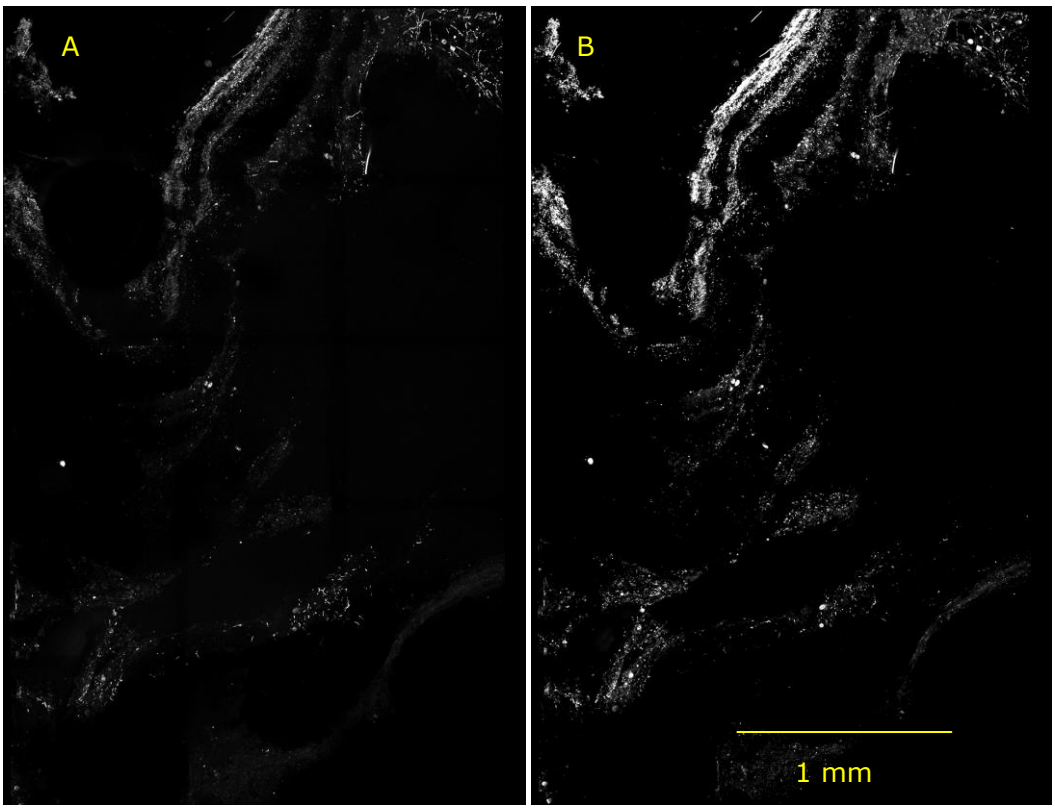

Figure 29. CLSM tilescan at 10 x magnification detailing a pit from a honeycomb mat from Lake Fryxell. The scale bar in B represents 1 mm for all images.

- **A** Fluorescence between 650 and 679 nm.
- **B** Fluorescence between 680 and 700 nm.

3.7.2 Pinnacle mats

As the pinnacle tips had collapsed, it was not possible to determine the spatial arrangements or distribution of the constituent organisms in these locations. In addition, sidewalls, depressions and pit boundaries could not be adequately analysed for these reasons. However, it was still possible to glean some information about the arrangement of fluorescent cells in the pinnacle mats as well as species composition. The most noticeable difference is the contrast in the present taxa. Thin trichome cyanobacteria were far more prevalent in the pinnacle mats than in the honeycomb mats. These cells were oriented vertically, in a base-surface direction and occupied the pinnacle mats across a 6 mm vertical section, decreasing in biomass concentration with depth. The first upper 2-3 mm of the mat was suspected to be the collapsed pinnacles (Figures 30 and 31).

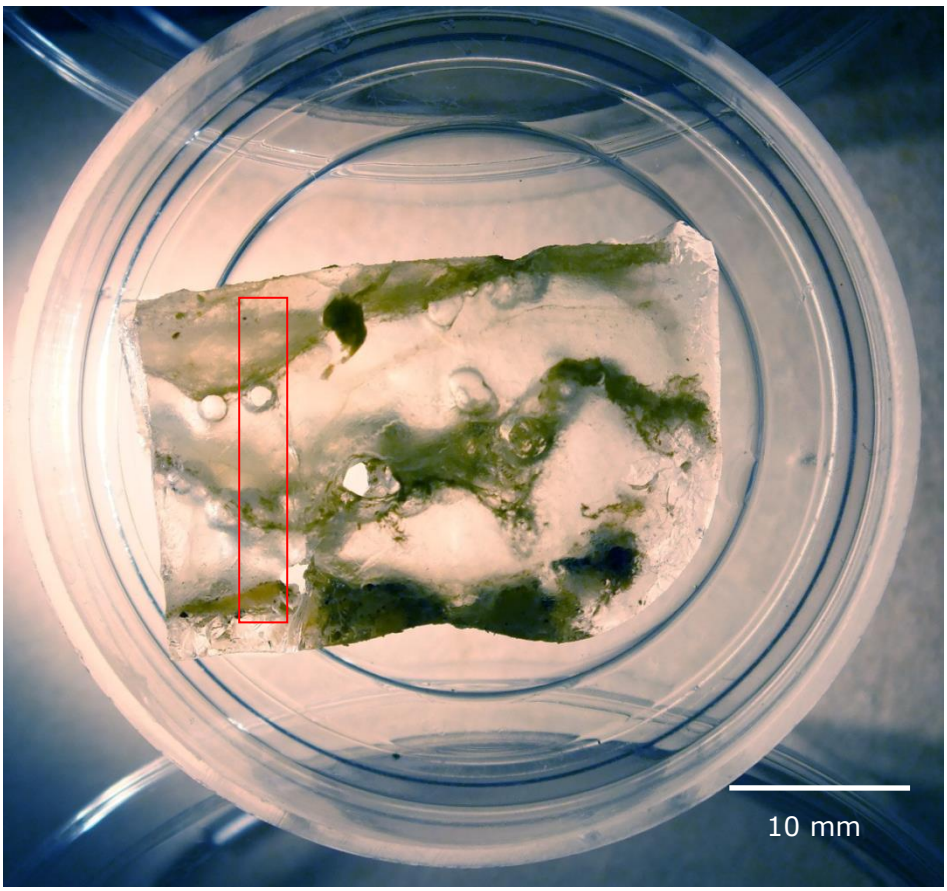

Figure 30. Vertical section of embedded pinnacle mat collected from Lake Fryxell. The red rectangle designates where the tile scan was conducted (Figure 31). The top of the microbial mat is oriented towards the top of the image.

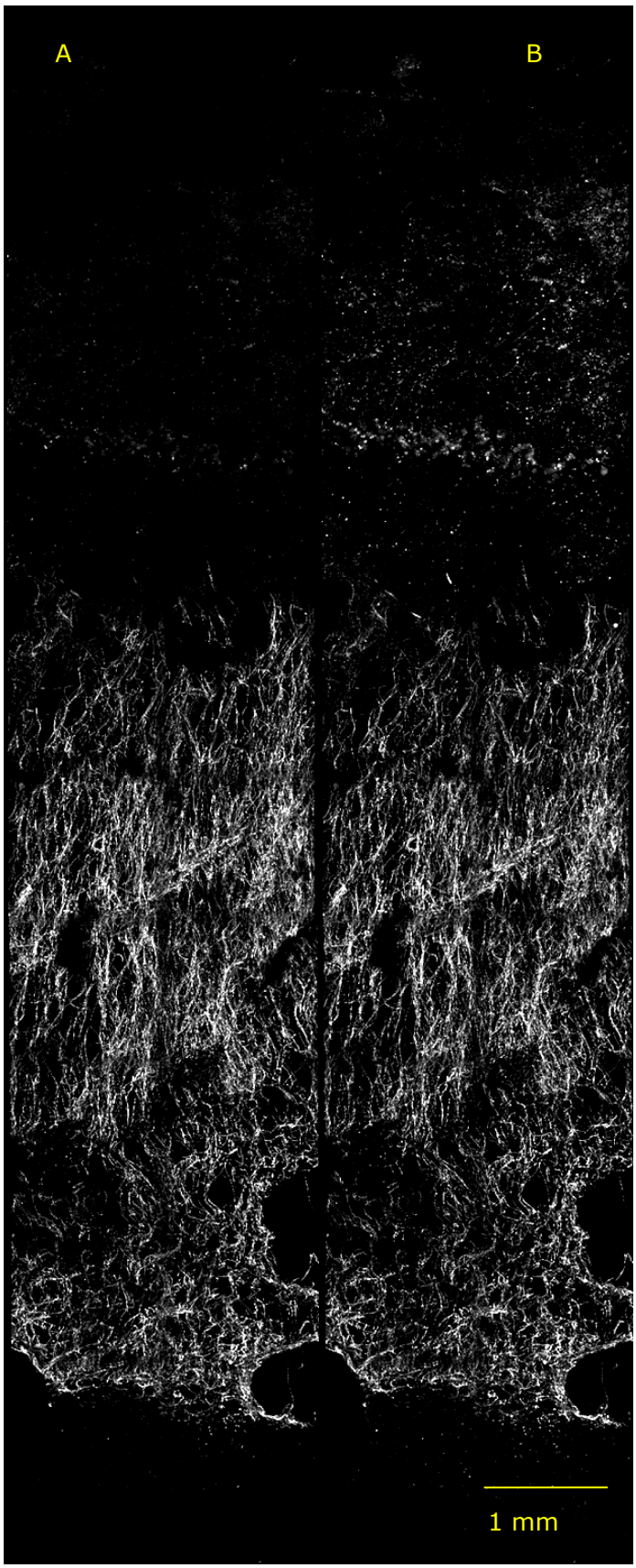

Figure 31. CLSM tilescan at 10 x magnification detailing a vertical section through a pinnacle mat from Lake Fryxell. The scale bar in B represents 1 mm for all images.

- **A** Fluorescence between 650 and 679 nm.
- **B** Fluorescence between 680 and 700 nm.

4. Discussion

The primary aim of this research was to investigate the structure of the benthic microbial mat communities at Lake Fryxell. This was addressed by developing new analytical approaches that utilised the spectral properties of the constituent mat species as a means of "finger-print" identification. Confocal microscopy was utilised to map their distribution within vertical section microbial mats. This approach was supplemented with conventional pigment extraction protocols. New preservative techniques were also tested for their efficacy in preserving mat structure for later analyses.

4.1 Methodology review

4.1.1 Sample Preservation

Of the three preservation techniques employed, freezing and embedding gave the best results for preserving mat structure. In contrast, fixing alone and transporting in liquid medium did not preserve structural integrity and resulted in them losing cohesiveness. Although freezing gave better preservation of pigments than fixing samples, freezing also brought risks of out-gassing, the production of gas bubbles when the sample freezes, and physical disruption caused by ice crystal growth. Both effects could have compromised structural integrity of the preserved mats. One possible way of avoiding bubble formation would be to replace the water around the mat with de-gassed water. Water stored under vacuum through the use of a simple vacuum pump will lose all its dissolved gases, and were the water around the mat replaced with such de-gassed water, and this allowed to equilibrate for some time before freezing for the remaining gas within the mat to diffuse out, bubbling within the mat on freezing might be reduced.

Two approaches were taken to viewing frozen samples. They were either thawed before viewing, or alternatively, viewed while still frozen. Preliminary trials with the frozen samples suggested that there were few changes in structure as the mats thawed, which suggests that this is a valid approach to observing mat structure. Some preliminary attempts were also made to view frozen samples by

confocal microscopy. Attempts at affixing frozen samples to metal stubs and designing a temperature controlled apparatus to view the samples using confocal microscopy encountered several technical problems. Ironically, cooling the metal stub in liquid nitrogen rendered them too cold to view properly using microscopy, due to the formation of ice crystals on the cover slip from frozen condensation. That these frozen samples were too cold for viewing suggests that there may be a way in which less severe cooling is used that would keep the samples frozen yet avoid the issue of ice formation on the cover-slip. This would allow microbial mats to be viewed while frozen without the issues of thawing changing structure. No further experiments were made with frozen samples and priority shifted to analysis of embedded material. While freezing is the standard procedure for preservation and transportation of Antarctic microbial mat specimens prior to imaging, it was speculated that more optimal procedures, such as fixation and embedding, could maintain structural integrity owing of the highly delicate frameworks which characterise benthic microbial communities from Lake Fryxell.

Acrylamide embedding has previously been used to help section and image other fragile samples such as embryonic tissues (Germroth *et al.,* 1995). The acrylamide-embedded mat samples were better preserved compared to fixed or frozen specimens, particularly amongst the samples that were kept in plastic containers during transport that prevented desiccation. The pinnacle samples, which were not so contained, dried and lost structural integrity as the acrylamide gel dried out and shrank. In hindsight, removing pinnacle samples from their containers after polymerization and wrapping in aluminium foil is an inadequate protocol. While Germroth *et al.* (1995) noted several drawbacks with the acrylamide embedding technique (such as the toxicity of liquid acrylamide) they did not mention dehydration of the polymerised material. It is apparent, therefore, that acrylamide-embedded specimens must be kept in a tightly-sealed, cool and moist environment at all times.

Acrylamide-embedded samples were prepared by sequential immersion in fixative, several rinses in filtered lake water and then the unpolmyerised acrylamide solution. During this procedure, repeated handling could have disrupted of the microbial matrix. An even better preservation of structure may be obtained if handling is minimised, particularly during the rinsing stage. A liquid displacement apparatus could be ideal for such work, where new fluids can

be slowly added over time, displacing the previous fluid. Additionally, these liquids should be de-gassed by storing them under vacuum prior to their use so that the generation of gas bubbles within the samples is minimised. While the embedding technique was specifically developed for this project, it could be feasibly used in studies of microbial mat structures at other lakes in the McMurdo Dry Valleys and elsewhere.

However, while the embedding approach was successful, many of the photosynthetic pigments (mainly the water-soluble phycobilins) were lost from the matrix, most likely during the fixative stage as the same was true of samples that were fixed but not embedded. Future research efforts must consider the effects of pigment loss before employing this technique. Fortunately, enough residual fluorescence was present to permit the acquisition of high quality images.

4.1.2 Confocal Microscopy

Confocal microscopy is a highly versatile imaging tool, which can use multiple lasers to generate a comprehensive image of a specimen. A major advantage of this type of microscopy is its ability to capture high-quality digital images of fluorescent samples and allows for 3-D reconstructions (Paddock, 1999). However, confocal microscopy is not without limitations. Light-induced bleaching can be a considerable problem and longer exposure times and higher excitation laser power result in more bleaching. Fluorescent molecules in their excited state can react with molecular oxygen to produce free radicals, which are highly damaging to cell components (Dailey *et al.,* 2005, Wynn-Williams, 1985). Sample bleaching was encountered during this experiment. Using a lower intensity laser with sufficient spectral coverage is one strategy that can be used to mitigate this effect.

The red HeNe 633 nm laser was chosen over the blue argon 488 nm laser for use in the structural studies for several reasons. Firstly, the embedding process had removed a large portion of the pigment content from the samples, particularly phycoerythrin, which would otherwise have been better imaged with the 488 nm excitation laser. Secondly, the 488 nm laser is more powerful than the 633 nm

and carried greater risks of further damaging already pigment-depleted samples. The green 561 nm laser was not considered for these experiments as it does not excite the chlorophylls present in diatoms well, and thus makes these cells difficult to see. Similarly, the violet 405 nm was not used as it has a higher energy and causes more rapid bleaching of samples. The different emission properties from diatoms and cyanobacteria trichomes viewed using 633 nm excitation allowed discrimination to be made between these groups. Specifically, the shift in emission peak from 660 nm in cyanobacteria to 680 nm in diatoms allowed the fluorescence emission windows on the Leica confocal to be set to between 650-679 nm for cyanobacteria and 680-700 nm for diatoms. Ultimately, the final technique used here to generate images of the microbial mats involved trade-offs between ease of sample handling, pigment preservation and image degradation by prolonged use of short wavelength laser excitation, and did not exploit the full potential of the multiple-laser fingerprinting technique developed.

4.2 Pigments and identification of mat constituents

While pigments have considerable potential in identifying specific groups of organisms, the resolution available in this study was limited. Precise pigment identification was not possible due to overlapping of spectral absorbance and emission between carotenoids, chlorophylls and bacteriochlorophylls. While it was possible to discriminate between cyanobacteria and diatoms based on spectral signatures, this project relied on visual identification to discriminate within these groupings. For example, the thick and thin trichomes both contained phycoerythrin and allophyococyanin, common pigments amongst cyanobacteria (Lawrenz *et al.,* 2011). While this distinguished them from the diatoms and green algae (containing a strong chlorophyll signature), each type could only be positively confirmed from the other by size and shape.

Use of pigments for species identification has previously been attempted by Millie *et al.* (2002), who attempted to use microscope-based absorption and fluorescence spectra to distinguish between planktonic organisms. Their goal was a robust, optically-based approach that allowed rapid discrimination of problematic algal blooms on the basis of their spectral traits, using traditional

and confocal microscopic examinations of specimens. Clearly optical approaches to algal identification, perhaps with alternative analytical approaches for studying pigment concentration, such the use of chromatography and *in situ* application of fibre-optic microprobes, have potential in resolving fine-scale algal distribution problems. The last of these has the further advantage of being minimally invasive as microprobes do not disturb the structural laminations of microbial mats or the steep environmental gradient variables, although proper calibration of these devices is difficult (Kuhl and Fenchel, 2000).

4.3 Mat morphologies

Results from this research demonstrated a clear relationship between mat morphology, pigment content, species composition and physical lake properties. As pH and temperature displayed minimal variation, their role in determining mat morphology dynamics was deemed minimal. Similarly, it was unlikely that conductivity was strongly correlated with changes in mat morphology either, as conductivity only changed from 5 mS/cm at D1 to a maximum of 9 mS/cm at D9. Essentially, marginally brackish water was only slightly increasing in salinity with depth. This served to illustrate that the transect was in the salinity stabilised component of the water column, a pre-requisite to steep gradients in other variables with depth. This suggested that the changes in mat composition and morphology along the transect were most likely to be linked to oxygen concentration and irradiance.

Pinnacle mats were located in the hyperoxic zone, from 8.9 to 9.4 m, while honeycomb and prostrate mats were found in the hypoxic (9.5-10.5 m) and anoxic zones (>10.5 m) respectively. The pigment extractions and spectral analyses from all sampling stations revealed changes in the abundances of chlorophylls, carotenoids, bacteriochlorophyll-a, allophycocyanin and phycoerythrin, which appeared to correspond to changes in the mat morphology and physical parameters. Phycoerythrin and chlorophyll mostly found in pinnacle mats, decreasing in amount in honeycomb mats, while prostrate mats contained higher amounts of carotenoids and bacteriochlorophyll-a.

Dissolved oxygen was only present in trace amounts at stations D4 to D6 and was virtually absent by stations D7 to D9. This also coincided with a substantial reduction in irradiance and decrease in chlorophyll and phycobilins (see Sections 3.1 and 3.3). This suggests that oxygenic photosynthesis was not the dominant form of primary production. Instead, anoxygenic photosynthesis would have been carried out by green sulfur bacteria at these depths (Karr *et al.,* 2005; Sattley and Madigan, 2010). This is consistent with the 750 nm absorbance peak in acetone extracts in this zone, indicative of the presence of bacteriochlorophyll-a. This pigment was first detected at D5 and then found throughout the hypoxic and anoxic zones. Bacteriochlorophyll-a is characteristic of green sulfur bacteria (Gerola and Olson, 1986). Honeycomb and prostrate mats were thus associated with low irradiance and increasing sulfide content. These findings also pointed towards link with the change in dominant metabolism and species composition. Cyanobacteria and diatoms were mostly found in the hyperoxic and hypoxic zones, while sulfate reducers would have been found in higher abundance further down, based on the divers reports of sulfide becoming detectable at D7. Observations beyond station D5 revealed the presence of thin cohesive films of trichomes overlying the mat communities. This would suggest that green-coloured cyanobacteria are more common at depth, and may be capable of employing both oxygenic and anoxygenic photosynthesis, while the phycoerythrin containing (purple) cyanobacteria are mainly restricted to areas of higher irradiance and dissolved oxygen. The switch to a sulfur-based metabolism in mats below the oxycline is consistent with similar reports of shifts in the planktonic microbial community in Lake Fryxell (Karr *et al*., 2003. 2005)

Previous research by Sabbe *et al.* (2004) has also indicated that the occurrence of mat morphology transitions was connected with (but not caused by) lake depth. Jorgensen *et al.* (1983) noted that the thick cyanobacterial from Solar Lake, in Sinai, also diminished in biomass with decreasing irradiance even though the latter is a different environmental context. It was not possible from this research to definitively conclude that irradiance was responsible for this metabolic, species and structural zonation but the results are suggestive. However, these physical parameters did seem to determine how emergent structures form.

4.4 Mat structure and organisation

Confocal microscopy of embedded honeycomb samples indicated that thick trichome cyanobacteria and diatoms were the dominant components, mainly in the first 3 mm of the surface and especially concentrated at the upper pit slopes. However, they were entirely absent from the pits. Thick trichomes were mainly located at the surface of the mat and oriented parallel to the mat surface. Thin trichomes were present and were mainly located underneath this diatom-thick trichome mosaic and oriented vertically. No diatoms or cyanobacteria were seen in the bases of the pits, where the black precipitate may have been iron sulfide that is generated by sulfate reducing bacteria (Baghoorn and Nichols, 1961). If so it suggests that the bottoms of the pits were anoxic, and the diatoms and cyanobacteria were avoiding these regions in favour of the localised oxygen-rich areas on the upper parts of the mat matrix. This localisation of photosynthetic biomass on the tops of the honeycomb structure would also account for the more rapid growth on the sides of the pits, as opposed to the rest of the mat. Such unequal vertical growth of pit rim and pit base is necessary for the evolution of the pit structure over time. In contrast, the pinnacle mats were almost entirely composed of thin trichome cyanobacteria arranged in the same vertical base-surface orientation as seen in the interior parts of the honeycomb mat. No fluorescent organisms were found at depths greater than 10 mm within the mat matrix in either pinnacle or honeycomb samples.

Interestingly, this diatom-cyanobacteria arrangement had some parallels with studies by Jorgensen *et al.* (1983) in Solar Lake, in the Sinai where thick, gelatinous cyanobacterial mats were present. There, dense diatom tufts 0.2-0.5 mm in diameter were also found overgrowing the cyanobacteria. Previous work by Krumbein and Cohen (1974, 1977) made similar findings. Exactly why the thick trichomes were oriented parallel to the surface is not known, although Vopel and Hawes (2006) have suggested that trichomes may form a horizontal layer during winter darkness, when no orientation cues are available, and some of these trichomes remain horizontal in the inter-laminar layer while a new lamination grows on top of them. This phenomenon has also been reported by Doemel and Brock (1977) for warm-water laminated mats. It is possible then that the layers observed could serve as the foundation for the next annual lamination.

Based on these findings, a model is proposed to describe pit formation in honeycomb mats (Figure 32). During winter darkness photoautotrophic growth must cease, and survival will depend on use of stored reserves and the winter "check" in growth will form. These checks were evident in the internal laminations within the mat structure (see Figure 10). Cyanobacteria are known to survive in anoxic environments and are also capable of chemoheterotrophic growth in darkness (Schmidt, 1988; Smith 1982). Diatoms are also capable of surviving in dark, anoxic sediments for months (Kamp *et al.,* 2011). When summer returns, the thick trichomes and diatoms clustered at the tops of the pit walls begin to grow again and secrete extracellular polysaccharide, allowing them to grow vertically, away from the anoxic zones and towards the irradiance, resulting in accumulation of mat at the surface of the pit, but not at the base. Organisms that either died or only survived (i.e. non-growing) bind with the detritus left behind by motile cells, thereby generating the new internal lamination.

While the poor preservation of the pinnacle samples prevented a growth model from being developed with any confidence, something similar may be proposed for this growth form, with the exception that there are no anoxic pit bases (Figure 33). Pinnacle mats are growing under higher irradiance than the honeycomb, and contain a different species balance evidenced by the abundance of phycoerythrin and the prevalence of narrow trichomes in confocal images. Pinnacle development to cm-scale relief requires that the emerging structures grow more rapidly than the background mat. This may be due to organism motility, whereby the trichomes oriented towards the pinnacle apex are migrating towards the tip, perhaps enhancing biomass accumulation at that tip. Observations made here that trichomes tend to be oriented towards the apex of the pinnacles is consistent with a general growth and migration towards that apex. Accumulation at the tip will provide more biomass, and it is also possible that this in turn reinforces enhanced apical growth.

The cuspate pinnacles and prostrate morphologies observed along the transect were similar to the emergent structures described by Hoffman (1969) for Precambrian stromatolites. These findings corroborate with the biogenic argument for stromatolite formation that has been forwarded by Flannery and

Walter (2012). Evidence that emergent structures in Lake Fryxell can calcify to form persistent stromatolites comes Parker *et al.* (1981) and Wharton *et al.* (1982). Collated data from this project does seem to support a model for emergent structure formation based on motility of constituent organisms that allows preferential apical growth, with both chemotactic and phototactic mechanisms potentially involved.

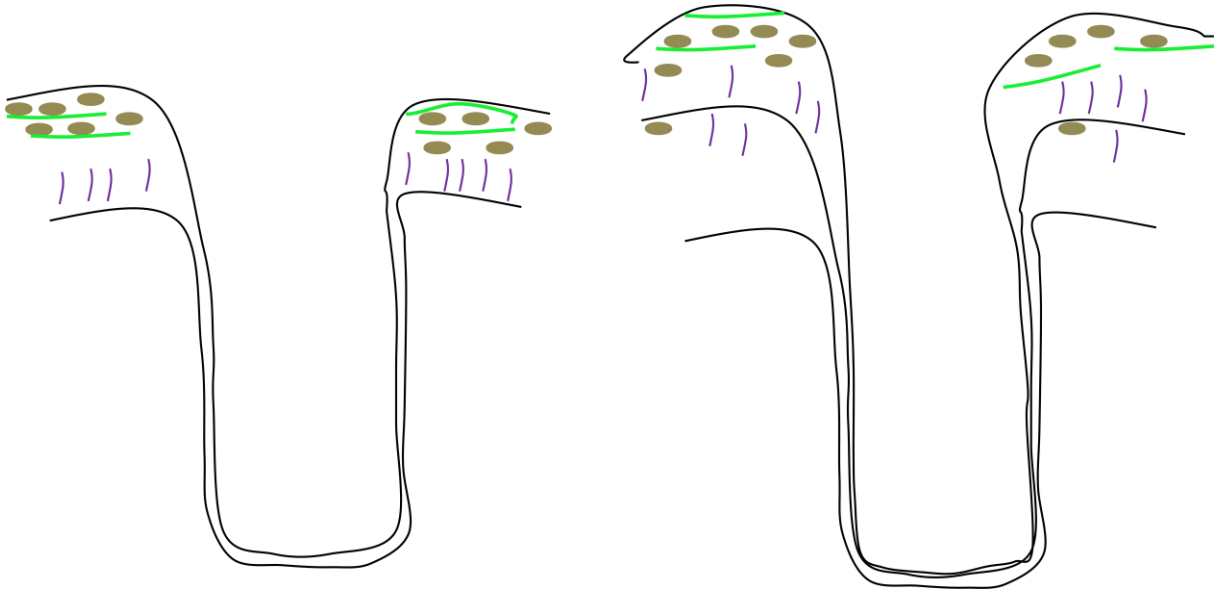

Figure 32. Proposed model of pit formation in honeycomb mats. The left illustration represents the first annual lamination while the right illustration represents two years of growth.

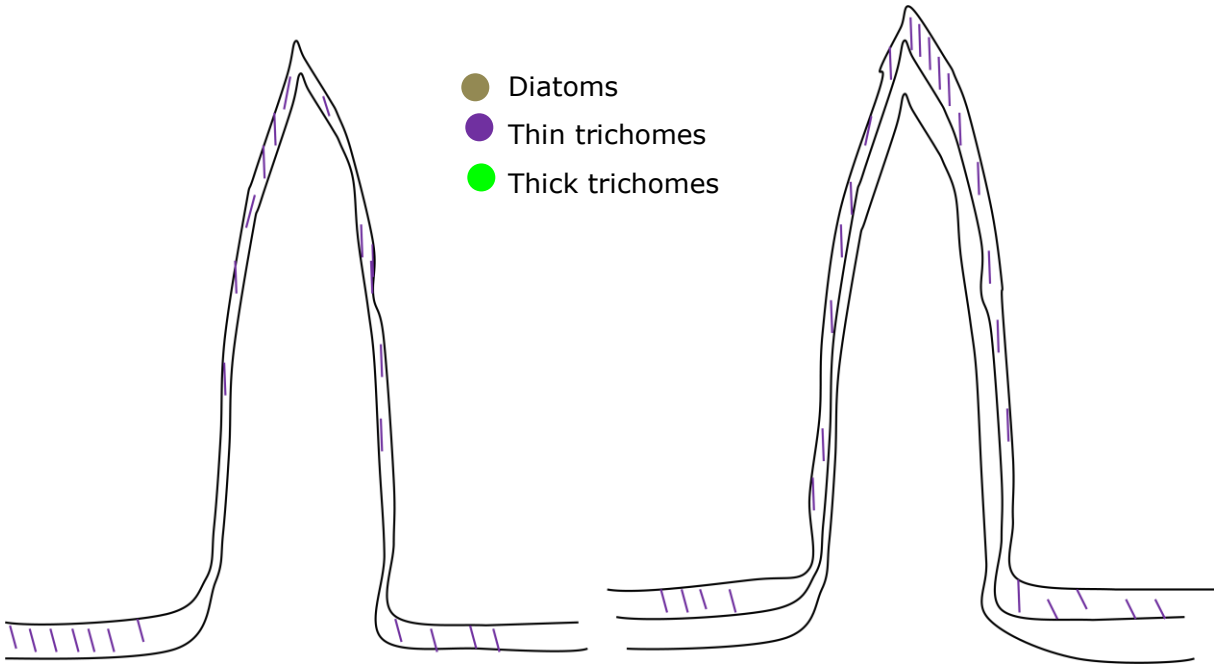

Figure 33. Proposed model of pit formation in pinnacle mats. The left illustration represents the first annual lamination while the right illustration represents two years of growth.

4.6 Future Directions

This research has generated a robust analytical protocol for embedding microbial mat samples and for cutting, sectioning and viewing those samples, and for generating "maps" of the distributions of specific groups of organisms within the mats. Future modifications and proposals to the embedding protocol include providing larger plastic containers and ensuring samples are more deeply embedded in liquid acrylamide prior to polymerization. New methods need to be developed to overcome the various challenges associated with sectioning and imaging before frozen samples can be similarly imaged. As no prostrate samples were acquired for confocal microscopy, future research expeditions should be aimed at acquiring these specimens.

5. Conclusions

At least three distinct microbial mat morphologies occur in Lake Fryxell – pinnacle, honeycomb and prostrate. The transitions between these coincided with notable changes in oxygen concentration and irradiance, with the pinnacle mats located in the areas with the highest amount of irradiance and dissolved oxygen, the honeycomb mats at lower irradiance and where oxygen concentration declined towards anoxia, and prostrate mats in the dim, anoxic waters below the oxycline. The shifts in mat morphology also coincided with changes in species composition and metabolic zoning.

Confocal microscopy established that the pinnacle mats were dominated by numerous thin trichomes that were oriented vertically. Honeycomb mats were dominated by thick trichomes and diatoms, with the thin trichomes seen in pinnacle mats less numerous and largely located underneath the diatom-thick trichome mosaic. No prostrate mats were examined, although spectral analysis indicated the presence of bacteriochlorophyll-a, which is characteristic of green sulfur bacteria.

Based on these findings, a model has been proposed to explain how emergent structures arise in benthic mat communities through a combination of environmentally-directed growth and motility. The biological basis of this model allows properties of pinnacle- and honeycomb-forming organisms to be defined, and by analogy what types of organisms are likely to have been necessary for the development of stromatolites displaying cuspate pinnacle peaks within an otherwise prostrate morphology. Although these studies findings were aimed at improving the understanding of emergent structure formation in MDV microbial mats, it has helped to support the biotic paradigm for formation of stromatolites.

6. References

Aiken G., McKnight D., Harnish R. and Wershaw R. (1996). Geochemistry of aquatic humic substances in the Lake Fryxell Basin, Antarctica. *Biogeochemistry* **34:** 157-188.

Allwood A.C., Grotzinger J.P., Knoll A.H., Burch I.W., Anderson M.S., Coleman M.L and Kanik I. (2009). Controls on development and diversity of Early Archean stromatolites. *Proceedings of the National Academy of Sciences of the USA* **106:** 9548-9555.

Andersen D.T., Sumner D.Y., Hawes I., Webster-Brown J. and McKay C.P. (2011). Discovery of large conical stromatolites in Lake Untersee, Antarctica. *Geobiology* **9:** 280-293.

Angino E.E., Armitage K.B. and Tash J.C. (1962). Chemical stratification in Lake Fryxell, Victoria Land, Antarctica. *Science* **138:** 34-36.

Barber J., Morris E.P. and da Fonseca P.C.A. (2003). Interaction of the allophyocyanin core complex with photosystem II. *Photochemical and Photobiological Sciences* **2:** 536-541.

Barghoorn E.S. and Nichols R.L. (1961). Sulfate-reducing bacteria and pyritic sediments in Antarctica. *Science* **134:** 190.

Batchelor M.T., Burne R.V., Henry B.I. and Watt S.D. (2003). Mathematical and image analysis of stromatolites morphogenesis. *Mathematical Geology* **35:** 789-803.

Bauld J. (1981). Occurrence of benthic microbial mats in saline lakes. *Hydrobiologica* **81:** 87-111.

Bomblies A., McKnight D.M. and Andrews E.D. (2001). Retrospective simulation of lake-level rise in Lake Bonney based on recent 21-year record: indication of recent climate change in the McMurdo Dry Valleys, Antarctica. *Journal of Paleoclimatology* **25:** 477-492.

Bosak T., Knoll A.H. and Petroff A.P. (2013). The meaning of stromatolites. *Annual Review of Earth and Planetary Sciences* **41:** 1-24.

Bosak T. and Newman D.K. (2005). Microbial kinetic controls on calcite morphology in supersaturated solutions. *Journal of Sedimentary Research* **75:** 190-199.

Brambilla E., Hippe H., Hagelstein A., Tindall B.J. and Stackebrandt E. (2001). 16S rDNA diversity of cultured and uncultured prokaryotes of a mat sample from Lake Fryxell, McMurdo Dry Valleys, Antarctica. *Extremophiles* **5:** 23-33.

Burne R.V. and Moore L.S. (1987). Microbialites: Organosedimentary deposits of benthic microbial communities. *Palaios* **2:** 241-254.

Canfield D.E. and Green W.J. (1985). The cycling of nutrients in a closed-basin Antarctic lake: Lake Vanda. *Biogeochemistry* **1:** 233-256.

Castenholz R.W. (1968). The behaviour of *Oscillatoria terebriformis* in hot springs. *Journal of Phycology* **4:** 132-139.

Craig H., Wharton R.A. and McKay C.P. (1992). Oxygen supersaturation in ice-covered Antarctic lakes: biological versus physical contributions. *Science* **255:** 318-321.

Dailey M.E. Manders E., Soll D.R. and Teraski M. (2005). Confocal microscopy of living cells. In: Pawley J.B. (ede.), *Handbook of Biological Confocal Microscopy*. Springer, New York, USA. pp 381-403.

Decho A.W. (1990). Microbial exopolymer secretions in ocean environments: their role(s) in food webs and marine processes. *Oceanography and Marine Biology* **28:** 73-153.

de los Rios A., Ascaso C., Wierzchos J., Fernandez-Valiente D. and Quesada A. (2004). Microstructural characterisation of cyanobacterial mats from the

McMurdo Ice Shelf, Antarctica. *Applied and Environmental Microbiology* **70:** 569-580.

Dillon J.G., Miller S., Bebout B., Hullar M., Pinel N. and Stahl D.A. (2009). Spatial and temporal variability in a stratified hypersaline mat microbial mat community. *FEMS Microbiology Ecology* **68:** 45-58.

Doemel W.N. and Brock T.D. (1977). Structure, growth and decomposition of laminated algal-bacterial mats in alkaline hot springs. *Applied and Environmental Microbiology* **34:** 433-452.

Dore J.E. and Priscu J.C. (2001). Phytoplankton phosphorus deficiency and alkaline phosphatase activity in the McMurdo Dry Valley lakes, Antarctica. *Limnology and Oceanography* **46:** 1331-1346.

Dupraz C., Reid P.R., Braissant O., Decho A.W., Norman S.R. and Visscher P.T. (2009). Process of carbonate precipitation in modern microbial mats. *Earth-Science Reviews* **96:** 141-162.

Dupraz C. and Visscher P.T. (2005). Microbial lithification in marine stromatolites and hypersaline mats. *Trends in Microbiology* **13:** 429-438.

Fenchel T. (1998). Formation of laminated cyanobacterial mats in the absence of benthic fauna. *Aquatic Microbial Ecology* **14:** 235-240.

Flannery D.T. and Walter M.R. (2012). Archean tufted microbial mats and the Great Oxidation Event: new insights into an ancient problem. *Australian Journal of Earth Sciences* **59:** 1-11.

Fountain A.G., Nylen T.H., Monaghan A., Basagic H.J. and Bromwich D. (2009). Snow in the McMurdo Dry Valleys, Antarctica. *International Journal of Climatology* **30:** 633-642.

Franks J. and Stolz J.F. (2009). Flat laminated microbial mat communities. *Earth-Science Reviews* **96:** 163-72.

Frigaard N.U., Larsen K.L. and Cox R.P. (1996). Spectrochromatography of photosynthetic pigments as a fingerprinting technique for microbial phototrophs. *FEMS Microbiology Ecology* **20:** 69-77.

Frigaard N.U., Takaichi S., Hirota M., Shimada K. and Matsuura K. (1997). Quinones in chlorosomes of green sulfur bacteria and their role in the redox-dependent fluorescence studied in chlorosome-like bacteriochlorophyll c aggregates. *Archives of Microbiology* **167:** 343-349.

Gerdes G. (2010). What are microbial mats? In: Seckbach J. and Oren A. (eds), *Microbial mats: modern and ancient microorganisms in stratified systems.* Springer, New York, USA. pp 3-25.

Germroth P.G., Gourdie R.G. and Thompson R.P. (1995.) Confocal microscopy of thick sections from acrylamide gel embedded embryos. *Microscopy Research and Techniques* **30**: 513-520.

Gerola P.D. and Olson J.M. (1986). A new bacteriochlorophyll *a*-protein complex associated with chlorosomes of green sulfur bacteria. *Biochimica et Biophysica Acta – Bioenergetics* **848:** 69-76.

Gleadow A.J.W., McKelvey B.C. and Ferguson K.U. (1984). Uplift history of the Transantarctic Mountains in the Dry Valleys area, southern Victoria Land, from apatite fission track ages. *New Zealand Journal of Geology and Geophysics* **27:** 457-464.

Grotzinger J.P. and Knoll A.H. (1999). Stromatolites in Precambrian carbonates: evolutionary mileposts or environmental dipsticks? *Annual Review of Earth and Planetary Sciences* **27:** 313-358.

Grotzinger J.P. and Rothman D.H. (1996). An abiotic model for stromatolites morphogenesis. *Nature* **383:** 423-425.

Hawes I. and Howard-Williams C. (1998). Primary production processes in streams of the McMurdo Dry Valleys, Antarctica. *Antarctic Research Series* **72:** 129-140.

Hawes I., Howard-Williams C. and Vincent W.F. (1992). Desiccation and recovery of Antarctic cyanobacterial mats. *Polar Biology* **12:** 587-594.

Hawes I., Moorhead D., Sutherland D., Schmeling J. and Schwarz A.-M. (2001). Benthic primary production in two perennially ice-covered Antarctic lakes: patterns of biomass accumulation with a model of community metabolism. *Antarctic Science* **13:** 18-27.

Hawes I. and Schwarz A-M. J. (2001). Absorption and utilisation of irradiance by cyanobacterial mats in two ice-covered Antarctic lakes with contrasting light climates. *Journal of Phycology* **37:** 5-15.

Hawes I. and Schwarz A-M. (1999). Photosynthesis in an extreme shade environment: benthic microbial mats from Lake Hoare, a permanently ice-covered Antarctic lake. *Journal of Phycology* **35:** 448-459.

Hawes I., Sumner D.Y., Andersen D.T. and Mackey T.J. (2011). Legacies of recent environmental change in the benthic communities of Lake Joyce, a perennially ice-covered Antarctic lake. *Geobiology* **9:** 394-410.

Hoare R.A., Popplewell K.B., House D.A., Henderson R.A., Prebble W.M. and Wilson A.T. (1965). Solar heating of Lake Fryxell, a permanently ice-covered Antarctic lake. *Journal of Geophysical Research* **70:** 1555-1558.

Hofmann H.J. (1969). *Stromatolites from the Proterozoic Animikie and Sibley groups, Ontario*. Department of Energy, Mines and Resources, Ottawa, Canada.

Howes B.L. and Smith R.L. (1990). Sulfur cycling in a permanently ice-covered amictic lake Antarctic lake, Lake Fryxell. *Antarctic Journal of the United States* **25:** 230-233.

Jørgensen B.B. and des Marais D.J. (1986). Competition for sulfide among colorless and purple sulfur bacteria in cyanobacterial mats. *FEMS Microbiology Letters* **38:** 179-186.

Jørgensen B.B., Revsbech N.P. and Cohen Y. (1983). Photosynthesis and structure of benthic microbial mats: Microelectrode and SEM studies of four cyanobacterial communities. *Limnology and Oceanography* **28:** 1075-1093.

Kalkowsky V.H.E. (1908). Oolith und stromatolith im norddeutschen Buntsandstein. *Zeitschrift der Deutschen Geologischen Gesellschaft* **60**:68-125.

Kamp A., de Beer D., Nitsch J.L., Lavik J. and Stief P. (2011). Diatoms respire nitrate to survive dark and anoxic conditions. *Proceedings of the National Academy of Sciences of the USA* **108:** 5649-5654.

Karr E.A., Ng J.M., Belchik S.M., Sattley W.M., Madigan M.T. and Achenbach L.A. (2006). Biodiversity of methanogenic and other *Archaea* in the permanently frozen Lake Fryxell, Antarctica. *Applied and Environmental Microbiology* **72:** 1663-1666.

Karr E.A., Sattley W.M., Jung D.O., Madigan M.T. and Achenbach L.A. (2003). Remarkable diversity of phototrophic purple bacteria in a permanently frozen Antarctic lake. *Applied and Environmental Microbiology* **69:** 4910-4914.

Karr E.A., Sattley W.M., Rice M.R., Jung D.O., Madigan M.T. and Achenbach M.T. (2005). Diversity and distribution of sulfate-reducing bacteria in permanently frozen Lake Fryxell, McMurdo Dry Valleys, Antarctica. *Applied and Environmental Microbiology***71:** 6353-6359.

Kepner R., Kortyna A., Wharton R.A., Doran P., Andersen D. and Roberts E. (2000). Effects of research diving on a stratified Antarctic lake. *Water Research* **34:** 71-84.

Kilian O., Steunou A-S., Fazeli F., Bailey F., Bhaya D. and Grossman A.R. (2007). Responses of a thermophilic *Synechococcus* isolate from the microbial mat of Octopus Spring to light. *Applied and Environmental Microbiology* **73:** 4268-4278.

Klock J-H., Wieland A., Seifert R. and Michaelis W. (2007). Extracellular polymeric substances (EPS) from cyanobacterial mats: characterisation and isolation method optimisation. *Marine Biology* **152:** 1077-1085.

Konfirst M.A., Sjunneskog C., Scherer R.P. and Doran P.T. (2011). A diatom record of environmental change in Fryxell Basin, Taylor Valley, Antarctica, late Pleistocene to present. *Journal of Palaeolimnology* **46:** 257-272.

Kowalewski D. Ice Stories: Dispatches from Polar Scientists (2009). Welcome to the Beacon Valley. (On Line). Available HTTP: http://icestories.exploratorium.edu/dispatches/welcome-to-beacon-valley/. (2013, June 07).

Krumbein W.E. and Cohen Y. (1974). Biogene, klastische und evaporitsche Sedimentation in einem mesothermen monomiktischen ufernahen See (Golf von Aqaba). *Geologische Rundschau* **63:** 1035-1065.

Krumbein W.E. and Cohen Y. (1977). Primary production, mat formation and lithification: Contribution of oxygenic and facultative anoxygenic cyanobacteria, *In* E. Flugel (ed), *Fossil algae*. Springer, Berlin, Germany. pp. 37-56.

Kühl M. and Fenchel T. (2000). Bio-optical characteristics and the vertical distribution of photosynthetic pigments and photosynthesis in an artificial cyanobacterial mat. *Microbial Ecology* **40:** 94-103.

Lampert W. and Sommer U. (1997). *Limnoecology: The Ecology of Lakes and Streams*. Oxford University Press, Oxford, England

Lawrence M.J.F. and Hendy C.H. (1985): Water column and sediment characteristics of Lake Fryxell, Taylor Valley, Antarctica. *New Zealand Journal of Geology and Geophysics* **28:** 543-552.

Lawrenz E., Fedewa E.J. and Richardson T.L. (2011). Extraction protocols for the quantification of phycobilins in aqueous phytoplankton extracts. *Journal of Applied Phycology* **23:** 865-871.

Lorenzen J., Glud R.N. and Revsbech N.P. (1995). Impact of microsensor-caused changes in diffusive boundary layer thickness on O_2 profiles and photosynthetic

rates in benthic communities of microorganisms. *Marine Ecology Progress Series* **119:** 237-241.

Millie D.F., Schofield O.M.E, Kirkpatrick G.J., Johnsen G. and Evens T.J. (2002). Using absorbance and fluorescence spectra to discriminate microalgae. *European Journal of Phycology* **37:** 313-322.

Moorhead D.L., Schmeling J. and Hawes I. (2005). Modelling the contribution of benthic microbial mats to net primary production in Lake Hoare, McMurdo Dry Valleys. *Antarctic Science* **17:** 33-45.

Moorhead D.L., Wolf C.F. and Wharton R.A. (1997). Impact of light regimes on productivity patterns of benthic microbial mats in an Antarctic lake: A modelling study. *Limnology and Oceanography* **42:** 1561-1569.

Paerl H.W. and Pinckney J.L. (1996). A mini-review of microbial consortia: their roles in aquatic production and biogeochemical cycling. *Microbial Ecology* **31:** 225-247.

Paddock S.W. (1999). Confocal laser scanning microscopy. *BioTechniques* **27:** 992-1004.

Parker B.C. and Simmons G.M. (1978). Ecosystem comparisons of oasis lakes and soils. *Antarctic Journal of the United States* **13:** 168-169.

Parker B.C., Simmons G.M., Love G.F., Wharton R.A. and Seaburg K.G. (1981). Modern stromatolites in Antarctic Dry Valley lakes. *BioScience* **31:** 656-661.

Petroff A.P., Sim M.S., Maslov A., Krupenin M., Rothman D.R. and Bosak T. (2010). Biophysical basis for the geometry of conical stromatolites. *Proceedings of the National Academy of Sciences of the USA* **107:** 9956-9961.

Quesada A., Fernandez-Valiente E., Hawes I. and Howard-Williams C. (2008). Benthic primary production in polar lakes and rivers. In: Vincent W.F., Laybourn-Parry, J. (eds), *Polar Lakes and Rivers - Arctic and Antarctic Aquatic Ecosystems*. Oxford University Press, Oxford, England, pp. 179-196.

Riding R. (2000). Microbial carbonates: the geological record of calcified bacterial-algal mats and biofilms. *Sedimentology* **47:** 179-214.

Rowan K.S. (1989). *Photosynthetic pigments of algae*. Cambridge University Press, Cambridge, United Kingdom.

Sabbe K., Hodgson D.A., Verleyen E., Taton A., Wilmotte A., Vanhoutte K. and Vyverman W. (2004). Salinity, depth and the structure and composition of microbial mats in continental Antarctic lakes. *Freshwater Biology* **49:** 296-319.

Sattley W.M. and Madigan M.T. (2010). Temperature and nutrient induced responses of Lake Fryxell sulfate-reducing prokaryotes and description of *Desulfovibrio lacufryxellense,* sp. nov. a pervasive, cold-active, sulfate reducing bacterium from Lake Fryxell, Antarctica. *Extremophiles* **14:** 357-366.

Schmidt A. (1988). Sulfur metabolism in cyanobacteria. *Methods in Enzymology* **167:** 572-583.

Sharma A., Sahgal M. and Johri B.N. (2003). Microbial communication in the rhizosphere: operation of quorum sensing. *Current Science* **85:** 1164-1172.

Shepard R.N. and Sumner D.Y. (2010). Undirected motility of filamentous cyanobacteria produces reticulate mats. *Geobiology* **8:** 179-190.

Smith A.J. (1982). Modes of cyanobacterial carbon metabolism. Carry N.G. and Whitton B.A. (eds). *The Biology of Cyanobacteria.* Blackwell, Oxford, United Kindgom. pp. 47-85.

Smith R.L., Miller L.G., Howes B.L. (1993). The geochemistry of methane in Lake Fryxell, an amictic, permanently ice-covered lake. *Biogeochemistry* **21:** 95-115.

Spaulding S.A., McKnight D.M., Smith R.L. and Dufford R. (1994). Phytoplankton population dynamics in perennially ice-covered Lake Fryxell, Antarctica. *Journal of Plankton Research* **16:** 527-541.

Spaulding S.A., McKnight D.M., Stoermer E.F. and Doran P.T. (1997). Diatoms in sediments of perennially ice-covered Lake Hoare, and implications for interpreting lake history in the McMurdo Dry Valleys of Antarctica. *Journal of Paleolimnology* **17:** 403-420.

Stevens E.W., Sumner D.Y., Harwood C.L., Crutchfield J., Hamann B., Kreylos O., Puckett E. and Senge P. (2011). Understanding microbialite morphology using a comprehensive suite of three-dimensional analysis tools. *Astrobiology* **11:** 1-10.

Taton A., Grubisic S., Brambilla E., De Wit R. and Wilmotte A. (2003). Cyanobacterial diversity in natural and artificial microbial mats of Lake Fryxell (McMurdo Dry Valleys, Antarctica): a morphological and molecular approach. *Applied and Environmental Microbiology* **69:** 5157-5169.

Tice M.M., Thornton D.C.O., Pope M.C., Olszewski T.D. and Gong J. (2011). Archean microbial mat communities. *Annual Review of Earth Planetary Sciences* **39:** 297-319.

Vermaas W.F.J. (1998). Gene modifications and mutation mapping to study the function of photosystem II. *Methods in Enzymology* **297:** 293-310.

Vincent W. (2000). Cyanobacterial dominance in the Polar regions. Whitton B. and Potts M. (eds). *The Ecology of Cyanobacteria*. Springer, Houten, The Netherlands. pp. 321-340

Vincent W.F. and Vincent C.L. (1982). Factors controlling phytoplankton production in Lake Vanda (77° S). *Canadian Journal of Fisheries and Aquatic Sciences* **39:** 1602-1609.

Vincent W.F. (1988). *Microbial ecosystems of Antarctica*. Cambridge University Press, Cambridge, United Kingdom.

Vopel K. and Hawes I. (2006). Photosynthetic performance of benthic microbial mats in Lake Hoare, Antarctica. *Limnology and Oceanography* **51:** 1801-1812.

Walter M.R., Bauld J. and Brock T.D. (1976). Microbiology and morphogenesis of columnar stromatolites (Conophyton, Vacerrilla) from hot springs in Yellowstone National Park. Walter M.R. (ed) *Stromatolites*. Elsevier, Amsterdam, The Netherlands. pp. 273-310.

Wharton R.A., Parker B.C. and Simmons G.M. (1983) Distribution, species composition and morphology of algal mats in Antarctic dry valley lakes. *Phycologia* **22:** 355-365.

Wharton R.A., Parker B.C. and Simmons G.M., Seaburg K.G. and Love F.G. (1982). Biogenic calcite structures forming in Lake Fryxell, Antarctica. *Nature* **295**: 403-405.

Whittaker T.E., Hall B.L., Hendy C.H. and Spaulding S.A. (2008). Holocene depositional environments and surface level changes at Lake Fryxell, Antarctica. *The Holocene* **18:** 775-786.

Wilson A.T. (1967). The lakes of the McMurdo Dry Valleys. *Tuatara* **15:** 152-164.

Wynn-Williams D.D. (1985). Photofading retardant for epifluorescence microscopy in soil micro-ecological studies. *Soil Biology and Biochemistry* **17:** 739-746.

Appendix 1: Fixatives

All preservatives were made at Lake Fryxell using stock solutions that had been prepared at the University of Canterbury, prior to the flight down to Antarctica. As it was impractical to transport large amounts of de-ionised water for the flight, instead water was taken directly from Lake Fryxell and filtered back at the lakeside laboratory using disposable 0.45 µm Millipore filters.

Table A1.1 Phosphate buffered saline (PBS) solution constituents.

Chemical	Final concentration in 1x solution (mM)	10x Stock solution concentration (mM)	mass for 1 litre of 10x stock (g)
NaCl	131	1310	76.56
$Na_2HPO_4.2H_2O$	5.1	51	9.09
KH_2PO_4	1.56	15.6	2.12
pH 7.2			

Table A1.2 Aldehyde fixative solution constituents.

Chemical	Final concentration	Stock solution concentration	Volume to make 200 ml (ml)	Volume to make 2 l (ml)
Formaldehyde	4%	29.2%	28	280
Triton X-100	0.1%	10%	2	20
PBS	1x	10x	20	200
Filtered water	-	-	150	1500

Table A1.3 Acrylamide embedding solution constituents.

Chemical	Final concentration	Stock solution concentration	Volume to make 50 ml (ml)	Volume to make 1 l (ml)
Acrylamide solution	16%	30%	26.67	533.4
Triton X-100	0.1%	10%	0.5	10
PBS	1x	10x	5	100
TEMED	0.075%	100%	0.0375	0.75
APS	0.1%	10%	0.5	10
Filtered water	-	-	17	340